UC San Diego

UC San Diego Electronic Theses and Dissertations

Title

Circadian and Diurnal Control of Metabolism in Cyanobacteria

Permalink

https://escholarship.org/uc/item/5z01761k

Author

Diamond, Spencer

Publication Date

2015

Supplemental Material

https://escholarship.org/uc/item/5z01761k#supplemental

Peer reviewed|Thesis/dissertation

eScholarship.org Powered by the California Digital Library
University of California

UNIVERSITY OF CALIFORNIA, SAN DIEGO

Circadian and Diurnal Control of Metabolism in Cyanobacteria

A dissertation submitted in partial satisfaction of the requirements for the degree Doctor of Philosophy

in

Biology

by

Spencer Diamond

Committee in Charge:

Professor Susan S. Golden, Chair
Professor William H. Gerwick
Professor Terence Hwa
Professor Stephen P. Mayfield
Professor Jose L. Pruneda-Paz

2015

Copyright

Spencer Diamond, 2015

All rights reserved.

The Dissertation of Spencer Diamond is approved, and it is acceptable in quality and form for publication on microfilm and electronically:

_____

_____

_____

_____

_____

Chair

University of California, San Diego

2015

DEDICATION

To My Mother, Julia Diamond, The Embodiment of Hard Work and Strength

To My Father, Scott Diamond, The Greatest Idol for Any Son

To the rest of my family,

La familia sticks together, thank you for always supporting my dream

TABLE OF CONTENTS

LIST OF FIGURES

LIST OF TABLES

LIST OF SUPPLEMENTARY FIGURES

LIST OF SUPPLEMENTARY DATA SETS

Supplementary Data Set 2-S1: **2_S1.xlsx**

Supplementary Data Set 2-S2: **2_S2.xlsx**

Supplementary Data Set 3-S1: **3_S1.xlsx**

Supplementary Data Set 3-S2: **3_S2.xlsx**

Supplementary Data Set 3-S3: **3_S3.xlsx**

ACKNOWLEDGEMENTS

First and foremost I would like to thank Dr. Susan Golden for taking me in when I had lost my way, and giving me just the right advice for each situation through this journey. You let me struggle to learn, gave me guidance when it was truly needed, and never lost your cool (even when I deleted the computer). Thank you Susan, for being a fantastic mentor and advisor.

I would like to specially thank, Benjamin Emery Rubin. You are the greatest colleague and friend that another graduate student could ask for. There is nobody else I would rather disagree with over ideas, and I could only hope to work together again this closely in the future.

I would also like to specially thank Darae Jun and Chase Dylan Barber, two of the most talented and dedicated undergraduate students I have ever come across. It was my great pleasure to mentor both of you and I know that you will each be very successful in your future endeavors.

I would also like to acknowledge the James Golden, Susan Golden, and Ralph Greenspan lab members for providing guidance, assistance with data analysis, feedback on presentations, and general support. In particular I would like to thank Dr. Arnaud Taton who sat behind me for many years and was always available for questions and discussion on a wide variety of topics, Dr. Mark Paddock for discussions on circadian clock outputs and general support, Dr. Ryan Simkovsky for always having good feedback on statistics and knowing the right experimental questions to ask, Dr. Ryan Shultzaberger

for helping me with sequencing and introducing me to R programing, and Blake Trial for always making sure our lab runs like clockwork (no pun intended).

Also, I would like to acknowledge my graduate committee, Dr. Stephen Mayfield for excellent suggestions on applying metabolomics to cyanobacteria, as well as Dr. Terry Hwa, Dr. Bill Gerwick, and Dr. Jose Pruneda-Paz for experimental guidance through this process.

I would also like to thank two of my most important mentors, Dr. Louise Glass and Dr. Andre Fleissner; my time at UC Berkeley was truly enriched by knowing both of you, and you are both model scientists that I hope to emulate (and make proud) during my career.

Personally, I would like to thank my family and friends for their unyielding support during my graduate career. First I would like to thank my mother, Julia Diamond, for always being interested in my work, even when you did not understand it, and my father, Scott Diamond, for always providing support when things got tough. I would also specially like to thank Elizabeth Beckman, who has been nothing but supportive, encouraging, and loving through the good and the bad of this process. Of my friends, I would particularly like to acknowledge Booth Ramsay, Kris Eklund, Zack Eklund, and Daniela Digregorio. You have all been great roommates and friends, and you put up with my long nights in the lab and inability to always do things together. I hope this dissertation provides some excuse of my absence at

times in the last 6 years. Finally, I would like to thank the people at Vin de Syrah for always being welcoming when I needed a break.

This work was supported by National Science Foundation grant MCB1244108 as well as the National Institute of Health cell and molecular genetics training grant T32GM007240

Chapter 1 is, in part, a reprint of material that appears in Shultzaberger, R. K., Boyd, J. S., Diamond, S., Greenspan, R. J., & Golden, S. S. (2015). Giving Time Purpose: The *S. elongatus* clock in a broader network context. Annu Rev Genet. (In Press). The dissertation author was a primary co-author and contributed to sections 3 and 4 of the manuscript and figures 2 and 3.

Chapter 2 is a reprint of Diamond, S., Jun, D., Rubin, B. E., & Golden, S. S. (2015). The circadian oscillator in *Synechococcus elongatus* controls metabolite partitioning during diurnal growth. *Pnas*, *112*(15), E1916–25. http://doi.org/10.1073/pnas.1504576112. The dissertation author was the primary author of this publication

Chapter 3 is a manuscript in preparation for publication under the tentative citation: Diamond, S., Rubin, B. E., Shultzaberger, R. K., Chen, Y., Barber, C. D., & Golden, S. S. (2015). Keeping the Balance: The Cyanobacterial Circadian Response Regulator RpaA is Critical for Metabolic Stability at Night. The dissertation author will be the primary author of this publication

VITA

EDUCATION

Ph.D. Biology, University of California, San Diego (2015)
Division of Biological Sciences Affiliated Doctoral Program with the Salk Institute for Biological Studies

B.S. Microbial Biology, University of California, Berkeley (2008)
College of Natural Resources

B.A. Molecular Cell Biology, University of California, Berkeley (2008)
College of Letters and Science

TEACHING

BGGN 200 Graduate School Fundamentals (Winter 2014)
BGGN 208 Biology Graduate Student Bootcamp (Winter 2012)
BIMM 120 Bacteriology (Winter 2012)
BIBC 140 Introduction to Biofuels (Spring 2012)
BIMM 101 Recombinant DNA Techniques Lab (Spring 2011)
MCB C148 Microbial Genetics and Genomics (Fall 2009)
Bio 1B General Biology 1B (Fall 2006)

FELLOWSHIPS AND AWARDS

First Prize Poster, FF21 Research Symposium (2015)
ASM Kadner Institute Fellow, ASM Kadner Institute (2014)
CMG Training Grant Fellow, NIH/UC San Diego (2010 - 2013)
BD Biosciences Fellowship, BD Biosciences (2010)
Distinction in General Scholarship, UC Berkeley L&S (2008)
Graduation with Honors, UC Berkeley CNR (2008)
Summer Undergraduate Research Fellowship, UC Berkeley (2007)

PUBLICATIONS

Diamond S, Rubin BE, Shultzaberger RK, Chen Y, Barber CD, and Golden SS (2015) Keeping the Balance: The Cyanobacterial Transcriptional Regulator RpaA is Critical for Metabolic Stability at Night. (In Progress)

Rubin BE, Wetmore KM, Price MN, **Diamond S**, Shultzaberger RK, Lowe LC, Curtin G, Arkin AP, Dutschbauer A, and Golden SS (2015) The Essential Gene Set of a Photosynthetic Organism. PNAS (Submitted)

Shultzaberger RK*****, Boyd JS*****, **Diamond S***, Greenspan RJ, and Golden SS (2015) Giving time purpose: The *S. elongatus* clock in a broader network context. Annu Rev Genet (In Press) ***Authors contributed equally to this work**

Diamond S, Jun D, Rubin BE, and Golden SS (2015) The circadian oscillator in *Synechococcus elongatus* controls metabolite partitioning during diurnal growth. PNAS 112(15): E1916-E1925.

Sun J, Tian C, **Diamond S**, and Glass NL (2012) Deciphering regulatory mechanisms associated with hemicellulose degradation in *Neurospora crassa*. Eukaryotic Cell 11: 482-493.

Fleissner A, **Diamond S**, and Glass NL (2009) The *Saccharomyces cerevisiae* PRM1 homolog in *Neurospora crassa* is involved in vegetative and sexual cell fusion events, but also has post-fertilization functions. Genetics 181:497-510.

ABSTRACT OF THE DISSERTATION

Circadian and Diurnal Control of Metabolism in Cyanobacteria

by

Spencer Diamond

Doctor of Philosophy in Biology

University of California, San Diego, 2015

Professor Susan S. Golden, Chair

Cyanobacteria are the architects of photosynthesis, and have evolved under the constant evolutionary pressure of predictable light and dark cycles. Consequently, they are the only bacterial lineage known to have a fully functional circadian clock. Due to their ubiquitous presence over the earth,

and their growing importance in human health and bioindustry, a complete understanding of how their core metabolism interacts with natural diel cycles and circadian rhythms is a critical knowledge area that can be broadly applied to the understanding of cyanobacteria in both natural and artificial environments. Unfortunately, few studies have addressed the metabolic and physiological influence of the cyanobacterial circadian clock under a natural diel cycle. Here we use the bacterium *Synechococcus elongatus* PCC 7942 to address critical knowledge gaps regarding how cyanobacteria integrate signals from light and circadian rhythms to orchestrate core metabolic processes. *S. elongatus* is an ideal model for this study as it has emerged as a proven metabolic engineering platform, is currently the most well studied model of the cyanobacterial circadian clock, and is ubiquitous in fresh water environments. Using a combinatorial approach employing untargeted metabolomics, we have directly demonstrated that the *S. elongatus* circadian clock is an important control mechanism for central carbon metabolism during light-dark transitions. Specifically, we show that the core oscillator exerts a repressive effect on the downstream circadian response regulator RpaA. In the morning, the repression of RpaA by the clock is important for suppressing the oxidative pentose phosphate pathway (OPPP), which normally performs carbon compound catabolism at night, such that carbon from photosynthesis can flow to secondary biosynthetic pathways. In turn, this shows that OPPP activation is highly dependent on RpaA activity. Also, the activation of the

OPPP is critical for survival at night, and we have shown that without RpaA mediated activation cell death ensues due to the inability to generate cellular reducing power. Characterization of the RpaA diurnal lethality phenotype has not only demonstrated the importance of diurnal reductant balance in *S. elongatus*, but also provides a new understanding as to why the circadian clock confers a fitness advantage to cyanobacteria under diurnal growth conditions.

Chapter 1

Introduction

1.1 Cyanobacteria: Global and Synthetic Importance

The green slime seen in a stream or on the surface of a pond has often been used to describe the lowest of the low. However, the dominant group of microorganisms in this green slime, cyanobacteria, are both a key to the Earth's past as well as its future. Cyanobacteria are the architects of photosynthesis, which is arguably the most widespread and influential biosynthetic process that occurs on our planet. In turn, photosynthesis may become the most important process in biotechnology in the coming century. Advancing the understanding of cyanobacterial biology will help us understand the history of the biosphere, its current state, and how humanity can work within it to thrive.

1.1.1 Evolutionary History of Cyanobacteria

The oldest solid evidence of microbial life dates from around 3.5 billion years ago [1]. During this period it is likely that most microbes functioned as heterotrophs and chemolithotrophs, and were dependent on the abiotically produced nutrients in the "primordial soup" of the oceans. The Earth of this era was a very different place than we know today. The atmosphere was devoid of oxygen, and many of the nutrients required for life were in

mineralized form and not biologically available [2]. Although the exact date of the emergence of cyanobacteria and oxygenic photosynthesis is debated, around 2.5 billion years ago cyanobacterial photosynthetic activity resulted in a massive influx of oxygen to the environment known as the great oxidation event (GOE) [1, 3]. The GOE had a enormous geologic impact as oxidation altered the geologic chemistry of the earth, and caused the solubilization and increased bioavailability of many nutrients such as nitrogen and sulfur oxides [1]. Additionally, the presence of oxygen allowed for the evolution of aerobic respiration, a far more efficient energy generating metabolic strategy than anoxic metabolism. If it were not for this event, it would be unlikely that cells would have had the energy to organize themselves into the large multicellular organisms we see today.

The earth altering invention of oxygenic photosynthesis, and the GOE that resulted, is not the only legacy of cyanobacteria. They also introduced oxygenic photosynthesis to eukaryotic plants and algae. The chloroplast arose from the symbiotic interaction and eventual integration of a free-living cyanobacterium with a eukaryotic host [4, 5]. There is still dispute how many times this process, known as endosymbiosis, has occurred through the evolution of plants and algae [5]. If a secondary endosymbiosis event did occur, however, it was likely from red or green algae that had originally derived their photosynthetic abilities from cyanobacteria [5]. Thus, the current evidence suggests that all forms of the chloroplast and oxygen evolving

photosynthetic machinery can be traced back to the primary endosymbiotic event between a free-living cyanobacterium and heterotroph.

1.1.2 Cyanobacterial Impact on Nutrient Cycling

Global primary productivity and carbon cycling are almost exclusively driven by oxygenic photosynthesis [6]. Marine and terrestrial ecosystems each contribute roughly 50% to the overall global productivity [7]. In marine ecosystems the cyanobacterial genera, *Prochlorococcus* and *Synechococcus,* are the most abundant bacteria found in ocean surface waters [6, 8, 9]. They alone account for over two-thirds of CO_2 fixation in ocean ecosystems, and in turn, over one-third of global primary production [6]. Even in light of this fact, these numbers are still likely an underrepresentation of the true contribution of cyanobacteria to global primary productivity, as they are often the most dominant photosynthetic microorganisms found in terrestrial freshwater systems [10]. Thus, an understanding of the global carbon cycle would be incomplete without consideration of cyanobacterial metabolism.

In addition to their role in the carbon cycle, cyanobacteria play a critical role in global nitrogen cycles as a wide number of species have the ability to fix atmospheric nitrogen into bioavailable forms [11, 12]. The widespread nitrogen fixing cyanobacterial genus *Trichodesmium* makes a substantial contribution to both marine and global nitrogen cycles [13, 14]. Some estimates for the quantity of nitrogen fixed by *Trichodesmium* are as high as

42% of the global total [11]. A number of other nitrogen fixing cyanobacteria species further inflate their input to the global nitrogen cycle. Thus cyanobacteria likely play a dominant role in the global nitrogen cycle.

The pervasive impact of cyanobacteria on two of the most important global nutrient cycles is a direct result of their core carbon and nitrogen metabolic processes. Thus, basic research into cyanobacterial metabolism, and metabolic control mechanisms, is critical for expanding the understanding of global nutrient cycling as well as for predicting the effects of human activity on the future global environment.

1.1.3 Evolution: Influence on Cyanobacterial Metabolism

Due to their importance as primary producers, and their extremely long evolutionary history, cyanobacteria are found in almost every environment on earth from arctic glaciers to geothermal hot springs [15-17]. Thus, many cyanobacterial lineages have become extremely niche adapted, with a huge amount of diversity within the phylum [18, 19]. This diversity is reflected in genetics and morphology, as cyanobacteria take a variety of filamentous, multicellular, and unicellular forms [20] Despite their extreme diversity and wide distribution two commonalities are shared by all cyanobacteria: (1) All cyanobacteria use oxygenic photosynthesis as their primary energy generating mechanism [21]; (2) Photosynthetic output is subject to daily changes in light availability from the earth's rotation. Thus,

metabolism in cyanobacteria follows daily cycles of reduction (during active photosynthesis) and oxidation (during inactivity) that are highly predictable. Given these facts it is not surprising that metabolism in cyanobacteria has evolved around photosynthesis [22], and that metabolic regulation in cyanobacteria shows a strong response to light [23-25], as well as anticipation of changes in light availability [26-28]. The cyclic and predictable availability of light over cyanobacterial evolution is likely why they are the only phylum of bacteria known to possess a fully functional circadian clock [28, 29].

Rhythmic metabolic processes in cyanobacteria have very deep evolutionary roots. After the GOE, organisms that either respired or evolved oxygen needed to acquire mechanisms for the detoxification of reactive oxygen species (ROS) generated during active metabolism [30]. One of the earliest proteins that evolved to detoxify ROS were the peroxiredoxins [31], which are conserved in almost all living organisms [32]. Although it is still not fully understood, these proteins exhibit circadian 24 h oxidation/reduction rhythms in cyanobacteria (and all other organisms tested) [32, 33] that occur independently of the known circadian clock. Thus, oxidation/reduction cycles are deeply engrained in cyanobacterial evolution, and this fact is highly reflected in cyanobacterial metabolic signaling mechanisms. Redox regulation has been shown to directly control a number of core metabolic systems in cyanobacteria including starch biosynthesis [34], nitrogen assimilation [35], and the Calvin Cycle [36, 37]. More recent work has shown that redox

dependent modifications of protein thiols can be detected over the entire cyanobacterial proteome [38-40].

Photosynthesis, circadian timing, and redox stress and regulation are the core that cyanobacterial metabolism, and its regulation, are built around. Thus, in attempting to understand metabolic processes in cyanobacteria, we must approach new questions in the context of their natural evolutionary history where natural oxidation reduction cycles are applied through the use of diurnal growth conditions.

1.1.4 Potential for Biotechnology

One of the most exciting and rapidly expanding areas of cyanobacterial biology is the application of cyanobacteria to the production of commodity chemicals and fuels [41-46]. A wide array of compounds are currently produced using heterotrophic microbes [47]. However, a commonality amongst these processes is that they require some carbohydrate feedstock to fuel the microorganisms involved, which constitutes a large fraction of the production cost [43]. The photosynthetic metabolism (and sometimes nitrogen fixation) used by cyanobacteria solves two problems: (1) The need for carbohydrate inputs are eliminated, as well as the need for nitrogen sources in some cases; (2) CO_2 fixed by cyanobacteria is removed from the atmosphere resulting in a net reduction of industrially produced CO_2. Humans have already been undertaking the large-scale culture of photosynthetic

organisms, in the form of farming, for thousands of years. The application of cyanobacteria as a bioproduction platform would be a natural next step in our millennium year old partnership with photosynthetic organisms.

In addition to their ability to perform oxygenic photosynthesis, cyanobacteria possess a number of traits that make them excellent candidates for bioindustrial applications. Relative to plants, cyanobacteria have a very short life cycle, and they convert solar energy into biomass at rates that generally exceed terrestrial plants by up to 3-fold [43]. In addition, in contrast to plants and algae, many species are extremely genetically tractable [48, 49], and a wide array of genetic tools are available [50-53]. Due to their need for an aquatic habitat, there has been some expressed concern that large-scale cultivation of cyanobacteria will compete for fresh water resources [43]. However, a life cycle analysis between plant and cyanobacterial cultivation systems shows that not only do cyanobacteria need less water than plants, but they also have the capability to utilize saline and polluted water as a growth medium [43, 54]. In fact, current *Spirulina sp.* biomass production uses highly alkaline conditions (pH ~11) and high salinity (1.2M NaCl), which has the added benefit of making their growth environment less hospitable to invasive species [55, 56]. Finally, the placement of cyanobacterial growth systems is only constrained by access to light and CO_2. Thus, cyanobacteria do not significantly compete for arable land mass, and can be placed close to downstream production processes.

In only the past 10 years a wide array of industrially relevant compounds have been successfully produced in cyanobacteria including: alcohols [57-61], organic acids [62-64], aldehydes [65], terpenes [66-68], alkanes [69], and sugars [70, 71]. Initial synthetic biology attempts in cyanobacteria resulted in product titers that were significantly lower than the theoretical yield from photosynthesis [72]. However, genome scale metabolic modeling performed on *Synechocystis sp.* PCC6803 suggests that cyanobacterial metabolism is not inherently flawed as a production platform, and likely has the potential to perform better than *E. coli* for most products [73]. The theoretically higher production ceiling is due to the fact that photosynthetic metabolism produces metabolic precursors with far less carbon loss in the form of CO_2 than heterotropic metabolism (**Figure 1-1**). Despite the initial low productivity, a number of products such as ethanol [57], sucrose [71], and 2,3-butanediol [61, 74] have now been produced at titers exceeding 2g/L.

The engineering strategies currently adapted for cyanobacterial strain improvement have been extensively reviewed by Oliver et al. [75]. A number of these strategies highlight the specific importance of light-dependent and circadian control over metabolism in cyanobacteria. It has been shown that factors dependent on light-dark cycles, such as redox cofactor abundance,

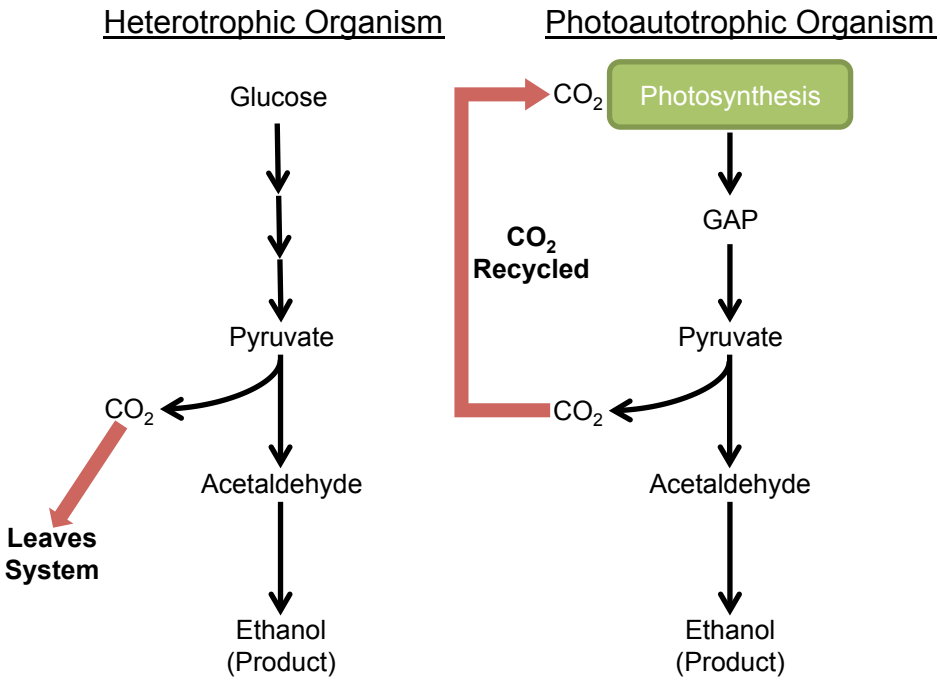

Figure 1-1. Theoretical Efficiency of Carbon Flow in Photoautotrophs. Ethanol production used as an example to demonstrate the conservation of carbon in photoautotrophic vs. heterotrophic metabolism. In heterotrophs one carbon in the form of CO_2 is lost for each product molecule formed, while in photoautotrophic metabolism the release of CO_2 from the system increases the local concentration and can be recycled back into photosynthesis. Thus the photoautotrophic system is inherently stoichometrically more efficient. Abbreviations are: glyceraldehyde-3-phosphate (GAP)

stoichiometry, and enzymatic specificity are all very influential over product yields [61, 62]. The ratio and the oxidation state of the reductant cofactors NADH and NADPH are directly related to the presence and absence of light in cyanobacteria [36]. Additionally, the ratio of NADPH/NADH is known to directly affect carbon fixation via modulation of Calvin Cycle enzymatic activity [36, 37]. Thus, enhanced knowledge of how global cellular redox state and stoichiometry affects cellular metabolism is likely to be beneficial for balancing the integration of reductant utilizing pathways under diurnal growth (**Figure 1-2A**). Indeed it has already been shown that both amino acid biosynthesis and fatty acid turnover can be increased by changes in overall cellular redox state [76, 77].

Another interesting observation is the ability of salt stress to enhance excreted sucrose biosynthesis by re-directing photosynthetic output to storage carbohydrates [71]. This indicates that global re-direction of carbon flux is a viable engineering strategy in cyanobacteira. Re-direction of carbon to storage compounds under stress conditions is a well characterized response in cyanobacteria, and recent work has shown that storage compound biosynthesis is often required for a proper stress response to occur [78-81]. This information has been directly leveraged to increase isobutanol production in cyanobacterial mutants that cannot store carbon by using isobutanol as an alternative carbon sink [82]. Unfortunately, a complex network with stoichiometric, redox, and circadian regulatory components

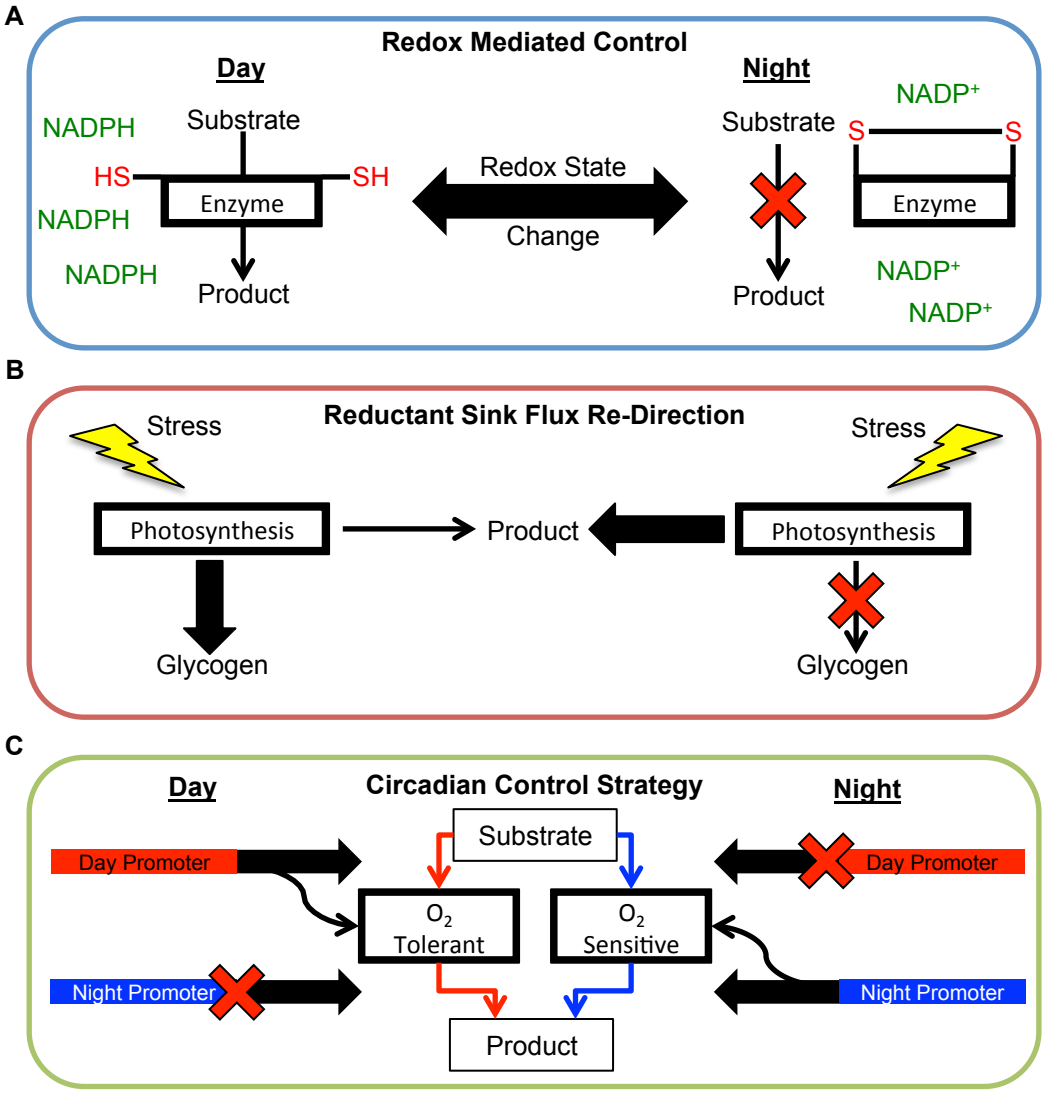

Figure 1-2. Metabolic Engineering Strategies Based on Redox and Circadian Driven Mechanisms. (A) Enzyme activity can change based on redox modification of cysteine residues that depend on the global redox state of the cell, which also changes with light availability. **(B)** Glycogen biosynthesis under stress as an example of a system that could be exploited to re-direct carbon flux to products. When glycogen synthesis is blocked reductant and carbon still need to flow out of photosynthesis and could be re-directed to a desired product. **(C)** An example engineered circadian regulon used for temporal expression control of oxygen sensitive and tolerant enzymes. Circadian clock driven promoters that drive peak expression during the day and night could be used to drive an oxygen tolerant and oxygen sensitive enzyme respectively, to maintain 24-h production of a product.

control stress driven flux re-direction (discussed further below), and this network is not fully characterized. A systems level understanding of flux re-direction control will likely improve the ability to leverage this strategy for other compounds where downstream precursor generation has proved difficult **(Figure 1-2B**).

The application of circadian control to bioproduction pathways is almost completely unexplored, and could be adapted to processes where incompatible processes must be segregated. As an example, production schemes that use oxygen sensitive enzymes are at a distinct disadvantage in an organism that evolves oxygen during normal growth. Although one production strategy for *n*-butanol production has adapted the use of oxygen-tolerant enzymes [83], it is likely that circadian control could be exploited to segregate incompatible processes such as photosynthesis and oxygen sensitive metabolism, which could further increase production titers (**Figure 1-2C**). A similar strategy is used by unicellular diazotrophic cyanobacteria to perform oxygenic photosynthesis and nitrogen fixation in the same cell [84].

Overall, any production system that uses solar energy will be subjected to natural diurnal cycles. It is known that cyanobacteria respond to these daily changes with large shifts in metabolism and physiology [85, 86]**,** and that these shifts are strongly influenced by circadian output and cellular redox state [36, 86]. Currently production systems only focus on product production during the light period. However, synthetic systems that can adapt and

respond to the dynamic intracellular environment of cyanobacteria may be able to take advantage of cellular metabolic state over the full 24 h period.

Given the success of synthetic feedback systems in *E. coli* that respond to intracellular metabolite levels to balance product output with metabolism [87], it is likely similar systems responding to redox state or exploiting circadian control would be highly beneficial in an inherently dynamic platform like cyanobacteria. Additionally, it has been shown that even synthetic promoters exhibit circadian expression patterns in cyanobacterial hosts [88]. Thus, it is clear that circadian regulation has a direct impact on heterologously expressed genes, and it is possible that peak expression of these genes may occur during a non-optimal metabolic state. However, the systems level understanding of redox and circadian regulation on metabolism is still far from comprehensive.

1.1.5 Overall Importance of Metabolic Study

Stretching back to the evolutionary beginnings of cyanobacteria, external diurnal cycles, circadian rhythms, and redox rhythms have had a major influence on their biology and metabolic control. Thus, future work on metabolism should be considered in a systems level context that includes signals of light availability, redox state, and circadian timing. Advancing understanding of metabolic control within the unique constraints of the diurnal photoautrophic lifestyle will be beneficial to almost all areas of cyanobacterial

biology. In the following sections we detail the current understanding of cyanobacterial core carbon and nitrogen metabolism, and how they are affected by natural diurnal cycles and circadian regulation. Subsequently we address some of the recent work where systems level analysis has been performed on cyanobacteria in an environmentally relevant diurnal cycle, as well as the current understanding of how the circadian clock elicits a global transcriptional response. We finish with a perspective on the gaps in existing knowledge and important future directions for the field. The focus of this review will primarily be on the metabolism occurring in non-nitrogen fixing cyanobacteria, however examples from nitrogen fixing cyanobacteria will be provided where relevant.

1.2 Carbon Metabolism: A Diurnal Perspective

Carbon metabolism in cyanobacteria is an extremely dynamic yet relatively predictable process due to its direct dependence on light availability. Cyanobacteria have evolved control mechanisms that generally separate carbon metabolic pathways into anabolic and catabolic regimes that occur during the light and dark, respectively. Although there are specific stimuli that result in re-direction of carbon metabolism, any response is also dependent on its timing within the light-dark cycle. Here we discuss the current state of understanding of core carbon metabolic pathways in cyanobacteria and their known circadian and diurnal regulatory mechanisms.

1.2.1 Glycogen Metabolism

1.2.1.1 Pathway Structure and Biochemistry

During active photosynthesis, cyanobacteria store fixed carbon as the glucose polymer glycogen [89]. Glycogen is the primary carbon storage polymer found in cyanobacteria and depending on the growth conditions can comprise between 20 to 60 percent of the dry cell mass [90, 91]. The structure of glycogen consists of α-1-4-linked glucose units with α-1-6-branch points at varying intervals depending on the cyanobacterial species [92]. Glycogen synthesis is initiated when glucose-6-phosphate (G6P) is isomerized to glucose-1-phosphate (G1P) via the activity of phosphoglucomutase (Pgm) (**Figure 1-3**), and is subsequently adenylated to ADP-glucose through the activity of ADP-glucose pyrophosphorylase (GlgC) in an irreversible reaction that consumes ATP [93]. The enzymatic activity of GlgC serves as the rate-limiting step in cyanobacterial glycogen biosynthesis [94]. The polymerization of glycogen and branching are accomplished through the enzymatic activities of glycogen synthase (GlgA) and glycogen branching enzyme (GlgB) respectively. During the breakdown of glycogen α-1-6-branch points are removed by the activity of glycogen debranching enzyme (GlgX), and α-1-4-linked glucose is depolymerized by glycogen phosphorylase (GlgP) [95, 96] (**Figure 1-3**).

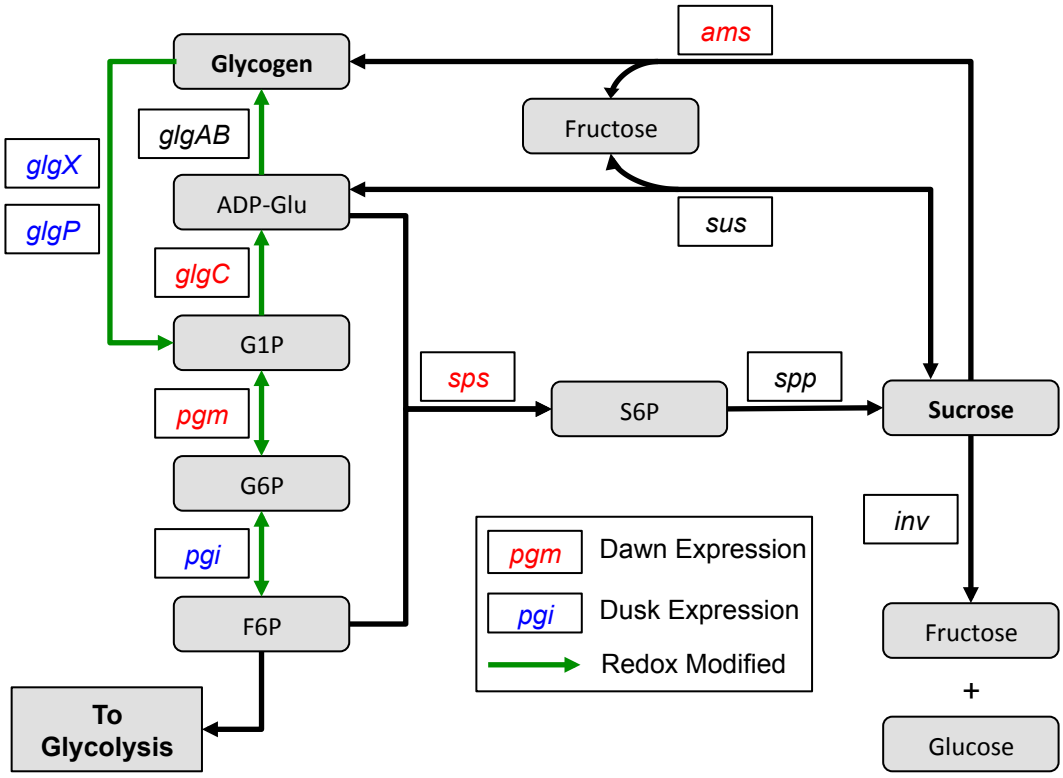

Figure 1-3. Metabolic Diagram of Glycogen and Sucrose Metabolism. This figure shows the interconnections between glycolysis, glycogen metabolism, and sucrose metabolism. Data about the peak expression time of circadian genes is indicated using data collected from *Synechococcus elongatus* PCC7942 (101). Genes colored in red peak in expression in the subjective morning, genes colored in blue peak in expression in the subjective evening, and genes colored in black have no detectable circadian rhythm in *S. elongatus*. Reactions where the respective enzyme had a detectable light-dark dependent redox modification in *Synechocystis sp.* PCC6803 (38) are colored green. The high degree of circadian controlled temporal segregation of anabolic and catabolic genes is evident, as well as the large numbers of redox modified enzymes participating in glycogen biosynthesis and degradation. Abbreviations are defined in the text.

For some time it has been known that glycogen accumulation and degradation in cyanobacteria occurs during day and night periods respectively, making glycogen metabolism a cyclic diurnal process [86, 95, 97-99]. Glycogen is also indispensible for diurnal viability as inactivation of *glgA* and *glgC*, blocking glycogen accumulation, and inactivation of *glgP*, blocking glycogen degradation, results in cells with severely attenuated viability under diurnal cycles [81, 96] (Rubin, et al. unpublished data). Thus, cyanobacterial cells do not simply go dormant when they enter the dark, but instead use stored carbon to drive metabolic processes critical for diurnal survival.

1.2.1.2 Regulatory Aspects

Control over glycogen content has both circadian and redox regulated components. It has recently been shown in *Synechococcus elongatus* PCC7942 that glycogen content continues to oscillate with a 24 h rhythm even when cells are held under constant light conditions [86, 100]. Transcriptional studies in diverse cyanobacteria have detected circadian patterns of gene expression for all glycogen metabolic genes [98, 101, 102]. Additionally, the anabolic and catabolic genes exhibit expression patterns that match their peak activity during glycogen accumulation and catabolism respectively. Experiments using *S. elongatus* cells lacking a functional circadian clock show that glycogen oscillations under constant light are

abolished when the clock is inactivated, however under diurnal conditions the glycogen accumulation and degradation cycle continues even in the absence of a functional clock [86]. The incomplete nature of circadian control is likely due to the fact that the glycogen metabolic enzymes are also subject to both redox and allosteric control mechanisms [94], which are in turn driven by diurnal cycles. Cysteine residues on GlgC in particular are substrates for thioredoxin dependent redox modification [34, 103] (**Figure 1-3**). In a reduced state GlgC increases in activity, while in an oxidized state enzymatic activity is significantly attenuated [34]. This regulatory activity is consistent with the expected pattern of glycogen synthesis and degradation following reduced and oxidized cellular states during light and dark periods respectively. Proteomic studies have also identified that the enzymes GlgA and GlgP are subject to light dependent cycles of thiol oxidation and reduction [38-40] (**Figure 1-3**). However, experiments have failed to detect redox regulation related to these residues in GlgA [34], and it is still unclear how redox modifications affect GlgA and GlgP enzymatic activity. Given the available data it is clear that glycogen regulation is governed by a complex interaction of circadian, redox, and allosteric signals that promote accumulation during the day and degradation during the night. Also, the ability of circadian, redox, and allosteric signals to influence glycogen metabolism changes over a 24 h diurnal cycle. Thus, future metabolic engineering strategies should not only

consider the importance of glycogen as a photosynthetic carbon sink, but also the current state of its control network over a 24 h period.

1.2.1.3 Connection of Glycogen to Sucrose Metabolism

In addition to its role as an energy storage polymer, glycogen has a strong metabolic connection to sucrose (**Figure 1-3**). Sucrose has classically been considered a compatible solute during osmotic stress in cyanobacteria, which has been reviewed extensively [78, 104]. However, recent work has shown that glycogen and sucrose likely play key roles in modulating photosynthetic output, and functioning as reductant sinks [71, 78]. The idea of a reductant sink is particularly important in cyanobacteria (**Figure 1-2B**), as they need mechanisms to buffer the redox state of the cell as light intensity changes over a normal diurnal cycle, as well as during periods of nutrient and oxidative stress.

Sucrose biosynthesis occurs through the sequential activity of sucrose-phosphate synthase (*sps*), which links ADP/UDP-glucose with fructose-6-phosphate to form sucrose-6-phosphate (S6P), and sucrose-phosphate phosphatase (*spp*), which dephosphorylates sucrose-6-phosphate to sucrose [104, 105] (**Figure 1-3**). Sucrose degradation occurs through one of three pathways depending on the cyanobacterial species: (1) Reversible degradation to ADP/UDP-glucose and fructose by sucrose synthase (*sus*); (2) Hydrolysis by invertase (*inv*) to form glucose and fructose; (3) Hydrolysis by

amylosucrase (*ams*) resulting in one fructose moiety and the linkage of the glucose moiety to an α-1-4-glycan (such as glycogen) [78] (**Figure 1-3**). Thus, sucrose inherently shares metabolic intermediates with glycogen, and there is evidence that direct interconversion between sucrose and glycogen can take place when degraded by the *sus* and *ams* routes [106, 107]. It has also been shown that the sucrose content in cyanobacteria increases when glycogen biosynthesis is inactivated [71, 108, 109]. Circadian studies in *S. elongatus* have detected a rhythm in both *sps* and *ams* expression that peaks at dawn [101]. This is consistent with an increase of sucrose and flux to glycogen in the morning in WT *S. elongatus* strains [86]. However, unlike glycogen metabolic enzymes, no studies have been able to detect redox-mediated regulation in the enzymes of sucrose metabolism. The primary connection between sucrose and redox state may come from sucrose acting as an electron valve during photosynthesis. Experiments using ^{13}C labeled bicarbonate indicate that glucose-6-phosphate and sucrose are the primary products of downstream photosynthetic output, and that labeled compounds were rapidly turned over [110]. Thus, while cyanobacteria do not accumulate large amounts of sucrose under normal growth conditions, flux through the pathway is high, as it represents the first destination of fixed carbon. Use of sucrose metabolism as a valve for photosynthetic activity was well illustrated by Ducat et al. [71]. By allowing sucrose to leave the cell through expression of a transporter (CscB), the investigators saw an increase in total fixed carbon,

photosynthetic oxygen evolution, and chlorophyll content relative to WT strains [71]. Thus movement of fixed carbon through sucrose may serve to alleviate photoinhibition by creating a larger electron sink. This also further illustrates the control and importance electron/redox balance has over photosynthetic systems. Interestingly, blocking glycogen biosynthesis in strains that export sucrose, increased total sucrose production. However, this carbon redirection resulted in severely attenuated growth rates under the tested conditions. Thus, even an expanded sucrose sink for electrons may not be sufficient when the glycogen sink is unavailable.

1.2.1.4 Function of Glycogen as an Electron and Carbon Sink

Although glycogen and sucrose are metabolically linked, and sucrose metabolism can play an important role as a valve for photosynthetic output, it is likely that glycogen serves as the primary carbon and electron sink in cyanobacterial metabolism. As redox conditions change over time, glycogen can act to store or release carbon as needed to balance reductant production. Some of the earlier work on glycogen metabolism identified that blocking glycogen production significantly attenuates photosynthetic activity and biomass production at high light intensities [111]. The negative effects on growth and productivity are consistent with electrons getting “backed up” in photosynthesis when they have no sink to flow to, resulting in a redox imbalance and the generation of ROS that damage the photosystems [112,

113]. The function of glycogen as a redox balancing electron sink is further supported by experiments showing that negative effects on growth and photosynthetic efficiency are alleviated when an alternative electron sink is synthetically provided [82]. Additionally, glycogen plays an important role in the response to macronutrient deprivation, specifically nitrogen limitation [79, 81, 114]. Nitrogen assimilation is a major reductant consuming process during photosynthetic growth [77], and during nitrogen deprivation there needs to be an alternative sink for electrons and carbon to avoid the generation of ROS. Glycogen provides a way to store electrons and carbon during the period of nutrient stress that can be utilized at a later time, and large amounts of glycogen accumulate under during nitrogen deprivation [80, 89]. Conversely, mutants that cannot accumulate glycogen do not exhibit a normal nitrogen deprivation response, and secrete large amounts of pyruvate and tricarboxylic acid (TCA) cycle intermediates [68, 79, 81, 114]. This is consistent with photosynthetic output being re-directed to organic acids when the glycogen sink is blocked. However, quantification of organic acids under these conditions reveals that they account for significantly less carbon than what would normally flow into glycogen [114]. Thus when glycogen biosynthesis is unavailable, cells must adopt sub-optimal routes to relieve carbon and electron buildup.

The buffering of cellular redox state through glycogen biosynthesis and degradation may be an important mechanism to allow the proper regulation of

cellular responses, and cellular redox state has been in fact shown to directly affect the metabolic enzymes and transcriptional regulators of nitrogen metabolism [35, 115]. However, glycogen accumulation is a general response observed during a number of nutrient limitation and stress conditions, and blocking glycogen biosynthesis also attenuates the stress responses to sulfur and phosphate deprivation [79, 116]. This suggests that glycogen serves as a general-purpose carbon and reductant buffer across stress conditions, and that this buffering capacity is important for proper metabolic regulatory control.

1.2.1.5 Summary

Overall, glycogen is a critical carbon and electron sink in cyanobacteria, and its regulation has broad effects on the movement of carbon through central metabolism. Additionally the essentiality of this pathway for diurnal growth indicates that active metabolism in the dark is critical for diurnal survival. New work on light dependent and circadian regulation of glycogen, as well as its importance for nutrient stress responses, highlights the fact that cyanobacteria likely strive to maintain some degree of redox stability through accumulation and degradation of this polymer (Diamond et al. unpublished data). The high degree redox modification detected on glycogen biosynthetic enzymes, indicates how the biosynthesis of this metabolite is directly responsive to cellular redox state. In turn the function of glycogen for cellular redox balance under dynamic conditions, and the negative regulatory impacts

of blocking its biosynthesis, highlight the influence of redox state on global metabolic regulation in cyanobacterial cells.

1.2.2 Glycolysis, the Oxidative Pentose Phosphate Pathway, and the Calvin Cycle

1.2.2.1 Pathway Structure and Biochemistry

In cyanobacteria, glycolysis, the oxidative pentose phosphate pathway (OPPP), and the Calvin Cycle constitute an interconnected superpathway of primary carbon metabolism that share a number of metabolic reactions (**Figure 1-4**). In contrast to heterotropic organisms where glycolysis serves as the first energy and reductant producing step of metabolism, glycolytic reactions in cyanobacteria serve to bridge and regulate the reactions of the OPPP and Calvin Cycle [117-119]. The evolutionary dependence on photosynthesis has driven cyanobacteria to instead use the Calvin Cycle and its oxidative equivalent, the OPPP, as the primary pathways for anabolic and catabolic carbon metabolism respectively [118-120]. Cyanobacteria oscillate between using photosynthesis and the Calvin cycle for reductant (NADPH), ATP, and fixed carbon generation during the day, and the OPPP as the primary method of carbon degradation and reductant (NADPH) generation at night [22, 118] (**Figure 1-4**). The importance of the OPPP for night metabolism is highlighted by the fact that the OPPP genes *zwf*, *gap1*, and

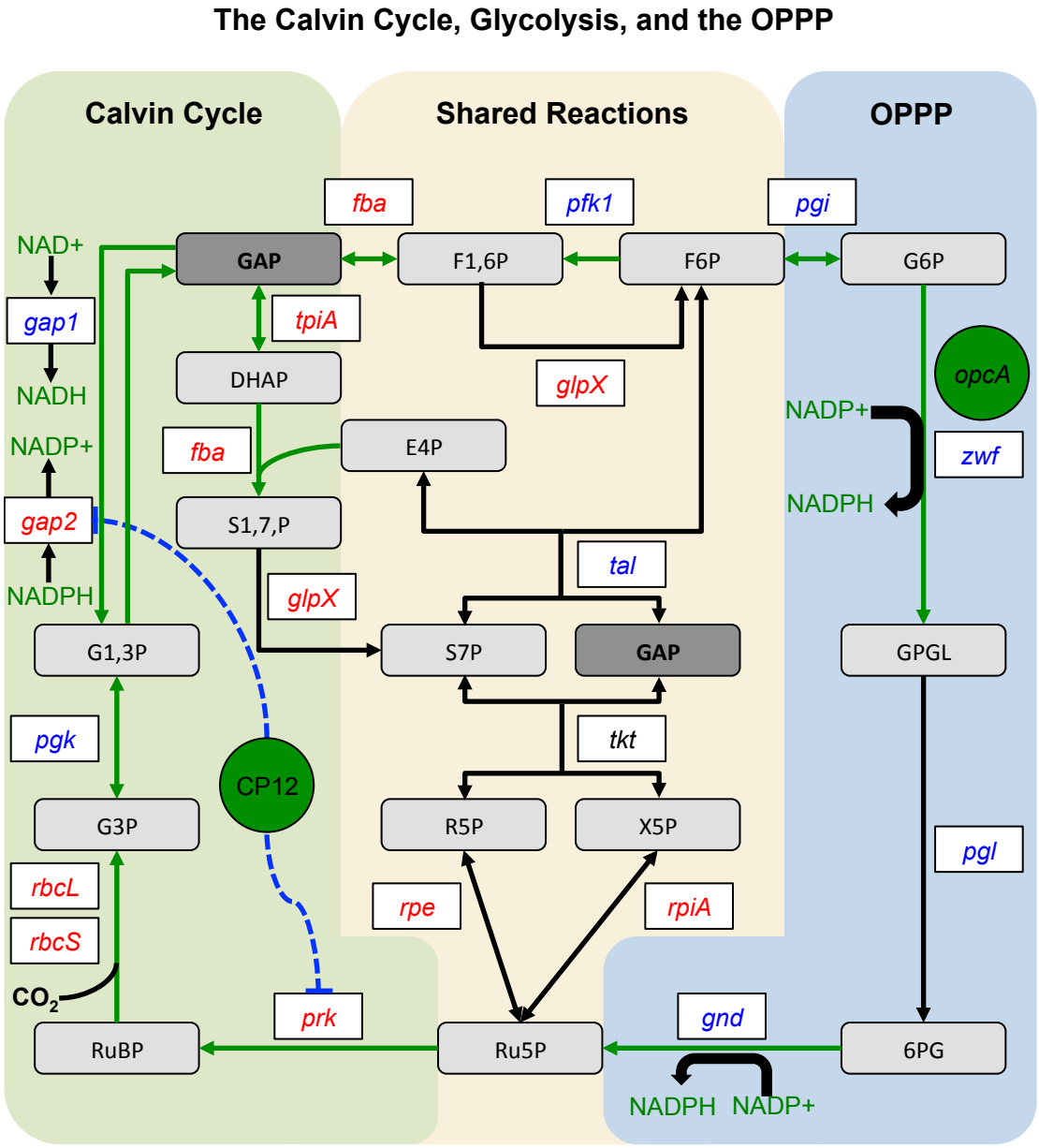

Figure 1-4. Metabolic Diagram of the Glycolysis, Calvin Cycle, OPPP Superpathway. This figure illustrates the significant overlap between the metabolic reactions of glycolysis, the Calvin Cycle, and the OPPP in cyanobacteria. Circadian control over gene expression and redox-regulated enzymes are indicated and determined using the same colors and data sources as in **Figure 1-3** (101, 38). Cyclic carbon flow switches back and forth between the Calvin Cycle and the OPPP during day and night periods respectively. The inhibitory activity of CP12 (green) on *gap2* and *prk* at night is indicated by the blue dotted line. The OpcA protein is indicated in green and promotes activation of Zwf, and in turn the OPPP route.

gnd are dispensable for growth in constant light, but their inactivation causes attenuated growth under light-dark cycles [121-123] (Rubin, et al. unpublished data). The oscillatory flux between the Calvin Cycle and the OPPP that follows diurnal cycles and photosynthesis, already hints at the fact that these pathways are heavily regulated by circadian and redox driven components.

1.2.2.2 Regulatory Aspects

The metabolic enzymes in the aforementioned pathways are highly conserved across almost all cyanobacteria [124], and a number of regulatory nodes are of particular note. The Calvin Cycle is strongly regulated at the reaction catalyzed by, phosphoribulokinase (Prk), which serves to regenerate ribulose-1,5-bisphosphate (RuBP) [125, 126] (**Figure 1-4**). Alternatively the OPPP is strongly regulated by its rate limiting enzyme Zwf, which irreversibly converts G6P into 6-phospho-D-glucono-1,5-lactone (6PGL) resulting in the generation of NADPH [127] (**Figure 1-4**). Also, there is a convergence of Calvin Cycle and OPPP regulation at the reaction that interconverts 1,3-bisphosphoglycerate (G1,3P) and glyceraldehyde-3-phosphate (GAP) (**Figure 1-4**). The Calvin Cycle (anabolic) reaction is catalyzed by glyceraldehyde-3-phosphate dehydrogenase 2 (Gap2), which can use both NADP(H) and NAD(H) as co-factors, while the OPPP (catabolic) reaction is catalyzed by the isozyme glyceraldehyde-3-phosphate dehydrogenase 1 (Gap1) that can only use NAD(H) as a cofactor [128] (**Figure 1-4**). This is

directly in line with the changing availability of these reductant species under light and dark conditions, as the NADPH/NADH ratio is considerably higher during active photosynthesis [36, 129]. Thus enzyme availability and reductant substrate specificity contribute to metabolic movement that favors either OPPP or Calvin Cycle activity.

High amplitude circadian rhythms have been detected in the transcripts for all of the genes that encode enzymes at regulatory nodes, as well as most genes in the Calvin Cycle, OPPP, and glycolysis [22, 101, 130]. Circadian oscillation of gene expression shows strong temporal segregation based on the pathway in which a gene participates. Thus, genes that favor Calvin Cycle activity peak in expression in the morning, while those that favor OPPP have their peak expression in the evening [22, 101, 130]. Interestingly, reactions catalyzed by two or more isozymes, such as between G1,3P and GAP, show out of phase circadian regulation that causes opposite directions of metabolic flux to be favored at opposite times. Consistent with their functions in photosynthesis and carbon catabolism, *gap2* peaks in expression in the morning while *gap1* peaks in expression in the evening; thus, circadian control can serve to drive the directionality of a metabolic reaction over a 24-h day [130]. Work on the circadian clock in *S. elongatus* has identified that the genes *gap1, zwf,* and *opcA* are direct targets of the transcription factor RpaA, which acts as the primary transcriptional output from the clock mechanism [131]. Although OpcA is not a metabolic enzyme it is required for full

activation of Zwf [132]. Also, inactivation of *rpaA* results in a strong global down regulation of *zwf*, *opcA, gap1, tal,* and *gnd* suggesting that it is an important activator of these genes and the OPPP in general [131]. Indeed, *rpaA* inactivation confers a similar diurnal growth sensitivity phenotype to the inactivation of *zwf*, *gap1*, or *gnd* [121, 123, 133].

Metabolic studies in *S. elongatus* seem to indicate that circadian regulation is particularly important for activating or repressing the OPPP, as its metabolites accumulate in the morning in circadian mutants where RpaA is de-repressed, and the OPPP fails to activate at night when RpaA is inactivated [86] (Diamond, et al. Ch. 3). It has also been observed that circadian control functions synergistically with environmental light-dark cycling in the expression of OPPP genes. When cyanobacteria are exposed to true light-dark cycles the expression of OPPP genes are significantly enhanced during their expected time of peak expression [134, 135].

Redox control mechanisms also have a role in modulating the fluctuation between Calvin Cycle and OPPP activity by the action of the small peptide CP12 [36, 37, 136]. CP12 responds to the redox state of the cell by detecting the NADPH/NADH ratio as well as through direct redox modification by thioredoxin proteins [36, 137]. During the light period when the NADPH/NADH ratio is high, and the cystines on CP12 are reduced, the protein exists in a disordered state (**Figure 1-4**). However when the NADPH/NADH ratio drops in the dark CP12 becomes ordered and binds and

sequesters Prk and Gap2 in a complex that inhibits their activity, causing flux to re-direct towards the OPPP [138, 139]. It has also been shown that Prk is directly redox regulated in a manner consistent with its role during the light period [125, 126] (**Figure 1-4**). A number of the other overlap points between the OPPP and Calvin Cycle also show direct redox (or light dependent) regulation including Fba (fructose-1,6,-bisphosphate aldolase) [140], Pgk (phosphoglycerate kinase) [40, 141], and Gap1 [40, 141]. With respect to the OPPP both Zwf and Gnd exhibit light dependent redox changes, and Zwf has been biochemically confirmed to respond to changes in redox state [38-40]. Thus, it is clear that in addition to the strong circadian regulation, most of the enzymes in these pathways are subject to direct redox modification. However, it is still unclear how redox modifications affect the enzymatic activity of most of these enzymes.

1.2.2.3 Engineering Perspective

While it is clear there is an extensive array of circadian, redox, and inherently light dependent mechanisms controlling the carbon flux through these pathways, none of these mechanisms have been directly exploited as engineering targets. However there is precedent for the modification of CP12, as the suppression of CP12 in tobacco using antisense RNA causes a re-direction of flux resulting in a decrease in stored carbohydrates with a corresponding increase in amines and organic acids [142]. Also,

cyanophages have been shown to express isoforms of CP12 and OPPP enzymes that result in increased flux to the OPPP resulting in increased NADPH and nucleotide precursors following infection [143]. Additionally, work on circadian clock mutants in *S. elongatus* shows that flux towards or away from the OPPP can be directly modulated by mutation of both the central oscillator or the output response regulator RpaA [86]. Thus, the modulation of these pathways using circadian or redox mediated strategies holds significant promise for metabolic engineering efforts, and specific circadian and redox regulatory aspects should always be considered during the evaluation of any engineering strategy.

1.2.2.4 Summary

With respect to future work on the regulation of primary carbon metabolism there is clearly a need to better understand the importance and breadth of individual redox modifications in the context of diurnal growth. However, one of the key observations from the aggregated data on Calvin Cycle, OPPP, and glycolytic control is that, unlike glycogen biosynthesis, transcription driven by the circadian clock seems to play a very influential role in OPPP activation, and this activation is critical for survival under diurnal conditions. Additionally, the OPPP likely acts as the catalytic “arm” of glycogen degradation that helps the cell maintain reductant balance, as its activity is clearly of critical importance under changing light conditions. Overall,

reductant production and cellular reductant balance is important for diurnal survival in cyanobacteria, however it is still not completely clear what exact purposes reductant production serves at night.

1.2.3 The Tricarboxylic Acid Cycle and Connections to Nitrogen Metabolism

1.2.3.1 Pathway Structure and Biochemistry (And Some History)

The tricarboxylic acid (TCA) cycle is one of the best metabolic examples of the unique carbon metabolism that occurs in cyanobacteria, as well as the extensive work that still needs to be done to fully understand how carbon is partitioned and controlled in these organisms. Classically this cycle completes the full oxidation of pyruvate, and thus serves as the primary source of reducing power generated in heterotrophic cells. Due to the ubiquity of the TCA cycle reactions across almost all organisms, and it's structure as a complete cycle, there has been a somewhat dogmatic expectation that the TCA cycle should be a significant source of reducing power in cells, and that its cyclic nature should be maintained. However, for more than four decades the failure to detect the enzymatic activity of 2-oxoglutarate dehydrogenase (OGDH), which forms part of the link between 2-oxoglutarate (2-OG) and succinate (**Figure 1-5**), led to it being generally accepted that cyanobacteria have an

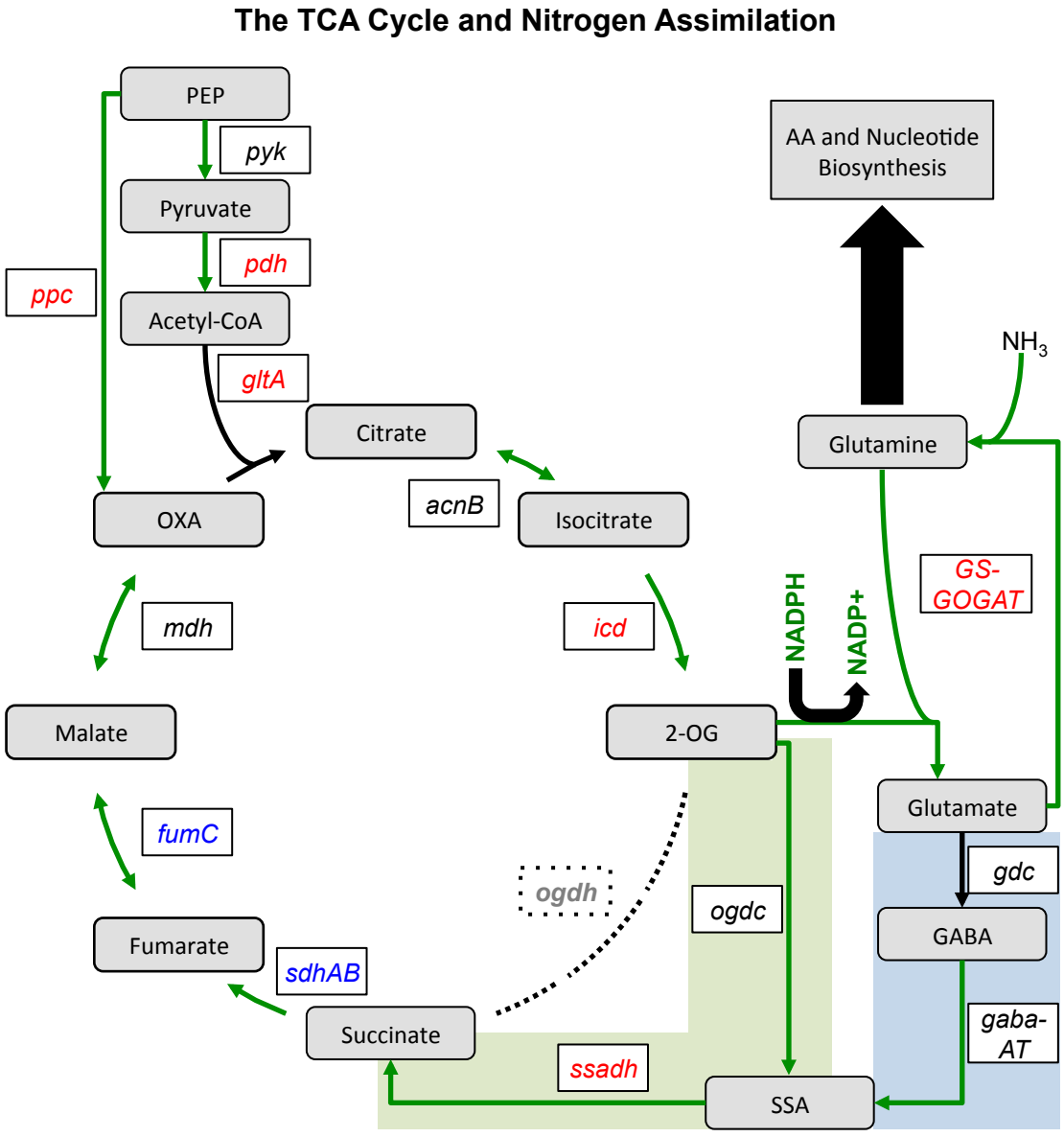

Figure 1-5. Metabolic Diagram of the TCA cycle and Nitrogen Assimilation Pathways. This figure illustrates the core TCA cycle as well as the SSA (green) and γ-aminobutyric acid (blue) bypasses from 2-OG to succinate. The glyoxylate shunt is not pictured, as it is only present in nitrogen-fixing cyanobacteria. The OGDH enzymatic step missing in cyanobacteria is indicated by a dotted black line and the enzyme is labeled in grey. Circadian control over gene expression and redox-regulated enzymes are indicated, and were determined, using the same colors and data sources as in **Figure 1-3** (38, 101). The large number of redox-regulated reactions highlight the importance of TCA cycle responsiveness to cellular redox sate.

incomplete TCA cycle [144]. This drove a number of hypotheses suggesting that the incomplete TCA cycle in cyanobacteria was responsible for specific phenotypic traits, such as obligate photoautotrophy in some strains [145]. However recent work has established that a number of bypasses are present, depending on cyanobacterial species, which generate succinate from 2-OG to complete the cycle (**Figure 1-5**). These bypasses include a functional glyoxylate shunt [146], a bypass through the γ-aminobutyric acid shunt [147], and a novel bypass where 2-OG is first converted to succinic semialdehyde (SSA) by 2-oxoglutarate decarboxylase (OGDC) and subsequently to succinate by succinic semialdehyde dehydrogenase (SSADH)[148]. The SSA bypass is by far the most conserved in a wide number of cyanobacteria with the exception of marine *Synechococcus* and *Prochlorococcus* species [124]. While finding novel closure mechanisms in a core cycle of metabolism is interesting in its own right, it still does not directly support the value of cycle closure for cyanobacterial fitness. Indeed, metabolic modeling conducted on *Synechocystis* PCC6803 suggests that flux through the TCA cycle is non-cyclic during photoautotrophic growth [118]. Subsequent studies in *Synechocystis* PCC6803 using ^{13}C isotopic tracing also directly show that flux through the proposed bypasses, as well as through succinate and fumarate, is extremely small under both photoautotrophic and heterotrophic conditions [120, 149]. In fact, these flux studies show that carbon actually primarily cycles within the OPPP or the Calvin Cycle depending on the availability of

light, not through the TCA cycle [120, 149]. This is further corroborated by a recent full genome transposon mutagenesis study in *S. elongatus* that determined the genes coding for the TCA cycle enzymes SSADH, succinate dehydrogenase (SdhB*)*, and fumarate hydratase (FumC*)*, were all dispensable for survival under photoautotrophic growth conditions, and conferred no measureable growth defect when inactivated (Rubin, et al. unpublished data). Nonetheless, there is conflicting evidence on the importance of succinate production from 2-OG across the cyanobacterial lineage, as the original work that identified the SSA bypass showed that the inactivation of *ogdc* in *Synechococcus sp.* PCC7002 causes a 30% growth reduction under photoautotrophic conditions [148]. Additionally, it is known that succinate can be an important contributor of electrons to the electron transport chain through the activities of SdhA and SdhB [150, 151]. Thus, while current evidence is consistent with the hypothesis that cyclic flux through the TCA cycle does not play a major role under standard photoautotrophic and heterotrophic conditions in most cyanobacteria, these reactions may serve a more important role under specific growth or stress conditions. This is consistent with results from a recent study on nitrogen deprivation in *Synechocystis sp.* PCC6803 that showed the abundance of succinate and fumarate significantly increase when cells were deprived of nitrogen [152]. However, the significance of these metabolic changes and the

importance of cyclic TCA flux under diverse conditions have yet to be determined.

In contrast to the uncertainty surrounding the second half of the TCA cycle, the first three steps of the cycle leading from oxaloacetate to 2-OG are highly conserved and essential in all cyanobacterial species [124] (Rubin, et al. unpublished data). In cyanobacteria 2-OG is the primary carbon precursor for glutamate during nitrogen assimilation, as well as an essential regulatory molecule controlling nitrogen assimilation (153). The action of the glutamine synthetase – glutamine synthase (GS-GOGAT) complex uses reducing power from photosynthesis to incorporate NH_4 and 2-OG into the amino acids glutamate and glutamine [153]. Glutamine is subsequently used as the primary nitrogen donor in a wide variety of metabolic reactions in the cell (**Figure 1-5**). The fact that these reactions sit at the interface between carbon and nitrogen metabolism makes the TCA cycle a critical regulatory point for Carbon/Nitrogen (C/N) balance in cyanobacteria [154]. Cyanobacteria strictly regulate their C/N balance due to the fact that carbon metabolism and nitrogen metabolism are the primary reductant generating and consuming systems, respectively, in cyanobacteria, and their balance is critical for preventing ROS generation or reductant deficits. A significant amount of work has been performed on the transcriptional mechanisms underlying C/N balance in cyanobacteria; thus, we will not cover the intricacies in this review. For an extensive review of C/N balance control mechanisms see Flores et al.

[12] However, more recent work indicates that C/N balance is important for modulating cellular redox state, and also that cellular redox state directly feeds back into mechanisms controlling C/N balance (35, 77). Thus we will cover some of the recent work on the TCA cycle/Nitrogen metabolism interface that specifically implicates redox-regulated components and their downstream impacts on cellular carbon flux.

Overall, the basic structure and functionality of the TCA cycle in cyanobacteria is still under some debate. The more recent work on TCA metabolism seems to suggest that the TCA reactions primarily serve as an interface between carbon and nitrogen metabolism, and as a source of carbon skeletons for downstream metabolic reactions. Thus, while a number of metabolic bypasses have been proposed for the cycle in cyanobacteria, and found, it seems that cyclic flux does not need to occur through the TCA cycle under normal growth conditions. However, the TCA cycle does play a critical role in the balance of carbon and nitrogen under normal growth conditions, which is important for cellular redox state regulation, and critical for viability.

1.2.3.2 Regulatory Aspects

Studies of circadian gene expression do not find a high degree of circadian control over TCA cycle genes. Within the limited studies that have been conducted, no TCA cycle genes show a circadian oscillation in

Synechocystis PCC6803 [130], however a number do show circadian regulation in *S. elongatus* [101] (**Figure 1-5**). In *S. elongatus* genes that function in the first half of the cycle and nitrogen assimilation show peak expression in the morning, while genes involved in succinate metabolism have a peak expression in the evening [101]. This is consistent with the first half of the TCA cycle acting as an important source of carbon skeletons during biosynthetic metabolism during the day period. However, the circadian oscillations detected in genes that do oscillate generally have low amplitude oscillations [101, 131]. This is in contrast to the genes of the Calvin cycle and the OPPP, which oscillate between extremely high and low levels of transcript abundance through a 24-h period [101] The lack of strong circadian control suggests that it is less important for the TCA cycle to preform periodic metabolic activities at specific times of the day, and more important for the reactions of the TCA cycle to be able to respond to unpredictable changes in the environment as needed.

The redox regulatory elements of the TCA cycle are far more pervasive than the circadian control elements. Two global redox proteomics experiments conducted in *Synechocystis* PCC6803 and *Synechococcus sp.* PCC7002 detected redox sensitive cysteine modifications across most TCA cycle enzymes as well as the enzymes of the GS-GOGAT complex [38, 39] (**Figure 1-5**). A number of studies have also specifically shown that isocitrate dehydrogenase (*icd*) and GS-GOGAT are specifically regulated by NADPH

content and light [155-157]. Due to the fact that nitrogen assimilation represents a major reductant sink for cyanobacteria, it is unsurprising that we find a significant amount of redox related control at the interface between carbon and nitrogen metabolism. In fact, work in *Synechocystis* PCC6803 has shown that in response to high light, cells require a coordinated response from both carbon and nitrogen regulatory pathways to properly acclimate [158]. Additionally, recent work in *S. elongatus* has further confirmed the importance of nitrogen assimilation as an electron sink, and that the movement of carbon from 2-OG to glutamine and glutamate has light and redox regulated components [77]. One particularly interesting, yet relatively unexplored, observation in *S. elongatus* is the strong activation of glutamine synthetase inactivating factor (IF7) when cells transition into the dark [135]. IF7 could potentially act to conserve reducing power by inhibiting nitrogen assimilation during the night. However, IF7 is not a significant circadian target and likely functions through complex regulatory networks that have light and subsequently redox regulated components.

1.2.3.3 Summary

The more limited understanding of the TCA cycle relative to other carbon metabolic pathways in cyanobacteria makes it an excellent target for further research. The cycle is a critical hub for control of C/N balance, and in turn likely plays many unexplored roles in redox homeostasis. Also, given that

the circadian control of the TCA cycle is not very pervasive, it is likely that it responds more strongly to acute environmental changes rather than the predictable changes of diurnal growth. Future work on the TCA cycle should consider its functionality under a wide range of growth and stress conditions, as there is still not conclusive data on the importance of the second half of the cycle for organism fitness.

1.3 Systems Level Analysis of Diurnal Growth

The centrality of photosynthesis and circadian timing in cyanobacterial metabolism results in metabolic networks and control mechanisms that are vastly different in comparison to well-studied heterotrophic bacteria. Thus, the response of cyanobacterial metabolism to any external or internal perturbation will be highly dependent the availability of light and the perceived circadian time within the organism. Recent metabolic engineering efforts have found that rational design approaches adapted from methods that were successful in heterotrophic organisms can often fail to produce desired outcomes in cyanobacterial strains [68]. However, engineering strategies that have accounted for the photoautotrophic differences in reductant co-factor species and cellular redox state have been more successful [62]. This is consistent with cyanobacteria having unique redox regulatory constraints on metabolism, resulting in responses to perturbations that cannot be predicted using a heterotrophic model. Thus a systems biology effort will be critical to

understanding how cyanobacterial metabolism will manifest itself under dynamic conditions of changing redox state and circadian timing at a systems wide level.

While a large number of high throughput transcriptomics, proteomics, and metabolomics studies have been conducted on cyanobacteria [159, 160], historical precedence and convenience has lead to the vast majority of studies being undertaken under a single light condition (either light or dark) and without consideration to circadian timing. Indeed, work on *S. elongatus*, the most well studied model for cyanobacterial circadian rhythms, has been primarily conducted using constant light because growth is more rapid in the light than in a light-dark cycle. Also, circadian measurements require constant light conditions to separate circadian influences from light driven responses. Thus, in the process of deconstructing the *S. elongatus* circadian clock there has been very little work done on how the clock affects metabolism and physiology of the organism in a natural diurnal cycle. Fortunately, in recent years there has been a renewed effort to conduct systems level studies with experimental designs that consider dynamic changes in light and time. Insights from these studies are beginning to dissect the interplay between circadian and light/redox driven control mechanisms. Additionally, the data from these analyses have been used to constrain cyanobacterial metabolic models that can take into account dynamic daily changes in circadian gene expression and light driven metabolic state (118).

Below we will detail the recent work performed on cyanobacterial transcriptomes and proteomes over true light-dark cycles. Subsequently, we will review the recent work on the systems characterization of protein redox modifications. Finally, we will look at the brief work performed on the how circadian clock interacts with true light-dark cycles. This will primarily be constrained to non-nitrogen fixing cyanobacteria because they are the most important strains for environmental carbon fixation as well as metabolic engineering.

1.3.1 Transcriptomics and Proteomics of Diurnal Growth

1.3.1.1 Transcript Abundance Over a Diurnal Period

The number of transcriptomics studies performed on cyanobacteria growing under diurnal conditions is limited. However, all studies that have been performed show that temporal segregation of carbon anabolic and catabolic gene expression, that follows light and dark periods respectively, is a consistent feature of cyanobacterial transcriptomes [22, 26, 135, 161, 162]. The data show that genes for the photosynthetic reaction centers, Calvin Cycle, CO_2 concentrating mechanism, and ATP synthase subunits are expressed in the morning hours and decrease through out the day period (**Figure 1-4**). Also, genes for nitrate uptake and amino acid biosynthesis generally show their maximum activity during the morning hours when ATP

and reducing power are the most abundant [124, 135] (**Figure 1-5**). Also, as mentioned before, genes for the OPPP and its supporting glycolytic reactions increase in expression in the late day period and peak near the beginning of the night. Also, all cyanobacterial transcriptomes show some degree of oscillation in the core circadian clock genes *kaiA, kaiB, kaiC*, and *rpaA* when they are present [26, 161, 162]. Finally, although we avoid discussion of nitrogen fixing species, it should be noted that transcriptomics performed over a diurnal period on *Cyanothece sp.* ATCC 51142 show very strong agreement with non-nitrogen fixing cyanobacteria in the peak expression times of most metabolic process [134, 163]. Thus, while diurnal gene expression may be slightly different among species, the general temporal pattern of expression for metabolic genes is conserved across the cyanobacterial phylum.

Although global metabolic gene expression patterns seem to be conserved among cyanobacteria, with anabolic genes peaking in the morning and catabolic genes peaking directly before entering the dark, there is a stark difference in how different species respond transcriptionally after entering a night period. Work on *S. elongatus* indicates that this species rapidly decreases its mRNA content when entering the dark [26] in an actively driven process of “nocturnal dormancy” [164]. This is in stark contrast to closely related *Prochlorococcus sp.*, which show increases in mRNA transcription, and the vast majority of their cell division during the dark period [22, 165]. The cyanobacterium *Synechocystis sp.* PCC6803 shows a response to darkness

that is between that of *S. elongatus* and *Prochlorococcus sp.*, where mRNA abundance does not increase but also does not steeply decline in the dark. Also, this species may increase total ribosomal RNA may occur over the dark period [162]. However, looking across the available datasets it does seem that a very small number of genes are consistently up-regulated across species when cells enter the dark, and even during actively driven “nocturnal dormancy” in *S. elongatus* there are a small subset of transcripts that show up-regulation 30 min to 1 h after entering a dark period [26, 135]. One gene that is strongly up regulated in both *S. elongatus* and *Synechocystis* PCC6803 after the dark transition is the small heat shock protein HspA [135, 162]. This protein is known to bind phycobilisomes and promote the integrity of the photosynthetic apparatus while conferring protection from oxidative stress [166-168]. Thus, one conserved function of dark driven *hspA* transcription may be to maintain photosystem integrity until the following light period. However, work in *S. elongatus* to characterize genes that are essential for diurnal growth has found that *hspA*, and a number of other dark activated genes, can be inactivated with no resulting fitness defect under diurnal conditions (Rubin, et al. unpublished data). Thus the specific activation of transcriptional responses after a dark transition, as well as the behavior of mRNA in the dark exhibited by diverse cyanobacteria, is still a poorly understood area of cyanobacterial biology.

1.3.1.2 Protein Abundance Over a Diurnal Period

Unlike the robust changes observed in many mRNA transcripts under diurnal growth conditions, cyanobacterial proteomes generally do not display large changes in protein abundance, and the vast majority of proteins display little to no change over a diurnal cycle [22, 169, 170]. Surprisingly, even for genes with very large changes in transcript abundance over a 24 h period, the protein abundance is often relatively constant or has even found to be in the opposite phase of transcript expression [22]. Proteins that show strong oscillations in abundance seem to be more of an exception than the standard in cyanobacterial cells. In line with these general observations, the rapid decrease in mRNA observed in *S. elongatus* cells after entering a dark period is not accompanied by a corresponding decrease in the associated proteins [169]. In fact, almost all proteins detected in the study by Guerreiro et al., where the proteome of *S.* elongatus was surveyed over a 48-h diurnal period, stayed at a constant level through both dark periods [169]. The fact that protein abundance is not strongly correlated with transcript oscillation is suggestive that posttranslational mechanisms such as redox modifications or the allosteric binding of metabolites modulates the activity of many proteins, particularly in the dark when transcription is less active. However, the abundance of proteins does not directly indicate their frequency of turnover, and studies have shown that there can be a significant level of protein turnover in cyanobacteria [171]. Thus, it is possible that protein turnover is in

phase with circadian transcriptional rhythms, which subsequently affects the relative levels of posttranslationally modified and unmodified protein species. Overall, the general stability of protein levels in cyanobacteria, specifically over the night period in some species, is highly suggestive that posttranslational regulatory mechanisms play a major role in the very dynamic metabolism observed in cyanobacteria under diurnal conditions.

1.3.1.3 Global Redox Modification of Proteins

Protein redox, or cysteine thiol, modifications have been well studied in plant chloroplasts [172], and in this review we have extensively outlined their importance in the control of cyanobacterial carbon metabolism. Additionally, it is clear that under diurnal conditions the redox state of the cell is closely coupled to light availability [36, 173]. Cyanobacteria contain a large array of proteins and small molecules such as thioredoxins, ferredoxins, peroxiredoxins, and glutathione, which can all directly modify protein thiols [31, 40, 103, 141, 174]. Early studies using various techniques of electrophoretic separation were able to identify that cyanobacterial proteomes contained a number of proteins that acquired redox modifications [103]. However, due to the techniques used, the throughput of these studies was small relative to the size of the proteomes examined. Two recent studies conducted in *Synechocystis* PCC6803 and *Synechococcus* PCC7002, using improved methods, have shown that shifts from light to darkness causes

redox modifications on 1060 and 350 proteins respectively [38, 39]. A separate study in *Synechocystis* PCC6803 was able to identify that 383 proteins specifically receive redox modifications through a possible interaction with glutathione [40]. In addition to the redox targets already mentioned in carbon metabolism, these studies found that proteins involved in amino acid biosynthesis were highly enriched in redox modifications [38-40]. It is not surprising that amino acid biosynthetic proteins represent a major target for global redox modifications, as this biosynthetic activity requires a large amount cellular reducing power [77], and must maintain a strict balance with carbon metabolism. These data are also consistent with the theory that maintaining C/N balance is important for redox control. A separate, and rather unexpected, finding from this work was a number of redox modifications on the core proteins of fatty acid metabolism. It had already been observed that fatty acid turnover in cyanobacteria is stimulated by high light intensity [76]. Also, one of the redox modified protein targets, FabH, is the rate limiting step in fatty acid biosynthesis [175]. The implication of fatty acid biosynthesis is particularly intriguing as these pathways are of strong interest for biotechnology, and very little is known about their regulation in cyanobacteria. Thus, although work on redox regulation of cyanobacterial metabolism is at the early stages, it is clear that this regulatory mechanism is highly pervasive among metabolic enzymes, and is directly responsive to diurnal cycles.

1.3.2 Circadian Mechanisms of Global Transcriptional Control

While significant advances have been made in our understanding of the maintenance and transference of temporal information in S. elongatus, the physiological and metabolic relevance of a functional clock has been largely unexplored. It is clear that control of the clock over cellular processes is extensive across the cyanobacterial lineage, but which processes the clock influences and to what degree are still open questions. Here, we briefly cover basic circadian clock functionality, as well as the recent work that examines the direct targets of clock output as well as its function in a diurnal context. Due to the fact that the vast majority of studies on circadian clock biochemistry and genetics have been conducted in the cyanobacterium *S. elongatus*, this section will primarily contain data collected from this organism, with other references where available.

1.3.2.1 Basic Circadian Clock Components

The cyanobacterial circadian clock has been extensively reviewed [28], so we will not cover the functionality in detail. However we will briefly summarize the key components to give context to recent work. The circadian clock in cyanobacteria is composed of two major components: A central oscillator that keeps the time, and an output pathway that relays timing information to gene expression. Three genes, *kaiA*, *kaiB*, and *kaiC*, encode the proteins of the central circadian oscillator, and inactivation of any of them

abolishes the clock [176]. KaiC displays a daily rhythm of phosphorylation at residues Ser431 and Thr432, and the oscillation of KaiC phosphorylation is the fundamental timekeeping mechanism in cyanobacteria [177] (**Figure 1-6A**). KaiA stimulates KaiC autophosphorylation and KaiB opposes KaiA's activity [178]. Temporal information from the cyanobacterial oscillator is broadcast to downstream genes via the histidine protein kinase SasA, whose autophosphorylation is stimulated by interaction with KaiC [179, 180]. SasA then transfers the phosphoryl group to RpaA, a response regulator with a DNA binding domain, which acts as the primary transcriptional output from the circadian clock [181] (**Figure 1-6A**). Disruption of either *sasA* or *rpaA* results in severely damped gene expression rhythms [133, 181]. Finally the timing of the clock is synchronized to the external environment by the interaction of KaiA, and the circadian input kinase (CikA) with the plastoquinone pool (**Figure 1-6A**). The redox state of plastoquinone is directly dependent on light intensity, and it has been shown that oxidized quinone moieties bind to CikA and KaiA, effectively resetting the timing of the clock mechanism [182-184].

1.3.2.2 Global Effects on Gene Expression

Work in *S. elongatus* showed that, as expected, global transcriptional control is RpaA-mediated, as the inactivation of RpaA eliminates circadian oscillations from a wide range of promoter-driven bioluminescence reporters,

and total bioluminescence decreases significantly at promoters controlling dusk-peaking circadian genes [181]. However, it was not clear from this work whether RpaA directly regulates the expression of all genes in *S. elongatus*, or acts indirectly through the regulation of other transcription factors or genome compaction rhythms. Significant insight was gained when Markson et al. characterized the global gene expression profile of an rpaA-null strain as well as the genomic binding sites of RpaA as measured by ChIP-seq [131]. Their data showed that RpaA binds to only about 110 loci in the genome, and the expression levels of only 84 genes are modulated by 2-fold or more in an rpaA-null mutant. Genes in RpaA's direct regulon include four sigma factors and two transcription factors, which presumably in turn control the rhythmic expression of the majority of cycling genes in the genome. Interestingly, they observed that the deletion of rpaA arrests the global transcription profile in a dawn-like expression state **(Figure 1-6B)**. That is, genes down-regulated in the mutant are highly enriched in transcripts that peak at dusk, while up-regulated genes are highly enriched in transcripts that peak at dawn. These data support the previously described claim that RpaA-mediated regulation can be either positive or negative [185]. Given that 69 of the 84 genes that change more than 2- fold were down-regulated, RpaA appears to be important to drive the expression of many dusk-peaking transcripts. This conclusion is supported by the finding that expressing a constitutively active form of RpaA (RpaA D53E) in an rpaA-null background leads to a rapid shift

from a dawn-like to a dusk-like expression state (**Figure 1-6B**) [131].

Global gene expression profiling has been done for a number of cyanobacterial species [101, 130, 162, 165]. However, while strong circadian rhythms of gene expression persist in *S. elongatus* even under constant light conditions, the majority of genes in many other species only exhibit rhythmic fluctuations when cells are grown under a diurnal cycle [162, 165]. Yet there are conflicting reports about circadian processes in some cyanobacteria, such as *Synechocystis* PCC6803. Some studies have reported that gene expression in *Synechocystis* PCC6803 is not rhythmic in constant light [162], while other studies have detected a small set of rhythmic transcripts under those conditions [130]. In the case where rhythmic transcripts were detected, they did overlap well with those known to have very strong amplitude in *S. elongatus*. Additionally, a recent study on *Synechocystis* PCC6803 has detected sustained circadian rhythms in growth rate and a number of other physiological parameters when cells were grown in constant light under strictly controlled conditions [186]. Thus, circadian rhythms may be harder to detect in some strains, and only appear robustly under specific growth conditions.

1.3.2.3 Global Metabolic Control

How the clock controls metabolic processes is still poorly understood, as few studies have provided a genetic link between metabolic observations

and clock output, and most circadian experiments have been conducted under constant light. Glycogen metabolism is one of the few metabolic systems where rhythmic activity has been genetically linked to the clock and studied in both constant light and diurnal contexts. Furthermore, the regulation of glycogen metabolism by the clock is conserved in higher eukaryotes; the mammalian clock has been shown to regulate liver glycogen synthesis [187]. It has been known for some time that glycogen in cyanobacteria accumulates during the day and degrades during the night under diurnal growth [95]. Recent work shows that the circadian clock directly influences the orchestration of glycogen and other carbon metabolism when cells are grown under both constant light and diurnal conditions [86, 100]. Glycogen content in S. elongatus grown under constant light oscillates with 24-h rhythmicity, and this rhythm is lost in a *kaiC*-null mutant that lacks a functional oscillator [100]. However, when glycogen was tracked for 72 h under diurnal growth conditions, accumulation oscillated in both WT and *kaiC*-null strains, showing that environmental light cycles can drive metabolic oscillations even in the absence of the clock. Nonetheless, the accumulation of glycogen during the day period in the *kaiC*-null strain occurred earlier, was significantly more rapid, and resulted in an overall higher glycogen content than in WT [86]. Thus, while environmental cycles can drive glycogen rhythms, there is a significant input from the circadian clock as to how these rhythms are modulated. Metabolomics measurements revealed that the *kaiC*-null

mutant significantly over-accumulates primary carbon metabolites in the OPPP and glycolysis, such as fructose-6-phosphate, in the morning hours of a diurnal cycle [86]. This is unsurprising as we have already detailed how several genes in the OPPP are direct RpaA targets (**Figure 1-6C**), and two of the most strongly down-regulated genes identified in *rpaA*-null strains are *zwf* and *gnd*, which code for enzymes that catalyze the two NADPH-producing steps of the OPPP (**Figure 1-4**) [117, 131]. The detection of increased OPPP activity in *kaiC*-null strains also sup- ports the hypothesis that the KaiABC complex acts as a repressor on SasA/RpaA-mediated output, specifically during the day period [185]. Without repressive output from the clock, RpaA is free to be active during the day and activates genes of the OPPP, resulting in an increased concentration of primary carbon metabolites (See Chapter 2).

Although *kaiC*-null strains grow normally under diurnal conditions, *rpaA*- and *sasA*-null strains do not [133, 181]. Understanding why *rpaA* and *sasA* mutants die under diurnal growth may elucidate what types of cellular processes are important for survival under diurnal conditions. Indeed, RpaA's control over the OPPP and glycogen degradation may be linked to the diurnal sensitivity of *rpaA* (and to a lesser extent, *sasA*) mutants. As mentioned earlier, the shift towards the OPPP during evening hours allows it to become the primary source of NADPH from degradation of stored glycogen when photosynthesis is inactive [120, 127], and the deletion of either *zwf* or *gnd* genes in cyanobacteria result in a decrease of viability under diurnal growth

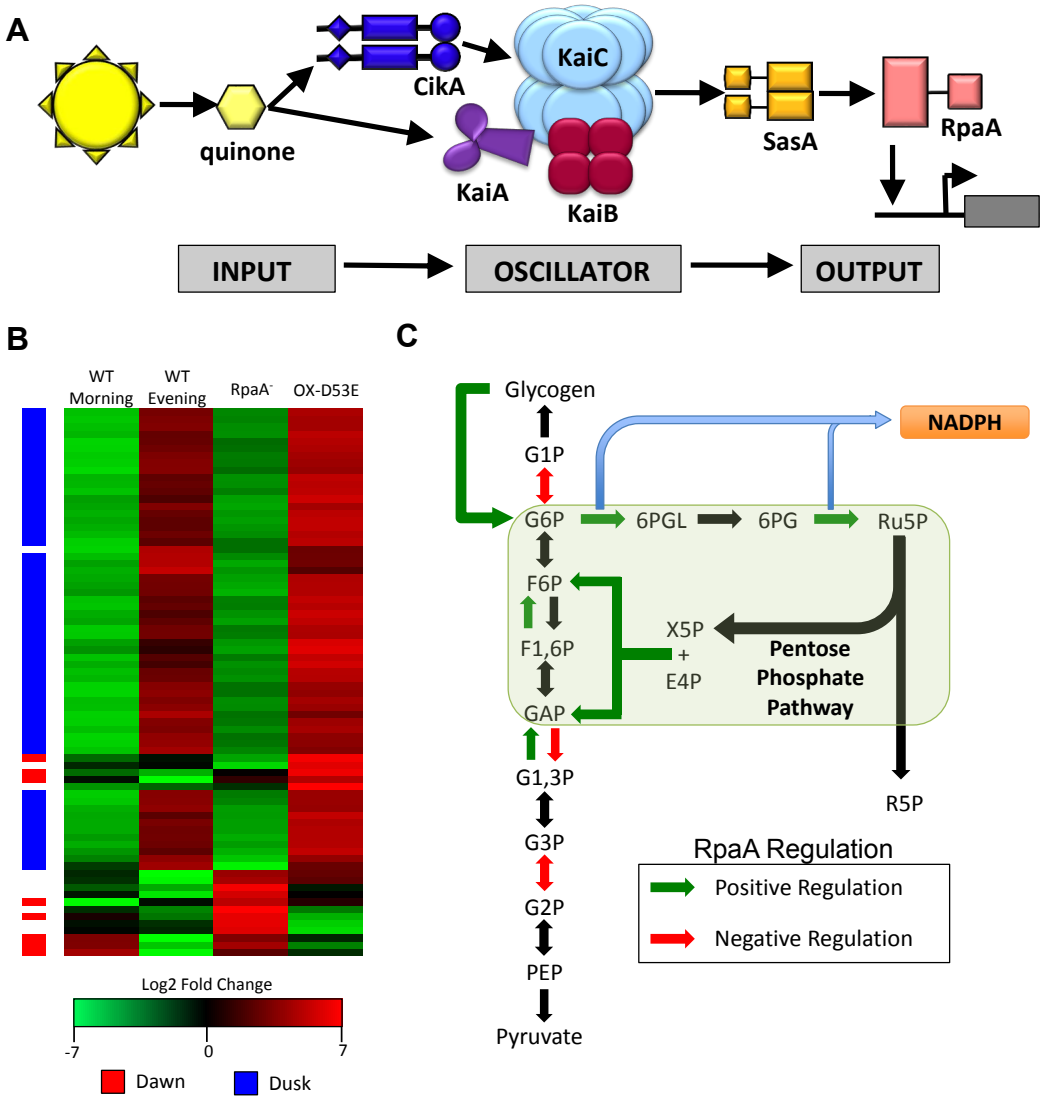

Figure 1-6. Cyanobacterial Circadian Clock and Effects of RpaA Transcriptional Output. (A) This cartoon illustrates the main components of the clock separated by their general function: light input components (left), central oscillator (center), and SasA-RpaA two-component output pathway (right). **(B)** Heatmap showing the expression of 76 genes that change more than 2-fold in an *S. elongatus* Δ*rpaA* strain The columns indicate the expression of these genes at morning and evening circadian time points as well as in a ΔrpaA and ΔrpaA::rpaA(D53E) strain, which has a mutation that simulates constitutively active RpaA. The column on the left indicates if a gene normally peaks in expression at dawn (red) or dusk (blue) based on data from Vijayan et al. (101). **(C)** Pathway diagram of glycolysis and the pentose phosphate pathway indicating reactions whose corresponding genes are either activated (green) or repressed (red) by RpaA. These genes change in overall expression level significantly when *rpaA* is inactivated

conditions [121, 123]. Additionally, *rpaA* mutants have attenuated glycogen degradation at night, and only degrade about half of their stored glycogen reserves over a 12 h period in the dark [86]. Experiments have also shown that an inability to store or degrade glycogen leads to loss of viability specifically under diurnal growth [81]. However, it is unclear if additional metabolic pathways are controlled by RpaA, and are important for viability at night, and why OPPP activity is important for nighttime viability.

Studies to elucidate the metabolic properties affected by circadian rhythms highlight the fact that genetic studies to parse apart circadian from diurnal influences in cyanobacteria are severely lacking. Additionally, the current studies are primarily focused on *S. elongatus*, and other cyanobacterial models should be considered. The current data suggests the major influence of the clock on metabolism is to balance OPPP activity over a 24 h period. However, it is still very unclear what the consequences of aberrant OPPP activity are, and what the purpose of reductant production at night is. With respect to clock output, a picture is forming that places the circadian oscillator as important for repression of SasA-RpaA output activity during the day, and active RpaA output as important for night-time metabolic processes. Future work should focus on both the biological relevance of temporally separating these classes of metabolic pathways.

1.4 Conclusions and Knowledge Gaps for Future Study

1.4.1 Main Summary Points

Cyanobacteria are a central part of Earth's history, play a major role in global carbon and nitrogen cycles, and are promising candidates for applications in the field of industrial biotechnology. Due to the evolution of photosynthetic metabolism under a predictable diurnal cycle, the most complete understanding of cyanobacterial metabolism will need to take into account the effect of light-to-dark transitions and circadian timing. Additionally, it is increasingly clear that metabolism in cyanobacteria is controlled and structured differently than metabolism in heterotropic bacteria. Thus, the classic approaches applied to engineering heterotrophic bacteria will need to be revised for cyanobacterial strains. Here we provide five main points to summarize the important data presented in this review on diurnal, circadian, and redox control of metabolism in cyanobacteria:

(1) The cellular redox state in cyanobacteria has a very strong bearing on metabolic flux and enzyme activity, and it is likely that cyanobacteria strive to maintain a redox balance within their cells to modulate enzymatic activity and mitigate the effects photosystem over-reduction.

(2) Glycogen serves a number of functions in cyanobacterial metabolism: It is the primary carbon storage polymer, it functions to buffer the production of excess fixed carbon and reductant under periods of nutrient stress, and it is critical for the survival of cyanobacterial cells at night.

(3) There are light and dark specific regimes for central carbon metabolism in cyanobacteria with the Calvin cycle running during the day and the OPPP running at night. These pathways form a “superpathway” with glycolysis and the shift between them is primarily mediated by protein redox modifications and circadian clock driven transcription.

(4) Despite the discovery of bypasses the close the cyanobacterial TCA cycle, it is likely that these reactions do not need to progress as a cycle under normal growth conditions. The TCA cycle is not the primary reductant producing pathway in cyanobacteria as it is in most other heterotrophic organisms

(5) The circadian clock is an important regulator of carbon metabolism, and in particular the OPPP is strongly controlled by the clock

response regulator RpaA. This clock output activity is critical for OPPP activation, and in turn diurnal survival.

1.4.2 Main Knowledge Gaps

Given the new direct evidence linking redox driven and circadian processes to central metabolism, a number of questions still remain as to how these processes interact as well as the exact purpose of metabolic processes at night. Here we provide six main questions that still remain and can be used to drive the future work on diurnal, circadian, and redox mediated metabolic processes in cyanobacteria.

(1) What effect do the light-dependent redox modifications, identified across cyanobacterial proteomes, have on enzymatic activity?

(2) Is there an interaction between circadian output, the overall cellular redox state, and the extent of protein redox modifications (ie: does redox regulation change depending on the timing of the circadian clock)?

(3) Although protein levels are stable, is protein turnover a circadian processes in cyanobacteria? If so, does the stoichiometry of modified to unmodified proteins play a role in turnover importance?

(4) What is the exact physiological function of OPPP activation and reductant production at night, and why is it essential for diurnal survival?

(5) What is the physiological importance of dark activated transcription in diverse cyanobacterial species, specifically if in some species genes that come on at night are dispensable for diurnal survival? In turn, what are all the essential genes for diurnal viability?

(6) Can metabolism be globally or locally re-directed for engineering purposes using modifications based on the understanding of circadian and/or redox control?

1.5 Acknowledgements

Chapter 1 is, in part, a reprint of material that appears in Shultzaberger, R. K., Boyd, J. S., Diamond, S., Greenspan, R. J., & Golden, S. S. (2015). Giving Time Purpose: The *S. elongatus* clock in a broader network context. Annu Rev Genet. (In Press). The dissertation author was a primary co-author and contributed to sections 3 and 4 of the manuscript and figures 2 and 3.

1.6 References

1. Schopf JW: **Geological evidence of oxygenic photosynthesis and the biotic response to the 2400-2200 ma "great oxidation event".** *Biochemistry Mosc* 2014, **79**:165–177.

2. Kharecha P, Kasting J, Siefert J: **A coupled atmosphere–ecosystem model of the early Archean Earth**. *Geobiology* 2005.

3. Knoll AH: **Paleobiological Perspectives on Early Microbial Evolution.** *Cold Spring Harb Perspect Biol* 2015, **7**:a018093.

4. Howe CJ, Barbrook AC, Nisbet RER, Lockhart PJ, Larkum AWD: **The origin of plastids**. *Philos Trans R Soc Lond, B, Biol Sci* 2008, **363**:2675–2685.

5. Dorrell RG, Howe CJ: **What makes a chloroplast? Reconstructing the establishment of photosynthetic symbioses.** *J Cell Sci* 2012, **125**:1865–1875.

6. Bryant DA: **The beauty in small things revealed.** *Proc Natl Acad Sci USA* 2003, **100**:9647–9649.

7. Field C, Behrenfeld M, Randerson J, Falkowski P: **Primary production of the biosphere: integrating terrestrial and oceanic components**. *Science* 1998, **281**:237–240.

8. Partensky F, Hess WR, Vaulot D: **Prochlorococcus, a marine photosynthetic prokaryote of global significance.** *Microbiology and Molecular Biology Reviews* 1999, **63**:106–127.

9. Scanlan DJ: **Physiological diversity and niche adaptation in marine Synechococcus.** *Adv Microb Physiol* 2003, **47**:1–64.

10. Ramaraj R, Tsai DD-W, Chen PH: **Freshwater microalgae niche of air carbon dioxide mitigation**. *Ecological Engineering* 2014, **68**:47–52.

11. Berman-Frank I, Lundgren P, Falkowski P: **Nitrogen fixation and photosynthetic oxygen evolution in cyanobacteria**. *Research in Microbiology* 2003.

12. Flores E, Herrero A: **Nitrogen assimilation and nitrogen control in cyanobacteria.** *Biochem Soc Trans* 2005, **33**:164–167.

13. Capone DG, Zehr JP, Paerl HW, Bergman B, Carpenter EJ: **Trichodesmium, a Globally Significant Marine Cyanobacterium**. *Science* 1997, **276**:1221–1229.

14. Bergman B, Sandh G, Lin S, Larsson J, Carpenter EJ: **Trichodesmium–a widespread marine cyanobacterium with unusual nitrogen fixation properties**. *FEMS Microbiology Reviews* 2013, **37**:286–302.

15. Musilova M, Tranter M, Bennett SA, Wadham J, Anesio AM: **Stable microbial community composition on the Greenland Ice Sheet**. *Front Microbiol* 2015, **6**:1–10.

16. Urbieta MS, González-Toril E, Bazán ÁA, Giaveno MA, Donati E: **Comparison of the microbial communities of hot springs waters and the microbial biofilms in the acidic geothermal area of Copahue (Neuquén, Argentina)**. *Extremophiles* 2015, **19**:437–450.

17. Glaring MA, Vester JK, Lylloff JE, Abu Al-Soud W, Sørensen SJ, Stougaard P: **Microbial Diversity in a Permanently Cold and Alkaline Environment in Greenland**. *PLoS ONE* 2015, **10**:e0124863–22.

18. Shi T, Falkowski PG: **Genome evolution in cyanobacteria: the stable core and the variable shell.** *Proc Natl Acad Sci USA* 2008, **105**:2510–2515.

19. Larsson J, Nylander JA, Bergman B: **Genome fluctuations in cyanobacteria reflect evolutionary, developmental and adaptive traits**. *BMC Evolutionary Biology* 2011, **11**:187.

20. Mariné MH, Clavero E, Roldán M: **Microscopy methods applied to research on cyanobacteria**. *Limnetica* 2004, **23**:179–186.

21. Woese CR: **Bacterial evolution.** *Microbiol Rev* 1987, **51**:221–271.

22. Waldbauer JR, Rodrigue S, Coleman ML, Chisholm SW: **Transcriptome and Proteome Dynamics of a Light-Dark Synchronized Bacterial Cell Cycle**. *PLoS ONE* 2012, **7**:e43432.

23. Golden SS: **Light-responsive gene expression in cyanobacteria.** *J Bacteriol* 1995, **177**:1651–1654.

24. Garcia-Dominguez M, Muro-Pastor MI, Reyes JC, Florencio FJ: **Light-Dependent Regulation of Cyanobacterial Phytochrome Expression**. *J Bacteriol* 2000, **182**:38–44.

25. Salem: **Light-to-dark transitions trigger a transient increase in intracellular Ca2+ modulated by the redox state of the photosynthetic**

electron transport chain in the cyanobacterium Anabaena sp. PCC7120. 2004:1–10.

26. Ito H, Mutsuda M, Murayama Y, Tomita J, Hosokawa N, Terauchi K, Sugita C, Sugita M, Kondo T, Iwasaki H: **Cyanobacterial daily life with Kai-based circadian and diurnal genome-wide transcriptional control in Synechococcus elongatus**. *Proc Natl Acad Sci USA* 2009, **106**:14168–14173.

27. Elvitigala T, Stöckel J, Ghosh BK, Pakrasi HB: **Effect of continuous light on diurnal rhythms in Cyanothece sp. ATCC 51142**. *BMC Genomics* 2009, **10**:226.

28. Mackey SR, Golden SS, Ditty JL: **The Itty-Bitty Time Machine**. In *Advances in Genetics*. *Volume 74*. Elsevier; 2011:13–53. [*Advances in Genetics*]

29. Dong G, Golden SS: **How a cyanobacterium tells time.** 2008, **11**:541–546.

30. Nathan C, Ding A: **SnapShot: Reactive Oxygen Intermediates (ROI).** *Cell* 2010, **140**:951–951.e2.

31. Dietz K-J: **Peroxiredoxins in Plants and Cyanobacteria**. *Antioxid Redox Signal* 2011, **15**:1129–1159.

32. Edgar RS, Green EW, Zhao Y, van Ooijen G, Olmedo M, Qin X, Xu Y, Pan M, Valekunja UK, Feeney KA, Maywood ES, Hastings MH, Baliga NS, Merrow M, Millar AJ, Johnson CH, Kyriacou CP, O'Neill JS, Reddy AB: **Peroxiredoxins are conserved markers of circadian rhythms.** *Nature* 2012, **485**:459–464.

33. Hoyle NP, O'Neill JS: **Oxidation–Reduction Cycles of Peroxiredoxin Proteins and Nontranscriptional Aspects of Timekeeping**. *Biochemistry* 2015, **54**:184–193.

34. Díaz-Troya S, López-Maury L, Sánchez-Riego AM, Roldán M, Florencio FJ: **Redox regulation of glycogen biosynthesis in the cyanobacterium Synechocystis sp. PCC 6803: analysis of the AGP and glycogen synthases.** *Mol Plant* 2014, **7**:87–100.

35. Alfonso M, Perewoska I, Kirilovsky D: **Redox control of ntcA gene expression in Synechocystis sp PCC 6803. Nitrogen availability and electron transport regulate the levels of the NtcA protein**. *PLANT PHYSIOLOGY* 2001, **125**:969–981.

36. Tamoi M, Miyazaki T, Fukamizo T, Shigeoka S: **The Calvin cycle in cyanobacteria is regulated by CP12 via the NAD(H)/NADP(H) ratio under light/dark conditions**. *The Plant Journal* 2005, **42**:504–513.

37. Wedel N, Soll J: **Evolutionary conserved light regulation of Calvin cycle activity by NADPH-mediated reversible phosphoribulokinase/CP12/ glyceraldehyde-3-phosphate dehydrogenase complex dissociation**. *Proceedings of the National Academy of …* 1998.

38. Guo J, Nguyen AY, Dai Z, Su D, Gaffrey MJ, Moore RJ, Jacobs JM, Monroe ME, Smith RD, Koppenaal DW, Pakrasi HB, Qian W-J: **Proteome-wide Light/Dark Modulation of Thiol Oxidation in Cyanobacteria Revealed by Quantitative Site-specific Redox Proteomics**. *Molecular & Cellular Proteomics* 2014, **13**:3270–3285.

39. Ansong C, Sadler NC, Hill EA, Lewis MP: **Characterization of protein redox dynamics induced during light-to-dark transitions and nutrient limitation in cyanobacteria**. *Frontiers in …* 2014.

40. Chardonnet S, Sakr S, Cassier-Chauvat C, Le Maréchal P, Chauvat F, Lemaire SD, Decottignies P: **First Proteomic Study of S-Glutathionylation in Cyanobacteria.** *J Proteome Res* 2014:140919143615000.

41. Robertson DE, Jacobson SA, Morgan F, Berry D, Church GM, Afeyan NB: **A new dawn for industrial photosynthesis**. *Photosynth Res* 2011, **107**:269–277.

42. Wijffels RH, Kruse O, Hellingwerf KJ: **Potential of industrial biotechnology with cyanobacteria and eukaryotic microalgae**. *Current Opinion in Biotechnology* 2013, **24**:405–413.

43. Ducat DC, Way JC, Silver PA: **Engineering cyanobacteria to generate high-value products**. *Trends in Biotechnology* 2011, **29**:95–103.

44. Lassen LM, Nielsen AZ, Ziersen B, Gnanasekaran T, Møller BL, Jensen PE: **Redirecting Photosynthetic Electron Flow into Light-Driven Synthesis of Alternative Products Including High-Value Bioactive Natural Compounds**. *ACS Synth Biol* 2014, **3**:1–12.

45. Angermayr SA, Gorchs Rovira A, Hellingwerf KJ: **Metabolic engineering of cyanobacteria for the synthesis of commodity products.** *Trends in Biotechnology* 2015, **33**:352–361.

46. Yu Y, You L, Liu D, Hollinshead W, Tang Y, Zhang F: **Development of**

Synechocystis sp. PCC 6803 as a Phototrophic Cell Factory. *Marine Drugs* 2013, **11**:2894–2916.

47. Chen X, Zhou L, Tian K, Kumar A, Singh S, Prior BA, Wang Z: **Metabolic engineering of Escherichia coli: A sustainable industrial platform for bio-based chemical production**. *Biotechnology Advances* 2013, **31**:1200–1223.

48. Clerico EM, Ditty JL, Golden SS: **Specialized techniques for site-directed mutagenesis in cyanobacteria.** *Methods Mol Biol* 2007, **362**:155–171.

49. Holtman CK, Chen Y, Sandoval P, Gonzales A, Nalty MS, Thomas TL, Youderian P, Golden SS: **High-throughput functional analysis of the Synechococcus elongatus PCC 7942 genome.** *DNA Res* 2005, **12**:103–115.

50. Taton A, Unglaub F, Wright NE, Zeng WY, Paz-Yepes J, Brahamsha B, Palenik B, Peterson TC, Haerizadeh F, Golden SS, Golden JW: **Broad-host-range vector system for synthetic biology and biotechnology in cyanobacteria.** *Nucleic Acids Res* 2014, **42**:e136.

51. Taton A, Lis E, Adin DM, Dong G, Cookson S, Kay SA, Golden SS, Golden JW: **Gene Transfer in Leptolyngbya sp. Strain BL0902, a Cyanobacterium Suitable for Production of Biomass and Bioproducts**. *PLoS ONE* 2012, **7**:e30901–15.

52. Pakrasi HB: **Synthetic biology of cyanobacteria: unique challenges and opportunities**. 2013:1–14.

53. Sakai Y, Abe K, Nakashima S, Ellinger JJ, Ferri S, Sode K, Ikebukuro K: **Scaffold-fused riboregulators for enhanced gene activation in Synechocystissp. PCC 6803**. *MicrobiologyOpen* 2015:n/a–n/a.

54. Habib M, Parvin M, Huntington TC, Hasan MR: *A Review on Culture, Production and Use of Spirulina as Food for Humans and Feeds for Domestic Animal and Fish. FAO Fisheries and Aquaculture Circular …*. FAO; 2008.

55. Nolla-Ardèvol V, Strous M: **Anaerobic digestion of the microalga Spirulina at extreme alkaline conditions: biogas production, metagenome, and metatranscriptome**. *Frontiers in …* 2015.

56. Chaiklahan R: **Cultivation of Spirulina platensis Using Pig Wastewater in a Semi-Continuous Process**. *J Microbiol Biotechnol* 2010, **20**:609–614.

57. Gao Z, Zhao H, Li Z, Tan X, Lu X: **Photosynthetic production of ethanol from carbon dioxide in genetically engineered cyanobacteria**. *Energy Environ Sci* 2012, **5**:9857–9.

58. Lan EI, Liao JC: **Metabolic engineering of cyanobacteria for 1-butanol production from carbon dioxide.** *Metabolic Engineering* 2011, **13**:353–363.

59. Lan EI, Liao JC: **ATP drives direct photosynthetic production of 1-butanol in cyanobacteria**. 2012.

60. Atsumi S, Cann AF, Connor MR, Shen CR, Smith KM, Brynildsen MP, Chou KJY, Hanai T, Liao JC: **Metabolic engineering of Escherichia coli for 1-butanol production**. *Metabolic Engineering* 2008, **10**:305–311.

61. Oliver J, Machado I: **Cyanobacterial conversion of carbon dioxide to 2, 3-butanediol**. 2013.

62. Li C, Tao F, Ni J, Wang Y, Yao F, Xu P: **Enhancing the light-driven production of D-lactate by engineering cyanobacterium using a combinational strategy.** *Sci Rep* 2015, **5**:9777.

63. Angermayr SA, Hellingwerf KJ: **On the Use of Metabolic Control Analysis in the Optimization of Cyanobacterial Biosolar Cell Factories**. *J Phys Chem B* 2013, **117**:11169–11175.

64. Varman AM, Yu Y, You L, Tang YJ: **Photoautotrophic production of D-lactic acid in an engineered cyanobacterium.** *Microbial Cell Factories* 2013, **12**:117.

65. Atsumi S, Higashide W, Liao JC: **Direct photosynthetic recycling of carbon dioxide to isobutyraldehyde**. *Nature Biotechnology* 2009, **27**:1177–1180.

66. Bentley FK, Melis A: **Diffusion-based process for carbon dioxide uptake and isoprene emission in gaseous/aqueous two-phase photobioreactors by photosynthetic microorganisms**. *Biotechnol Bioeng* 2011, **109**:100–109.

67. Kiyota H, Okuda Y, Ito M, Hirai MY, Ikeuchi M: **Engineering of cyanobacteria for the photosynthetic production of limonene from CO2**. *Journal of Biotechnology* 2014, **185**:1–7.

68. Davies FK, Work VH, Beliaev AS, Posewitz MC: **Engineering Limonene and Bisabolene Production in Wild Type and a Glycogen-Deficient Mutant of Synechococcus sp. PCC 7002.** *Front Bioeng Biotechnol* 2014, **2**:21.

69. Schirmer A, Rude MA, Li X, Popova E, del Cardayre SB: **Microbial biosynthesis of alkanes.** *Science* 2010, **329**:559–562.

70. Niederholtmeyer H, Wolfstadter BT, Savage DF, Silver PA, Way JC: **Engineering Cyanobacteria To Synthesize and Export Hydrophilic Products**. *Applied and Environmental Microbiology* 2010, **76**:3462–3466.

71. Ducat DC, Avelar-Rivas JA, Way JC, Silver PA: **Rerouting Carbon Flux To Enhance Photosynthetic Productivity**. *Applied and Environmental Microbiology* 2012, **78**:2660–2668.

72. Deng MD, Coleman JR: **Ethanol synthesis by genetic engineering in cyanobacteria.** *Applied and Environmental Microbiology* 1999, **65**:523–528.

73. Gudmundsson S, Nogales J: **Cyanobacteria as photosynthetic biocatalysts: a systems biology perspective**. *Mol BioSyst* 2015.

74. Oliver JWK, Machado IMP, Yoneda H, Atsumi S: **Combinatorial optimization of cyanobacterial 2,3-butanediol production.** *Metabolic Engineering* 2014, **22**:76–82.

75. Oliver J, Atsumi S: **Metabolic design for cyanobacterial chemical synthesis**. *Photosynth Res* 2014.

76. Takatani N, Use K, Kato A, Ikeda K, Kojima K, Aichi M, Maeda S-I, Omata T: **Essential Role of Acyl-ACP Synthetase in Acclimation of the Cyanobacterium Synechococcus elongatus Strain PCC 7942 to High-Light Conditions.** *Plant and Cell Physiology* 2015:pcv086–8.

77. Klotz A, Reinhold E, Doello S, Forchhammer K: **Nitrogen Starvation Acclimation in Synechococcus elongatus: Redox-Control and the Role of Nitrate Reduction as an Electron Sink.** *Life (Basel)* 2015, **5**:888–904.

78. Kolman MA, Nishi CN, Perez-Cenci M, Salerno GL: **Sucrose in cyanobacteria: from a salt-response molecule to play a key role in nitrogen fixation.** *Life (Basel)* 2015, **5**:102–126.

79. Hickman JW, Kotovic KM, Miller C, Warrener P, Kaiser B, Jurista T, Budde M, Cross F, Roberts JM, Carleton M: **Glycogen synthesis is a required component of the nitrogen stress response in Synechococcus elongatus PCC 7942**. *Algal Research* 2013.

80. Joseph A, Aikawa S, Sasaki K, Teramura H, Hasunuma T, Matsuda F, Osanai T, Hirai MY, Kondo A: **Rre37 stimulates accumulation of 2-oxoglutarate and glycogen under nitrogen starvation in Synechocystis sp. PCC 6803**. *FEBS Letters* 2014, **588**:466–471.

81. Grundel M, Scheunemann R, Lockau W, Zilliges Y: **Impaired glycogen synthesis causes metabolic overflow reactions and affects stress responses in the cyanobacterium Synechocystis sp. PCC 6803**. *Microbiology* 2012, **158**:3032–3043.

82. Li X, Shen CR, Liao JC: **Isobutanol production as an alternative metabolic sink to rescue the growth deficiency of the glycogen mutant of Synechococcus elongatus PCC 7942**. *Photosynth Res* 2014.

83. Lan EI, Ro SY, Liao JC: **Oxygen-tolerant coenzyme A-acylating aldehyde dehydrogenase facilitates efficient photosynthetic n-butanol biosynthesis in cyanobacteria**. *Energy Environ Sci* 2013, **6**:2672–10.

84. Welkie D, Zhang X, Markillie ML, Taylor R, Orr G, Jacobs J, Bhide K, Thimmapuram J, Gritsenko M, Mitchell H, Smith RD, Sherman LA: **Transcriptomic and proteomic dynamics in the metabolism of a diazotrophic cyanobacterium, Cyanothece sp. PCC 7822 during a diurnal light–dark cycle**. *BMC Genomics* 2014, **15**:1185.

85. Stöckel J, Jacobs JM, Elvitigala TR, Liberton M, Welsh EA, Polpitiya AD, Gritsenko MA, Nicora CD, Koppenaal DW, Smith RD, Pakrasi HB: **Diurnal rhythms result in significant changes in the cellular protein complement in the cyanobacterium Cyanothece 51142.** *PLoS ONE* 2011, **6**:e16680.

86. Diamond S, Jun D, Rubin BE, Golden SS: **The circadian oscillator in Synechococcus elongatus controls metabolite partitioning during diurnal growth.** *Proc Natl Acad Sci USA* 2015, **112**:E1916–25.

87. Zhang F, Carothers JM, Keasling JD: **Design of a dynamic sensor-regulator system for production of chemicals and fuels derived from fatty acids**. *Nature Biotechnology* 2012, **30**:354–359.

88. Nakahira Y, Katayama M, Miyashita H, Kutsuna S, Iwasaki H, Oyama T, Kondo T: **Global gene repression by KaiC as a master process of prokaryotic circadian system.** *Proc Natl Acad Sci USA* 2004, **101**:881–885.

89. Lehmann M, Wöber G: **Accumulation, mobilization and turn-over of glycogen in the blue-green bacterium Anacystis nidulans**. *Arch Microbiol* 1976, **111**:93–97.

90. Allen MM: **Cyanobacterial cell inclusions.** *Annual Review of Microbiology* 1984, **38**:1–25.

91. Sherman DM, Sherman LA: **Effect of iron deficiency and iron restoration on ultrastructure of Anacystis nidulans.** *J Bacteriol* 1983,

156:393–401.

92. Nakamura Y, Takahashi J-I, Sakurai A, Inaba Y, Suzuki E, Nihei S, Fujiwara S, Tsuzuki M, Miyashita H, Ikemoto H, Kawachi M, Sekiguchi H, Kurano N: **Some Cyanobacteria synthesize semi-amylopectin type alpha-polyglucans instead of glycogen.** *Plant and Cell Physiology* 2005, **46**:539–545.

93. Suzuki E, Ohkawa H, Moriya K, Matsubara T, Nagaike Y, Iwasaki I, Fujiwara S, Tsuzuki M, Nakamura Y: **Carbohydrate Metabolism in Mutants of the Cyanobacterium Synechococcus elongatus PCC 7942 Defective in Glycogen Synthesis**. *Applied and Environmental Microbiology* 2010, **76**:3153–3159.

94. Ballicora MA, Iglesias AA, Preiss J: **ADP-Glucose Pyrophosphorylase, a Regulatory Enzyme for Bacterial Glycogen Synthesis**. *Microbiology and Molecular …* 2003.

95. Suzuki E, Umeda K, Nihei S, Moriya K, Ohkawa H, Fujiwara S, Tsuzuki M, Nakamura Y: **Role of the GlgX protein in glycogen metabolism of the cyanobacterium, Synechococcus elongatus PCC 7942**. *Biochimica et Biophysica Acta (BBA) - General Subjects* 2007, **1770**:763–773.

96. Osanai T, Azuma M, Tanaka K: **Sugar catabolism regulated by light- and nitrogen-status in the cyanobacterium Synechocystis sp. PCC 6803**. *Photochem Photobiol Sci* 2007, **6**:508.

97. Hanai M, Sato Y, Miyagi A, Kawai-Yamada M, Tanaka K, Kaneko Y, Nishiyama Y, Hihara Y: **The Effects of Dark Incubation on Cellular Metabolism of the Wild Type Cyanobacterium Synechocystis sp. PCC 6803 and a Mutant Lacking the Transcriptional Regulator cyAbrB2**. *Life (Basel)* 2014, **4**:770–787.

98. Wyman M, Thom C: **Temporal Orchestration of Glycogen Synthase (GlgA) Gene Expression and Glycogen Accumulation in the Oceanic Picoplanktonic Cyanobacterium Synechococcus sp. Strain WH8103**. *Applied and Environmental Microbiology* 2012, **78**:4744–4747.

99. Gaudana SB, Alagesan S, Chetty M, Wangikar PP: **Diurnal rhythm of a unicellular diazotrophic cyanobacterium under mixotrophic conditions and elevated carbon dioxide**. *Photosynth Res* 2013.

100. Pattanayak GK, Phong C, Rust MJ: **Rhythms in Energy Storage Control the Ability of the Cyanobacterial Circadian Clock to Reset**. *Current Biology* 2014:1–5.

101. Vijayan V, Zuzow R, O'Shea EK: **Oscillations in supercoiling drive circadian gene expression in cyanobacteria**. *Proc Natl Acad Sci USA* 2009, **106**:22564–22568.

102. Gaudana SB, Krishnakumar S, Alagesan S, Digmurti MG, Viswanathan GA, Chetty M, Wangikar PP: **Rhythmic and sustained oscillations in metabolism and gene expression of Cyanothece sp. ATCC 51142 under constant light.** *Front Microbiol* 2013, **4**:374.

103. Lindahl M, Florencio FJ: **Thioredoxin-linked processes in cyanobacteria are as numerous as in chloroplasts, but targets are different.** *Proc Natl Acad Sci USA* 2003, **100**:16107–16112.

104. Klähn S, Hagemann M: **Compatible solute biosynthesis in cyanobacteria.** *Environmental Microbiology* 2011, **13**:551–562.

105. Kolman MA, Torres LL, Martin ML, Salerno GL: **Sucrose synthase in unicellular cyanobacteria and its relationship with salt and hypoxic stress**. *Planta* 2011, **235**:955–964.

106. Curatti L, Giarrocco LE, Cumino AC, Salerno GL: **Sucrose synthase is involved in the conversion of sucrose to polysaccharides in filamentous nitrogen-fixing cyanobacteria.** *Planta* 2008, **228**:617–625.

107. Perez-Cenci M, Salerno GL: **Functional characterization of Synechococcus amylosucrase and fructokinase encoding genes discovers two novel actors on the stage of cyanobacterial sucrose metabolism**. *Plant Science* 2014, **224**:95–102.

108. Miao X, Wu Q, Wu G, Zhao N: **Sucrose accumulation in salt-stressed cells of agp gene deletion-mutant in cyanobacterium Synechocystis sp PCC 6803.** *FEMS Microbiol Lett* 2003, **218**:71–77.

109. Xu Y, Guerra LT, Li Z, Ludwig M, Dismukes GC, Bryant DA: **Altered carbohydrate metabolism in glycogen synthase mutants of Synechococcus sp. strain PCC 7002: Cell factories for soluble sugars.** *Metabolic Engineering* 2013, **16**:56–67.

110. Huege J, Goetze J, Schwarz D, Bauwe H, Hagemann M, Kopka J: **Modulation of the major paths of carbon in photorespiratory mutants of synechocystis.** *PLoS ONE* 2011, **6**:e16278.

111. Miao X, Wu Q, Wu G, Zhao N: **Changes in photosynthesis and pigmentation in an agp deletion mutant of the cyanobacterium Synechocystis sp.** *Biotechnol Lett* 2003, **25**:391–396.

112. Posewitz MC: **Lauric acid production in a glycogen-less strain of Synechococcus sp. PCC 7002**. 2015:1–12.

113. Latifi A, Ruiz M, Zhang C-C: **Oxidative stress in cyanobacteria.** *FEMS Microbiology Reviews* 2009, **33**:258–278.

114. Jackson SA, Eaton-Rye JJ, Bryant DA, Posewitz MC, Davies FK: **Dynamics of Photosynthesis in the Glycogen-Deficient glgC Mutant of Synechococcus sp. PCC 7002.** *Applied and Environmental Microbiology* 2015:AEM.01751–15.

115. McDonagh B, Domínguez-Martín MA, Gómez-Baena G, López-Lozano A, Diez J, Bárcena JA, García Fernández JM: **Nitrogen starvation induces extensive changes in the redox proteome of Prochlorococcus sp. strain SS120**. *Environmental Microbiology Reports* 2012, **4**:257–267.

116. Schwarz R: **Acclimation of unicellular cyanobacteria to macronutrient deficiency: emergence of a complex network of cellular responses**. *Microbiology* 2005, **151**:2503–2514.

117. Knowles VL, Plaxton WC: **From genome to enzyme: analysis of key glycolytic and oxidative pentose-phosphate pathway enzymes in the cyanobacterium Synechocystis sp. PCC 6803.** *Plant and Cell Physiology* 2003, **44**:758–763.

118. Knoop H, Gründel M, Zilliges Y, Lehmann R, Hoffmann S, Lockau W, Steuer R: **Flux Balance Analysis of Cyanobacterial Metabolism: The Metabolic Network of Synechocystis sp. PCC 6803**. *PLoS Comput Biol* 2013, **9**:e1003081.

119. Young JD, Shastri AA, Stephanopoulos G, Morgan JA: **Mapping photoautotrophic metabolism with isotopically nonstationary 13C flux analysis**. *Metabolic Engineering* 2011, **13**:656–665.

120. You L, He L, Tang YJ: **Photoheterotrophic Fluxome in Synechocystis sp. Strain PCC 6803 and Its Implications for Cyanobacterial Bioenergetics**. *J Bacteriol* 2015, **197**:943–950.

121. Scanlan DJ, Sundaram S, Newman J, Mann NH, Carr NG: **Characterization of a zwf mutant of Synechococcus sp. strain PCC 7942.** *J Bacteriol* 1995, **177**:2550–2553.

122. Broedel SE, Wolf RE: **Genetic tagging, cloning, and DNA sequence of the Synechococcus sp. strain PCC 7942 gene (gnd) encoding 6-phosphogluconate dehydrogenase.** *J Bacteriol* 1990, **172**:4023–4031.

123. Doolittle WF, Singer RA: **Mutational analysis of dark endogenous metabolism in the blue-green bacterium Anacystis nidulans.** *J Bacteriol* 1974, **119**:677–683.

124. Beck C, Knoop H, Axmann IM, Steuer R: **The diversity of cyanobacterial metabolism: genome analysis of multiple phototrophic microorganisms**. *BMC Genomics* 2012, **13**:56.

125. WADANO A, KAMATA Y, IWAKI T, NISHIKAWA K, HIRAHASHI T: **Purification and Characterization of Phosphoribulokinase From the Cyanobacterium Synechococcus Pcc7942**. *Plant and Cell Physiology* 1995, **36**:1381–1385.

126. Kobayashi D, Tamoi M, Iwaki T, Shigeoka S, Wadano A: **Molecular characterization and redox regulation of phosphoribulokinase from the cyanobacterium Synechococcus sp. PCC 7942.** *Plant and Cell Physiology* 2003, **44**:269–276.

127. Yang C, Hua Q, Shimizu K: **Integration of the information from gene expression and metabolic fluxes for the analysis of the regulatory mechanisms in Synechocystis.** *Appl Microbiol Biotechnol* 2002, **58**:813–822.

128. Koksharova O, Schubert M, Shestakov S, Cerff R: **Genetic and biochemical evidence for distinct key functions of two highly divergent GAPDH genes in catabolic and anabolic carbon flow of the cyanobacterium Synechocystis sp. PCC 6803 - Springer**. *Plant Molecular Biology* 1998, **36**:183–194.

129. Tamoi M, Ishikawa T, Takeda T, Shigeoka S: **Enzymic and molecular characterization of NADP-dependent glyceraldehyde-3-phosphate dehydrogenase from Synechococcus PCC 7942: resistance of the enzyme to hydrogen peroxide.** *Biochem J* 1996, **316 (Pt 2)**:685–690.

130. Kucho KI, Okamoto K, Tsuchiya Y, Nomura S, Nango M, Kanehisa M, Ishiura M: **Global Analysis of Circadian Expression in the Cyanobacterium Synechocystis sp. Strain PCC 6803**. *J Bacteriol* 2005, **187**:2190–2199.

131. Markson JS, Piechura JR, Puszynska AM, O'Shea EK: **Circadian Control of Global Gene Expression by the Cyanobacterial Master Regulator RpaA**. *Cell* 2013, **155**:1396–1408.

132. Sundaram S, Karakaya H, Scanlan DJ, Mann NH: **Multiple oligomeric forms of glucose-6-phosphate dehydrogenase in cyanobacteria and the**

role of OpcA in the assembly process. *Microbiology (Reading, Engl)* 1998, **144 (Pt 6)**:1549–1556.

133. Boyd JS, Bordowitz JR, Bree AC, Golden SS: **An allele of the crm gene blocks cyanobacterial circadian rhythms.** *Proc Natl Acad Sci USA* 2013, **110**:13950–13955.

134. Toepel J, Welsh E, Summerfield TC, Pakrasi HB, Sherman LA: **Differential Transcriptional Analysis of the Cyanobacterium Cyanothece sp. Strain ATCC 51142 during Light-Dark and Continuous-Light Growth**. *J Bacteriol* 2008, **190**:3904–3913.

135. Hosokawa N, Hatakeyama TS, Kojima T, Kikuchi Y, Ito H, Iwasaki H: **Circadian transcriptional regulation by the posttranslational oscillator without de novo clock gene expression in Synechococcus**. *Proc Natl Acad Sci USA* 2011, **108**:15396–15401.

136. Michelet L, Zaffagnini M, Morisse S, Sparla F, Pérez-Pérez ME, Francia F, Danon A, Marchand CH, Fermani S, Trost P, Lemaire SD: **Redox regulation of the Calvin-Benson cycle: something old, something new.** *Front Plant Sci* 2013, **4**:470.

137. Howard TP, Metodiev M, Lloyd JC, Raines CA: **Thioredoxin-mediated reversible dissociation of a stromal multiprotein complex in response to changes in light availability.** *Proc Natl Acad Sci USA* 2008, **105**:4056–4061.

138. Gontero B, Maberly SC: **An intrinsically disordered protein, CP12: jack of all trades and master of the Calvin cycle**. *Biochem Soc Trans* 2012, **40**:995–999.

139. Marri L, Thieulin-Pardo G, Lebrun R, Puppo R, Zaffagnini M, Trost P, Gontero B, Sparla F: **CP12-mediated protection of Calvin-Benson cycle enzymes from oxidative stress.** *Biochimie* 2014, **97**:228–237.

140. Tabei Y, Okada K, Makita N, Tsuzuki M: **Light-induced gene expression of fructose 1,6-bisphosphate aldolase during heterotrophic growth in a cyanobacterium, Synechocystis sp. PCC 6803**. *FEBS Journal* 2008, **276**:187–198.

141. Li M, Yang Q, Zhang L, Li H, Cui Y, Wu Q: **Identification of novel targets of cyanobacterial glutaredoxin.** *Arch Biochem Biophys* 2007, **458**:220–228.

142. Howard TP, Fryer MJ, Singh P, Metodiev M, Lytovchenko A, Obata T,

Fernie AR, Kruger NJ, Quick WP, Lloyd JC, Raines CA: **Antisense Suppression of the Small Chloroplast Protein CP12 in Tobacco Alters Carbon Partitioning and Severely Restricts Growth**. *PLANT PHYSIOLOGY* 2011, **157**:620–631.

143. Thompson LR, Zeng Q, Kelly L: **Phage auxiliary metabolic genes and the redirection of cyanobacterial host carbon metabolism**. 2011.

144. Pearce J, Leach CK, Carr NG: **The incomplete tricarboxylic acid cycle in the blue-green alga Anabaena variabilis.** *J Gen Microbiol* 1969, **55**:371–378.

145. Zhang CC, Jeanjean R, Joset F: **Obligate phototrophy in cyanobacteria: more than a lack of sugar transport.** *FEMS Microbiol Lett* 1998, **161**:285–292.

146. Zhang S, Bryant DA: **Biochemical validation of the glyoxylate cycle in the cyanobacterium Chlorogloeopsis fritschii strain PCC 9212.** *Journal of Biological Chemistry* 2015.

147. Xiong W, Brune D, Vermaas WFJ: **The γ-aminobutyric acid shunt contributes to closing the tricarboxylic acid cycle in Synechocystissp. PCC 6803**. *Molecular Microbiology* 2014, **93**:786–796.

148. Zhang S, Bryant DA: **The Tricarboxylic Acid Cycle in Cyanobacteria**. *Science* 2011, **334**:1551–1553.

149. You L, Berla B, He L, Pakrasi HB, Tang YJ: **13C-MFA delineates the photomixotrophic metabolism of Synechocystissp. PCC 6803 under light- and carbon-sufficient conditions**. *Biotechnol J* 2014, **9**:684–692.

150. Cooley JW, Vermaas WF: **Succinate dehydrogenase and other respiratory pathways in thylakoid membranes of Synechocystis sp. strain PCC 6803: capacity comparisons and physiological function.** *J Bacteriol* 2001, **183**:4251–4258.

151. Cooley JW, Howitt CA, Vermaas WF: **Succinate:quinol oxidoreductases in the cyanobacterium synechocystis sp. strain PCC 6803: presence and function in metabolism and electron transport.** *J Bacteriol* 2000, **182**:714–722.

152. Osanai T, Oikawa A, Shirai T, Kuwahara A, Iijima H, Tanaka K, Ikeuchi M, Kondo A, Saito K, Hirai MY: **Capillary electrophoresis-mass spectrometry reveals the distribution of carbon metabolites during nitrogen starvation in Synechocystis sp. PCC 6803.** *Environmental*

Microbiology 2014, **16**:512–524.

153. Muro-Pastor MI, Reyes JC, Florencio FJ: **Ammonium assimilation in cyanobacteria.** *Photosynth Res* 2005, **83**:135–150.

154. Herrero A, Muro-Pastor AM, Flores E: **Nitrogen Control in Cyanobacteria**. *J Bacteriol* 2001, **183**:411–425.

155. Marqués S, Mérida A, Candau P, Florencio FJ: **Light-mediated regulation of glutamine synthetase activity in the unicellular cyanobacterium Synechococcus sp. PCC 6301.** *Planta* 1992, **187**:247–253.

156. Jin M-M, Wang P, Li X, Zhao X-Y, Xu L, Song P, Zhu G-P: **Biochemical characterization of NADP$^+$-dependent isocitrate dehydrogenase from Microcystis aeruginosa PCC7806.** *Mol Biol Rep* 2013, **40**:2995–3002.

157. Muro-Pastor MI, Reyes JC, Florencio FJ: **The NADP+-isocitrate dehydrogenase gene (icd) is nitrogen regulated in cyanobacteria.** *J Bacteriol* 1996.

158. Singh AK, Elvitigala T, Bhattacharyya-Pakrasi M, Aurora R, Ghosh B, Pakrasi HB: **Integration of Carbon and Nitrogen Metabolism with Energy Production Is Crucial to Light Acclimation in the Cyanobacterium Synechocystis**. *PLANT PHYSIOLOGY* 2008, **148**:467–478.

159. Hernández-Prieto MA, Semeniuk TA: **Toward a systems-level understanding of gene regulatory, protein interaction, and metabolic networks in cyanobacteria**. *Frontiers in …* 2014.

160. Baroukh C, Muñoz-Tamayo R, Steyer J-P, Bernard O: **A state of the art of metabolic networks of unicellular microalgae and cyanobacteria for biofuel production**. *Metabolic Engineering* 2015, **30**(C):49–60.

161. Straub C, Quillardet P, Vergalli J, de Marsac NT, Humbert J-F: **A Day in the Life of Microcystis aeruginosa Strain PCC 7806 as Revealed by a Transcriptomic Analysis**. *PLoS ONE* 2011, **6**:e16208.

162. Beck C, Hertel S, Rediger A, Lehmann R, Wiegard A, Kölsch A, Heilmann B, Georg J, Hess WR, Axmann IM: **Daily Expression Pattern of Protein-Encoding Genes and Small Noncoding RNAs in Synechocystis sp. Strain PCC 6803.** *Applied and Environmental Microbiology* 2014, **80**:5195–5206.

163. Stöckel J, Welsh EA, Liberton M, Kunnvakkam R, Aurora R, Pakrasi HB: **Global transcriptomic analysis of Cyanothece 51142 reveals robust**

diurnal oscillation of central metabolic processes. *Proc Natl Acad Sci USA* 2008, **105**:6156.

164. Takano S, Tomita J, Sonoike K, Iwasaki H: **The initiation of nocturnal dormancy in Synechococcus as an active process.** *BMC Biol* 2015, **13**:36.

165. Zinser ER, Lindell D, Johnson ZI, Futschik ME, Steglich C, Coleman ML, Wright MA, Rector T, Steen R, McNulty N, Thompson LR, Chisholm SW: **Choreography of the Transcriptome, Photophysiology, and Cell Cycle of a Minimal Photoautotroph, Prochlorococcus**. *PLoS ONE* 2009, **4**:e5135–18.

166. Nakamoto H, Suzuki N, Roy SK: **Constitutive expression of a small heat-shock protein confers cellular thermotolerance and thermal protection to the photosynthetic apparatus in cyanobacteria.** *FEBS Letters* 2000, **483**:169–174.

167. Sakthivel K, Watanabe T, Nakamoto H: **A small heat-shock protein confers stress tolerance and stabilizes thylakoid membrane proteins in cyanobacteria under oxidative stress**. *Arch Microbiol* 2009, **191**:319–328.

168. Nakamoto H, Honma D: **Interaction of a small heat shock protein with light-harvesting cyanobacterial phycocyanins under stress conditions**. *FEBS Letters* 2006, **580**:3029–3034.

169. Guerreiro ACL, Benevento M, Lehmann R, van Breukelen B, Post H, Giansanti P, Altelaar AFM, Axmann IM, Heck AJR: **Daily rhythms in the cyanobacterium Synechococcus elongatus probed by high-resolution mass spectrometry based proteomics reveals a small-defined set of cyclic proteins.** *Mol Cell Proteomics* 2014.

170. Matallana-Surget S, Derock J, Leroy B, Badri H, Deschoenmaeker F, Wattiez R: **Proteome-Wide Analysis and Diel Proteomic Profiling of the Cyanobacterium Arthrospira platensis PCC 8005**. *PLoS ONE* 2014, **9**:e99076–12.

171. Aryal UK, Stöckel J, Krovvidi RK, Gritsenko MA, Monroe ME, Moore RJ, Koppenaal DW, Smith RD, Pakrasi HB, Jacobs JM: **Dynamic proteomic profiling of a unicellular cyanobacterium Cyanothece ATCC51142 across light-dark diurnal cycles**. *BMC Systems Biology* 2011, **5**:194.

172. Lindahl M, Kieselbach T: **Disulphide proteomes and interactions with thioredoxin on the track towards understanding redox regulation in chloroplasts and cyanobacteria.** *J Proteomics* 2009, **72**:416–438.

173. Sadler NC, Melnicki MR, Serres MH, Merkley ED, Chrisler WB, Hill EA, Romine MF, Kim S, Zink EM, Datta S, Smith RD, Beliaev AS, Konopka A, Wright AT: **Live Cell Chemical Profiling of Temporal Redox Dynamics in a Photoautotrophic Cyanobacterium**. *ACS Chem Biol* 2014, **9**:291–300.

174. Zaffagnini M, Bedhomme M, Marchand CH, Morisse S, Trost P, Lemaire SD: **Redox regulation in photosynthetic organisms: focus on glutathionylation.** *Antioxid Redox Signal* 2012, **16**:567–586.

175. Kuo J, Khosla C: **The initiation ketosynthase (FabH) is the sole rate-limiting enzyme of the fatty acid synthase of Synechococcus sp. PCC 7002.** *Metabolic Engineering* 2014, **22**:53–59.

176. Ishiura M, Kutsuna S, Aoki S, Iwasaki H, Andersson CR, Tanabe A, Golden SS, Johnson CH, Kondo T: **Expression of a gene cluster kaiABC as a circadian feedback process in cyanobacteria**. *Science* 1998, **281**:1519–1523.

177. Nakajima M, Imai K, Ito H, Nishiwaki T, Murayama Y, Iwasaki H, Oyama T, Kondo T: **Reconstitution of circadian oscillation of cyanobacterial KaiC phosphorylation in vitro**. *Science* 2005, **308**:414–415.

178. Williams SB, Vakonakis I, Golden SS, LiWang AC: **Structure and function from the circadian clock protein KaiA of Synechococcus elongatus: a potential clock input mechanism**. *Proc Natl Acad Sci USA* 2002, **99**:15357–15362.

179. Iwasaki H, Williams SB, Kitayama Y, Ishiura M, Golden SS, Kondo T: **A KaiC-interacting sensory histidine kinase, SasA, necessary to sustain robust circadian oscillation in cyanobacteria**. *Cell* 2000, **101**:223–233.

180. Smith RM, Williams SB: **Circadian rhythms in gene transcription imparted by chromosome compaction in the cyanobacterium Synechococcus elongatus**. *Proc Natl Acad Sci USA* 2006, **103**:8564–8569.

181. Takai N, Nakajima M, Oyama T, Kito R, Sugita C, Sugita M, Kondo T, Iwasaki H: **A KaiC-associating SasA-RpaA two-component regulatory system as a major circadian timing mediator in cyanobacteria.** *Proc Natl Acad Sci USA* 2006, **103**:12109–12114.

182. Schmitz O: **CikA, a Bacteriophytochrome That Resets the Cyanobacterial Circadian Clock**. *Science* 2000, **289**:765–768.

183. Mackey SR, Choi JS, Kitayama Y, Iwasaki H, Dong G, Golden SS: **Proteins Found in a CikA Interaction Assay Link the Circadian Clock,**

Metabolism, and Cell Division in Synechococcus elongatus. *J Bacteriol* 2008, **190**:3738–3746.

184. Wood TL, Bridwell-Rabb J, Kim Y-I, Gao T, Chang Y-G, LiWang A, Barondeau DP, Golden SS: **The KaiA protein of the cyanobacterial circadian oscillator is modulated by a redox-active cofactor.** *Proc Natl Acad Sci USA* 2010, **107**:5804–5809.

185. Paddock ML, Boyd JS, Adin DM, Golden SS: **Active output state of the Synechococcus Kai circadian oscillator.** *Proc Natl Acad Sci USA* 2013.

186. van Alphen P, Hellingwerf KJ: **Sustained Circadian Rhythms in Continuous Light in Synechocystis sp. PCC6803 Growing in a Well-Controlled Photobioreactor**. *PLoS ONE* 2015, **10**:e0127715–12.

187. Doi R, Oishi K, Ishida N: **CLOCK regulates circadian rhythms of hepatic glycogen synthesis through transcriptional activation of Gys2.** *Journal of Biological Chemistry* 2010, **285**:22114–22121.

Chapter 2

The Circadian Oscillator in *Synechococcus elongatus* Controls Metabolite Partitioning During Diurnal Growth

2.1 Abstract

Growth of engineered cyanobacteria in outdoor environments is increasingly considered for large-scale bio-production of industrial products. *Synechococcus elongatus* PCC 7942 is a genetically tractable model cyanobacterium that has been successfully engineered to produce industrially relevant biomolecules, and it is the best-studied model for a prokaryotic circadian clock. However, the organism is commonly grown in continuous light in the laboratory, and data on metabolic processes in a diel cycle are lacking. Moreover, the influence of the circadian clock on diurnal metabolism has been only briefly investigated. Here, we demonstrate that the circadian oscillator influences rhythms of metabolism during diurnal growth, even though light-dark cycles can drive metabolic rhythms when a key oscillator protein, KaiC, is absent. Moreover, the phenotype associated with loss of KaiC is distinct from that caused by absence of the circadian output transcriptional regulator, RpaA. While RpaA activity is important for carbon degradation at night and survival in a diel cycle, KaiC is dispensable for those

processes. Untargeted metabolomics analysis and glycogen kinetics suggest that functional KaiC is primarily important for metabolite partitioning when cells re-enter a light period. Additionally, output from the oscillator primarily functions to inhibit RpaA activity at morning time points, as mimetic strains locked in the morning KaiC-pST phosphostate phenocopy *ΔrpaA* strains. Inhibition of RpaA by the oscillator in the morning suppresses metabolic processes that are normally active at night, and a *kaiC*-null strain shows indications of oxidative pentose phosphate pathway activation as well as increased abundance of primary metabolites. Overall, inhibitory clock output may serve to allow secondary metabolite biosynthesis in the morning, and some of the metabolites resulting from these processes likely feedback to reinforce clock timing.

2.2 Introduction

Cyanobacteria comprise a promising engineering platform for the production of fuels and industrial chemicals. These organisms have already been engineered to produce ethanol, isobutyraldehyde, alkanes, and hydrogen [1-4]. However, the efficient industrial-scale application of these photosynthetic organisms will require their growth and maintenance in the outdoors where they will be subjected to light-dark (LD) cycles [5]. Phototrophic cyanobacteria present a novel engineering challenge relative to heterotrophic bacteria such as *Escherichia coli*: their cellular activities respond strongly to the presence

and absence of light because their metabolism is centered around photosynthesis [6, 7]. Diverse cyanobacteria also possess a true circadian clock that synchronizes with external LD cycles, and has been demonstrated to drive both gene expression and metabolic rhythms [8-10]. It is important to understand how signals from the external environment and the internal circadian clock are integrated to modulate metabolic processes in environmentally relevant LD cycles in order to optimize the engineering of these organisms. In this work we attempt to separate the influences of environment and circadian control using the cyanobacterium *Synechococcus elongatus* PCC7942, as it is both a highly tractable genetic system and the foundational model for the prokaryotic circadian clock.

The circadian clock in *S. elongatus* is based on a central oscillator formed by the proteins KaiA, KaiB, and KaiC [11]. The reversible phosphorylation of KaiC over a 24-h period sets the timing of the clock mechanism. The clock synchronizes to the environment through KaiA and a histidine protein kinase, CikA. Both proteins bind quinone cofactors, likely plastoquinone present in the photosynthetic membrane, that reflect the cellular redox state [12, 13]. KaiC activity is also modulated by the cellular ATP/ADP ratio [14], and both the cellular redox state and ATP/ADP ratio are dependent on external light availability. Thus, it has been demonstrated that changes in energy metabolism feed back in setting the timing of clock oscillations [15]. The output of the clock is relayed to gene expression through

the SasA-RpaA two-component system [16], in which RpaA is a transcription factor that binds over 170 gene targets. Many of the genes strongly activated by RpaA function in nighttime metabolic processes, including glycogen degradation, glycolysis, and the oxidative pentose phosphate pathway (OPPP) [17].

Under constant-light (LL) growth conditions circadian control in *S. elongatus* is quite pervasive, with up to 64% of transcripts displaying 24-h clock-dependent oscillations [10]. Gene expression has roughly two distinct phases in LL: genes with an expression peak at subjective dusk (Class 1) and genes with an expression peak at subjective dawn (Class 2) [18]. Recent work by Paddock et al. suggests that a single output from the central oscillator is responsible for both out-of-phase rhythms, and that the oscillator has maximum output activity in the morning when KaiC-pST becomes the most prevalent phosphorylation state [19]. Furthermore, there is evidence that oscillator activity is inhibitory [20], and rhythms may manifest as different responses to the alleviation and return of this inhibition over a daily period. It is also likely that metabolism is strongly influenced by the clock in constant light, as a statistically high proportion of genes involved in energy metabolism are rhythmic in LL [21]. However, no metabolic pathways are specifically enriched in Class 1 or Class 2 genes with the exception of ribosome biogenesis and photosynthesis, respectively [10].

A few studies have investigated the transcriptome, proteome, and physiological dynamics of particular species of cyanobacteria over a 24-h period under LD growth [6, 22, 23]. In general, systems for oxygenic photosynthesis are activated during the day and systems for respiratory metabolism are activated at night. Additionally, the day and night periods are used by cyanobacteria to segregate incompatible metabolic processes [22]. For example, *S. elongatus* activates light-independent protochlorophilide reduction, which is an oxygen-sensitive process, at night, a time when oxygen is not being produced by photosystem II [24]. However, the degree to which the circadian clock and light availability independently affect metabolic events is poorly understood. In *S. elongatus*, there are only two studies that investigate the behavior of mutants that lack a functional clock under an LD cycle [21, 25]. The available studies investigate these effects only over a light-to-dark transition, so there is currently an incomplete understanding of the circadian influence on cellular events over a full 24-h LD cycle. Finally, while there is a proteomics dataset for *S. elongatus* that covers a full 24-h LD period, that study tracked only wild-type (WT) cells and does not de-couple clock and environmental influences [23].

When cyanobacteria are grown in a 24-h LD cycle, cells perform photosynthesis and store fixed carbon as the branched glucose polymer glycogen during the day. Glycogen is subsequently degraded at night for energy and reducing power via the OPPP [26, 27]. Pattanayak et al. recently

showed that glycogen in *S. elongatus* oscillates in LL and that this oscillation depends on a functional clock [1-4, 15]. Rhythms of glycogen accumulation and degradation have also been observed during LD growth in *S. elongatus* [28]; however, the influence of the clock under LD conditions is not clear. In fact, enzymes in glycogen metabolism are sensitive to cellular redox state and LD transitions alone may trigger changes in glycogen content [29]. Glycogen is essential for survival in LD: mutants defective for the *glgA* or *glgC* genes, which are required for glycogen synthesis, are not viable under LD growth regime**s** [30]. In turn, deletion of the OPPP gene *zwf* or glycolysis gene *gap1*, both of which participate in pathways that consume glycogen, results in mutants that are impaired in LD growth [31, 32]. Null mutations in the circadian oscillator, including deletions of *kaiA, kaiB,* or *kaiC*, do not impair LD growth. However, disruptions in the SasA-RpaA clock output pathway dramatically stifle growth in LD [16, 33], and genes involved in catabolism of carbon including *glgP*, *gap1*, and *zwf* are all known RpaA targets [17]. Thus, while the clock output pathway likely activates important metabolic processes that occur at night, it is not clear if or how the circadian oscillator modulates these processes.

In this study we applied genetic, biochemical, and metabolomic methods to *S. elongatus* to dissect how the circadian oscillator and activation of the clock output pathway specifically control metabolism under an LD growth regime. We tracked glycogen content in WT and a Δ*kaiC* mutant over

a 72-h time course under both LL and LD conditions. Subsequently, we characterized glycogen kinetics at LD transitions in WT, Δ*kaiC*, Δ*rpaA*, and a Δ*kaiC*::KaiC-pST phosphomimetic mutant (KaiC-ET) to address whether circadian oscillator output exerts a negative or positive control over glycogen levels. Finally, we performed untargeted metabolic profiling of WT and Δ*kaiC* mutants to investigate how oscillator activity affects global metabolite abundance at the transition from darkness into light. We present a hypothesis for clock regulation of diurnal metabolism that combines our data with previous reports on *S. elongatus* transcript and protein rhythms [17, 21, 23] and that highlights the importance of circadian output for proper metabolite partitioning under LD growth regimes.

2.3 Results

2.3.1 The Circadian Clock Segregates Anabolic and Catabolic Carbon Metabolism in LL.

To determine whether carbon metabolic pathways are under circadian control we mined existing datasets using a bioinformatic approach that breaks larger pathways into anabolic and catabolic components. Using the Kyoto Encyclopedia of Genes and Genomes (KEGG) we determined which reactions of glycolysis, OPPP, and the Calvin Cycle act exclusively within the OPPP (catabolic) or the Calvin Cycle (anabolic). We subsequently annotated

the enzymes that enable these reactions with their circadian class of transcript (peaks at dusk = Class 1 and at dawn = Class 2) using available microarray data collected from cells grown in LL [10]. Our analysis showed that catabolic reactions are catalyzed exclusively by enzymes with Class 1 gene expression profiles whereas anabolism is catalyzed almost exclusively by enzymes with Class 2 gene expression profiles (**Figure 2-1A and 2-1B**).

Like the OPPP and the Calvin Cycle, glycogen metabolism shows strong temporal segregation in the expression of anabolic and catabolic pathway genes (**Figure 2-1A, boxed inset**). To gauge circadian influence on cellular flux of carbon we tracked glycogen content for 72 h in WT and a clockless Δ*kaiC* mutant grown in a photobioreactor under constant and stringently controlled turbidity, temperature, and light conditions (**Materials and Methods**). A recent report from Pattanayk, et al. demonstrated that WT cells show 24-h glycogen oscillations under LL conditions, whereas Δ*kaiC* mutants lack these oscillations [15]. Our data confirmed a *kaiC*-dependent 24-h rhythm of glycogen oscillation in LL (period = 24.7±0.13 h) (**Figure 2-2A**). We propose that oscillations in glycogen content under constant light conditions result from clock-controlled oscillations of gene expression that segregate pathways for storage and degradation of carbon temporally.

A

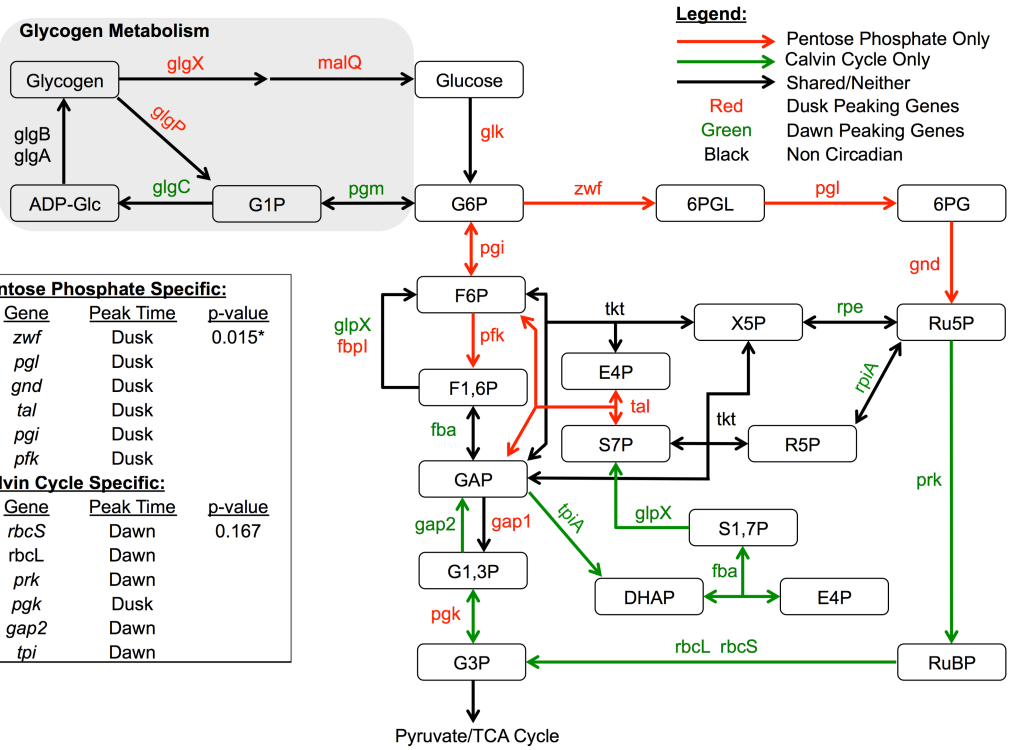

B

Pentose Phosphate Specific:

Gene	Peak Time	p-value
zwf	Dusk	0.015*
pgl	Dusk	
gnd	Dusk	
tal	Dusk	
pgi	Dusk	
pfk	Dusk	

Calvin Cycle Specific:

Gene	Peak Time	p-value
rbcS	Dawn	0.167
rbcL	Dawn	
prk	Dawn	
pgk	Dusk	
gap2	Dawn	
tpi	Dawn	

Figure 2-1. Overview of shared metabolic pathways among glycolysis, the OPPP, and the Calvin cycle, as well as the circadian patterns of genes for their enzymatic steps. (A) A diagram of the metabolic pathway which includes overlapping reactions from glycolysis, the OPPP, and the Calvin cycle and overlays the timing of circadian gene expression onto each pathway. Genes exclusively part of the OPPP generally peak at dusk (red), whereas genes exclusively part of the Calvin cycle generally peak at dawn (green). Additionally, glycogen metabolism (gray box) shows a similar pattern in which anabolic genes peak at dawn and catabolic genes peak at dusk. **(B)** The table indicates the probability of observing the set of coincident peak times strictly by chance. P values were calculated using Fisher's exact test. 6PG, 6-phosphogluconate; 6PGL, 6-phosphogluconolactone; ADP-Glc, ADP-glucose; DHAP, dihydroxyacetone phosphate; E4P, erythrose- 4-phosphate; F1,6P, fructose-1,6-bisphosphate; F6P, fructose-6-phosphate; G1,3P, 1,3-bisphosphoglycerate; G1P, glucose-1-phosphate; G3P, 3-phosphoglycerate; G6P, glucose-6-phosphate; GAP, glyceraldehyde-3-phosphate; R5P, ribose-5-phosphate; Ru5P, ribulose-5-phosphate; RuBP, ribulose-1,5-bisphosphate; S1,7P, sedoheptulose-1,7-bisphosphate; S7P, sedoheptulose-7-phosphate; X5P, xylose-5-phosphate.

2.3.2 During LD Growth KaiC has a Repressive Effect on Glycogen Synthesis, and is not Required for Glycogen Degradation

The daily oscillations in glycogen abundance that occur when cells are grown in a 24-h LD cycle [28] could be controlled by the circadian oscillator or driven by the environmental cycle. We observed glycogen synthesis and degradation rhythms in both WT and a *ΔkaiC* mutant during growth in an 12:12 LD cycle over a 72-h period (**Figure 2-2B**). Thus, the environment can drive cycles of glycogen accumulation independently of the clock. However, the kinetics of glycogen accumulation were different between the WT and Δ*kaiC* strains. Kinetic profiling revealed that accumulation of glycogen in Δ*kaiC* mutants occurs significantly faster during the 12-h light period than in WT, particularly within the first 6-h of light exposure (**Figure 2-3A and 2-3B**). More rapid accumulation resulted in glycogen reaching its peak content 4-5 h earlier in the Δ*kaiC* mutants than in WT. The Δ*kaiC* mutant had different rates of glycogen accumulation in the first and last 6-h blocks of the light period, whereas accumulation in WT was maintained at a steady rate over the full 12-h period (**Figure 2-3B**). Also, Δ*kaiC* mutants had higher overall glycogen levels than WT cells through the time course (**Supplementary Figure 2-S1**). Thus the rapid observed accumulation kinetics are not the result of normalization to a smaller starting pool size, but occur despite elevated glycogen content in these cells.

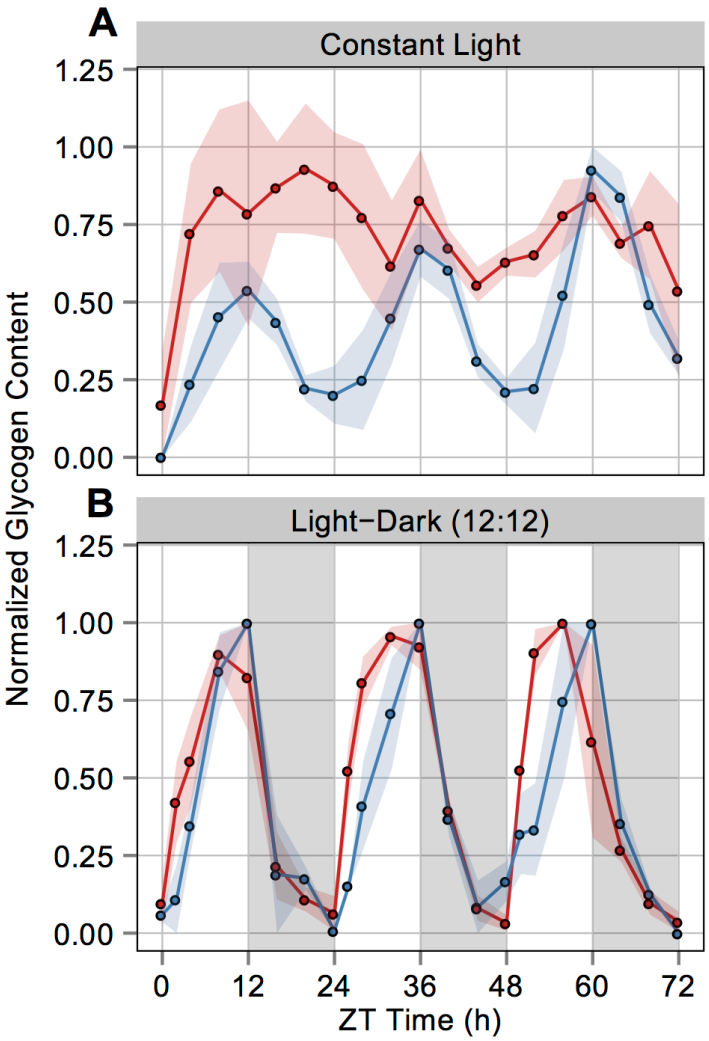

Figure 2-2. Average of normalized glycogen content in WT and ΔkaiC strains of S. elongatus over a 72-h period under both LL and LD growth conditions. The area of shaded color around the solid lines represents SEM. ZT0 represents subjective dawn after circadian entrainment (Materials and Methods). **(A)** Glycogen sampling every 4 h from cells grown in LL for 72 h. The WT (blue) strain shows a 24-h rhythm of glycogen content, whereas ΔkaiC (red) has arrhythmic fluctuations. Glycogen was normalized for each biological replicate to the maximum value in that replicate's 72-h period; the solid line is the av- erage of these values. The experiment was performed in triplicate for each strain. **(B)** Glycogen sampling every 4 h from cells grown in alternating periods of 12 h light and 12 h darkness; darkness is indicated by the gray bars. Both WT (blue) and ΔkaiC (red) strains display a 24-h rhythm of glycogen content. Glycogen was normalized for each biological replicate to the maximum value in that repli- cate's 24 h period; the solid line is the average of these values. The experiment was performed in duplicate for WT cells and in triplicate for ΔkaiC.

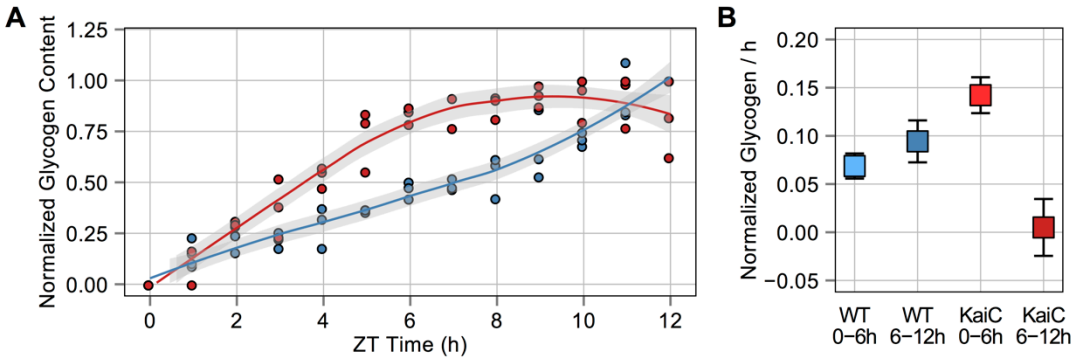

Figure 2-3. Summary of glycogen accumulation data over a 12-h light period collected from WT and ΔkaiC cells growing in a 12:12 LD cycle. (A) Normalized glycogen content from WT (blue circles) and ΔkaiC (red circles) cells collected at 1-h intervals after cells were released into the light. Glycogen content for each replicate was normalized to the maximum value in the 12-h period. The data indicate that ΔkaiC accumulates glycogen more rapidly than WT early in the day. Best-fit curves were calculated for WT (blue line) and ΔkaiC (red line) cells using LOESS regression; the gray shaded area indicates the 95% CI for the regression line. Sampling for each strain was conducted in triplicate. **(B)** Slope calculated using liner regression of normalized glycogen content for the given time intervals. The glycogen accumulation rate for WT does not significantly differ over the time course, whereas ΔkaiC displays significantly different rates of glycogen accumulation in the first and last 6 h of the day period. The ΔkaiC strain also shows significantly more rapid accumulation than WT in the first 6 h. Error bars indicate the 95% CI of the slope estimate. Each slope was calculated from 18 data points.

In contrast, kinetic profiling of glycogen degradation when cultures were transferred to darkness showed little difference between WT and Δ*kaiC* strains (**Figure 2-4A and Supplementary Figure 2-S2**). In all tested cases glycogen degradation could be modeled as a first-order decay process. The decay constant for Δ*kaiC* was slightly higher than that for WT (λ_{KaiC} = 0.318±0.069 ; λ_{WT} = 0.210±0.022). However, the terminal glycogen fraction after a night period was not significantly different for the two strains (G_24h_{KaiC} = 0.186±0.062 ; G_24_{WT} = 0.125±0.039). Thus, although glycogen degradation occurs slightly faster in the Δ*kaiC* strain, both strains degrade a similar fraction of their glycogen over the night period. These data demonstrate that the circadian oscillator refines the timing of glycogen accumulation so that it occurs at a constant rate through the light period, whereas darkness is sufficient to drive glycogen degradation. The kinetics observed when the clock is disrupted suggest that oscillator output has a negative effect on glycogen accumulation rate. This is further supported by an increased overall glycogen content observed when the oscillator is not present.

2.3.3 RpaA Activity is Important for Glycogen Degradation and Viability in LD, and is Negatively Regulated by Oscillator Output

Mutations in the SasA-RpaA circadian output pathway result in acute LD sensitivity [16]. To determine whether disruptions in the circadian output

pathway affect carbon catabolism at night we tracked glycogen degradation kinetics in a Δ*rpaA* mutant. Subsequently, we evaluated how the circadian oscillator affects RpaA activity by additionally tracking glycogen degradation kinetics in a Δ*kaiC*::KaiC-pST phosphomimetic mutant (KaiC-ET). In the KaiC-ET mutant the circadian oscillator is locked in the most active output state, which is most prevalent in the morning of a circadian cycle [19]. Thus, we can assess how active output from KaiC affects downstream RpaA activity with respect to glycogen metabolism.

The RpaA-null mutant displayed an initial drop in glycogen content but terminated glycogen degradation much earlier than WT (**Figure 2-4B and Supplementary Figure 2-S2)**. The terminal glycogen fraction determined by our model for Δ*rpaA* (G_24h_{RpaA} = 0.585±0.071) is significantly higher than that determined for WT (G_24h_{WT+km} = 0.222±0.085). However, the decay constant during the time glycogen degradation is active in each strain is not significantly different for Δ*rpaA* (λ_{RpaA} = 0.607±0.364) and WT (λ_{WT+km} = 0.291±0.077). The primary difference between the two strains is that glycogen degradation in Δ*rpaA* is incomplete and an unusually large fraction of glycogen remains in these strains at the end of a night period. The KaiC-ET mutant showed a glycogen degradation defect similar to that of Δ*rpaA* (**Figure 2-4C and Supplementary Figure 2-S2**). The decay constant does not significantly differ from WT ($\lambda_{WT+SpSm}$ = 0.165±0.062 ; $\lambda_{KaiC-ET}$ = 0.294±0.085); however, the terminal glycogen fraction was again significantly higher in this

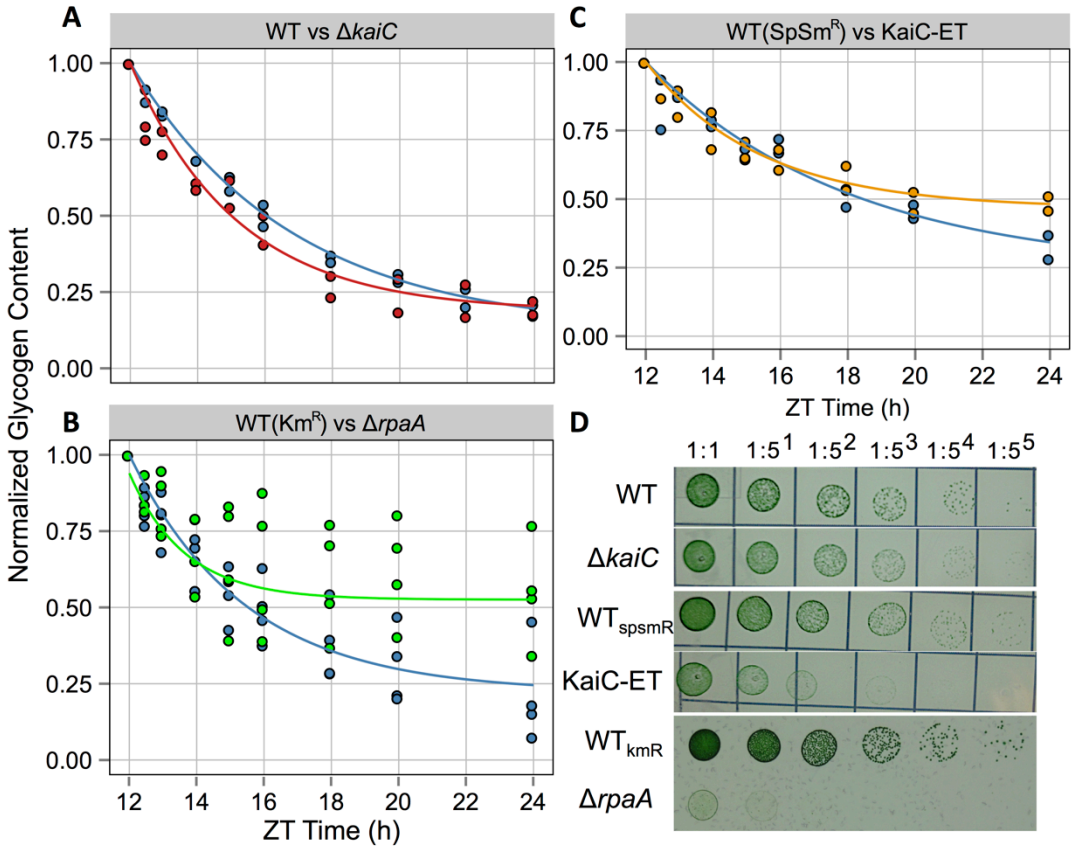

Figure 2-4. Summary of glycogen degradation data and LD growth phenotypes for WT, ΔkaiC, ΔrpaA, and KaiC-ET strains. Samples for all glycogen degradation rate experiments were collected at 0, 0.5-, 1-, 2-, 3-, 4-, 6-, 8-, and 12-h time points after cells entered a dark period during a 12:12 LD diurnal cycle. Glycogen content for each replicate was normalized to the glycogen value at 12 h after lights on. The best fit for each set of data was modeled using first-order decay and is indicated by a solid line; coefficients are given in the text. **(A)** Normalized glycogen content from WT (blue circles) and ΔkaiC (red circles). First-order decay model for WT (blue line) and ΔkaiC (red line) indicates that glycogen degradation is similar in these strains. The experiment was performed in duplicate for both strains. **(B)** Normalized glycogen content from WT (blue circles) and ΔrpaA (green circles). The first-order decay model for WT (blue line) and ΔrpaA (green line) indicates that glycogen degrada- tion is severely attenuated in the ΔrpaA strain. The experiment performed in quadruplicate because of the known high variability in the ΔrpaA strain. **(C)** Normalized glycogen content from WT (blue circles) and KaiC-ET (orange circles). The first-order decay model for WT (blue line) and KaiC- ET (green line) indicates that glycogen degradation is attenuated in the KaiC-ET strain. The experiment was performed in duplicate. **(D)** Dilution series of strains grown on solid BG-11 medium for 5–7 d in a 12:12 LD cycle. (Top) WT and ΔkaiC have similar growth kinetics under these conditions. However, KaiC-ET (Middle) and ΔrpaA (Bottom) have severely attenuated growth when grown in a diel cycle. Images are representative of multiple experiments.

strain ($G\_24h_{WT+SpSm}$ = 0.238±0.154 ; $G\_24h_{KaiC-ET}$ = 0.466±0.062). KaiC-ET mutants also exhibit an LD growth defect similar to, yet less severe than, that of Δ*rpaA*. (**Figure 2-4D**).

The results suggest that KaiC output activity has a negative effect on RpaA activity, as the KaiC-ET phosphomimetic is locked in the most active output state of the clock, and phenocopies an RpaA-null strain. This finding agrees with previous reports that over-expression of KaiC has a repressive effect on expression of Class 1 genes, which are normally activated by RpaA [17, 20]. Finally, this result demonstrates that RpaA has a positive effect on carbon catabolism; moreover, the ability to grow in a diel cycle strongly correlates with the extent to which glycogen is metabolized in the dark.

2.3.4 Metabolomic Profiling During Dark-to-Light Transition Reveals that the Clock is Important for Proper Metabolite Partitioning in the Morning

Because disruption of *kaiC* does not cause major changes in glycogen degradation (**Figure 2-4A**)**,** the difference in glycogen accumulation observed between WT and Δ*kaiC* (**Figure 2-3A**) suggests that a functioning circadian oscillator may be important for metabolite partitioning in the morning. To gain a clearer understanding of early-day metabolic changes in an LD cycle, we performed untargeted metabolic profiling using Gas Chromatography - Time of Flight - Mass Spectrometry (GC-TOF-MS) on both entrained WT and Δ*kaiC* strains directly before (0 h) and 4 h after a dark-to-light transition. The

analysis successfully identified 130 known metabolites across a broad array of metabolic pathways and an additional 195 unknown metabolites that correspond to previously observed mass spectra for which no purified standard compound has been matched [34] (**Supplementary Data Set 2-S1**).

2.3.4.1 Factors Contributing to Metabolite Variability

Because both sampling time and genotype potentially contribute to differences between samples we first used Partial Least Squares Discriminate Analysis (PLS-DA) to determine which factors contribute most of the variability in the dataset [35]. Plotting PLS-DA components 1 and 2 showed that the sample replicates are well segregated from each other, and that the variability from genotype differences is captured by component 1, while the variability from sampling time is captured by component 2 (**Figure 2-5A**). Given the association of time and genotype with the respective components, it is apparent that genotype explains a much larger percentage of dataset variability than response to an environmental signal (41.2% and 14.3%, respectively). Also, samples collected at 0 h are not very different from each other, as there is a slight overlap of the 95% CI ellipse between these groupings (**Figure 2-5A**).

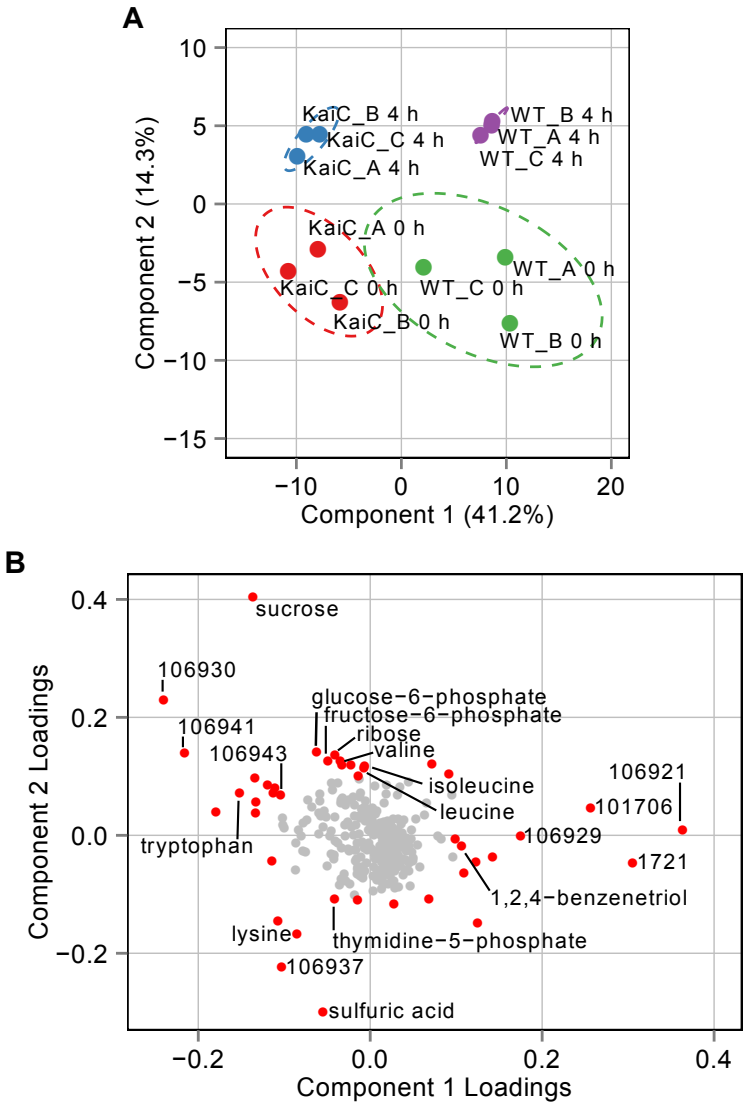

Figure 2-5. Summary of dimension reduction performed on metabolomics data from WT and ΔkaiC cells. (A) Plot of PLS-DA components 1 and 2 for all metabolomics samples. Components 1 and 2 account for 55.5% of the variance in the dataset, and all samples show good clustering by biological replicate. Component 1 associates with genotype-derived variability, whereas component 2 associates with sampling time-derived variability. Ellipses indicate the 95% CI of each grouping of samples on the plot. “W” indicates a WT sample while “K” indicates a ΔkaiC mutant. The letters A, B, and C represent the three biological replicates taken for each sample time point. **(B)** Loading plot derived from PLS-DA components 1 and 2 indicating the importance of each metabolite to the variability of a given component. Points in red are compounds for which one of the loadings was at least ±0.1. Points in gray are compounds for which no loading was greater than ±0.1. The plot shows that many unknown compounds drive variability in component 1 whereas known and unknown compounds drive variability in component 2.

A loading plot was produced that gives a relative score of how much an individual compound influences the variability of each component among samples (**Figure 2-5B**). Unknown compounds contribute strongly to genotype-derived variability (Component 1), whereas many compounds that contribute to sampling-time-derived variability (Component 2) are known primary metabolites such as glucose-6-phosphate and branched-chain amino acids. The connection of primary metabolites to time is indicative of the activation of primary metabolism after a dark-to-light transition. Some metabolites also contribute strongly to both components. These metabolites, such as sucrose and tryptophan, are interesting because, although they change after the dark-to-light transition, the nature of their variability is strongly affected by the presence or absence of KaiC. Overall, status of the circadian oscillator contributes more to the variability than a dark-to-light transition. Strikingly, the compounds that contribute most strongly to genotype-related differences are unknowns. Finally, it is likely that metabolic differences accumulate over the time course, as the most divergent samples are the WT and Δ*kaiC* mutant at 4 h after lights on.

2.3.4.2 Metabolites Significantly Altered in Dynamics or Abundance

We identified 21 known and 29 unknown compounds that differed significantly in at least one pair-wise comparison between sample types (**Supplementary Data Set 2-S1**). Based on PLS-DA we focused on

compounds that: (i) changed significantly between the 0 h and 4 h time points (**Figure 2-6A**), and (ii) had significantly different abundances between WT and *ΔkaiC* at the 4 h time point (**Figure 2-6B**). The metabolites that changed significantly over time in both WT and Δ*kaiC* are primarily known metabolites (**Figure 2-6A and Table 2-1**). Also, the direction of change over time was similar for many of these compounds in both strains. In contrast the majority of metabolites (11 of 12) that change over time only in WT are unknown species. Some of these metabolites, such as BBID#106943 and BBID#101299, change strongly with time in WT cells but show effectively no change over time in the *kaiC* mutant (**Figure 2-6A and Table 2-1**). Only 4 compounds changed significantly over time uniquely in Δ*kaiC*. One target, fructose-6-phosphate, is a known intermediate of the OPPP and shows a 4-fold increase. Previous work on *S. elongatus* suggests that flux through this compound is indicative of OPPP activity [36]. Additionally, the Δ*kaiC* mutant showed a 2.5-fold decrease of the unknown BBID#106921. This compound shows opposite metabolic movement between genotypes over the time course.

In Δ*kaiC* a number of primary metabolites were elevated by 4 h in the light relative to WT (**Figure 2-6B**). Most notably, sucrose was elevated more than 6-fold. Glucose-6-phosphate, fructose-6-phosphate, and inulotriose, which are connected to glycolysis, the OPPP, and glycogen biosynthesis, were also significantly elevated (**Figure 2-6B and 2-6C**). Tryptophan, a

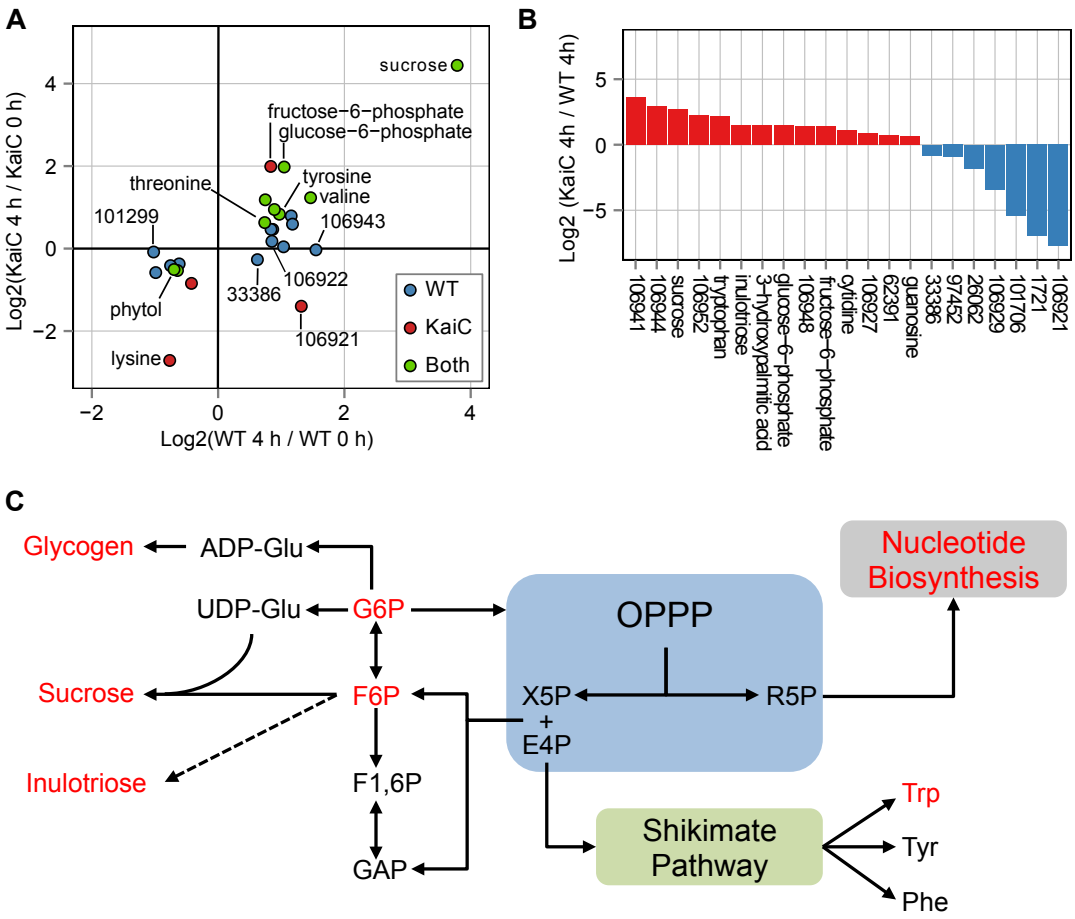

Figure 2-6. Summary of metabolites that differ significantly in the WT and ΔkaiC strains. **(A)** Scatter plot of metabolites that show a significant change in abundance from 0 h to 4 h in WT, ΔkaiC, or both strains. A significant change of a compound in a strain is indicated by the dot color. The log2 fold change from 0 h to 4 h after entering light is indicated on the x axis for WT and on y axis for ΔkaiC strains. **(B)** Plot of all metabolites that differ in abundance between WT and ΔkaiC at the 4-h sampling time point. Metabolite bars in red are significantly elevated and metabolite bars in blue are significantly reduced in ΔkaiC relative to WT. Although many primary metabolites are relatively elevated in ΔkaiC strains, all the metabolites in which ΔkaiC is reduced relative to WT are unknown compounds. Some of the unknowns are >100-fold less abundant in ΔkaiC strains. **(C)** Pathway diagram detailing the interconnections of the OPPP to glycolysis/glycogen metabolism, the Shikimate pathway, and nucleotide metabolism and indicating compounds that were significantly elevated in ΔkaiC relative to WT at the 4-h time point (red). Many of the elevated metabolites share the OPPP as a precursor hub; the monomers of many elevated sugar polymers were elevated also.

product of the shikimate pathway, which is directly fed by the OPPP, was ~4.5-fold more abundant in Δ*kaiC* at 4 h. In contrast, a number of unknown compounds that were very abundant in WT had extremely depressed levels in Δ*kaiC* mutants. Two of these compounds, BBID#106921 and BBID#1721, were more than 100-fold less abundant in Δ*kaiC*, but they were the 3rd and 6th most abundant compounds detected in WT at 4 h, respectively (**Figure 2-6B and Table 2-2**). In Δ*kaiC* these metabolites are only the 219th and 187th most abundant at 4 h, respectively.

In summary, the inactivation of *kaiC* appears to have a direct impact on how metabolites are partitioned in the cell after a dark-to-light transition. Both strains increase pool sizes of primary metabolites over the time course; however; Δ*kaiC* accumulates much larger amounts of primary metabolites, specifically those involved in and directly connected to the OPPP, such as fructose-6-phosphate and sucrose. In contrast, WT cells mobilize carbon into a number of unknown compounds that are present only at low levels in Δ*kaiC* and make up a significant portion of the overall WT sample.

2.3.5 Correlations in Metabolite Abundance can Help Classify Unknown Compounds

To identify shared pathways and suggest biochemical context for the unknown metabolites that change remarkably in WT, we applied inter-metabolite correlation analysis to look for groups of metabolites that share

similar patterns of abundance [37]. We compared the set of 50 metabolites with significant changes identified by ANOVA, which includes our unknown metabolites of interest (**Supplementary Data Set 2-S1**), to all of the known metabolites that were used in the ANOVA analysis (**Materials and Methods**). Pearson correlations were computed between the abundances of compounds in these two groups, which contained 50 and 111 compounds, respectively (**Supplementary Data Set 2-S2**). This analysis yielded 5,550 correlation coefficients from all possible pairwise comparisons. Subsequently, we used hierarchical clustering to group the correlation coefficients into clusters with similarity to each other. For the 50 metabolites with at least one significant change between samples we could identify 3 distinct groups that we call Target Clusters (TC), for which the correlations to the 111 known metabolites formed a unique pattern. Similarly, when we looked at all 111 known metabolites we could identify 6 distinct groups, which we call Metabolite Clusters (MC), for which a group of known metabolites has a unique pattern of correlations across TCs. The correlations are presented as an ordered heat map with TCs on the x-axis and MCs on the y-axis (**Figure 2-7, Table 2-3, and Supplementary Data Set 2-S2**).

We found that 11 out of 14 metabolites identified as more abundant in Δ*kaiC* at 4 h are clustered in TC2, while all 7 metabolites significantly depressed in KaiC relative to WT at 4 h are found in TC3 (**Table 2-3**). While TC1 and TC2 share similar correlation patterns across the 6 Metabolite

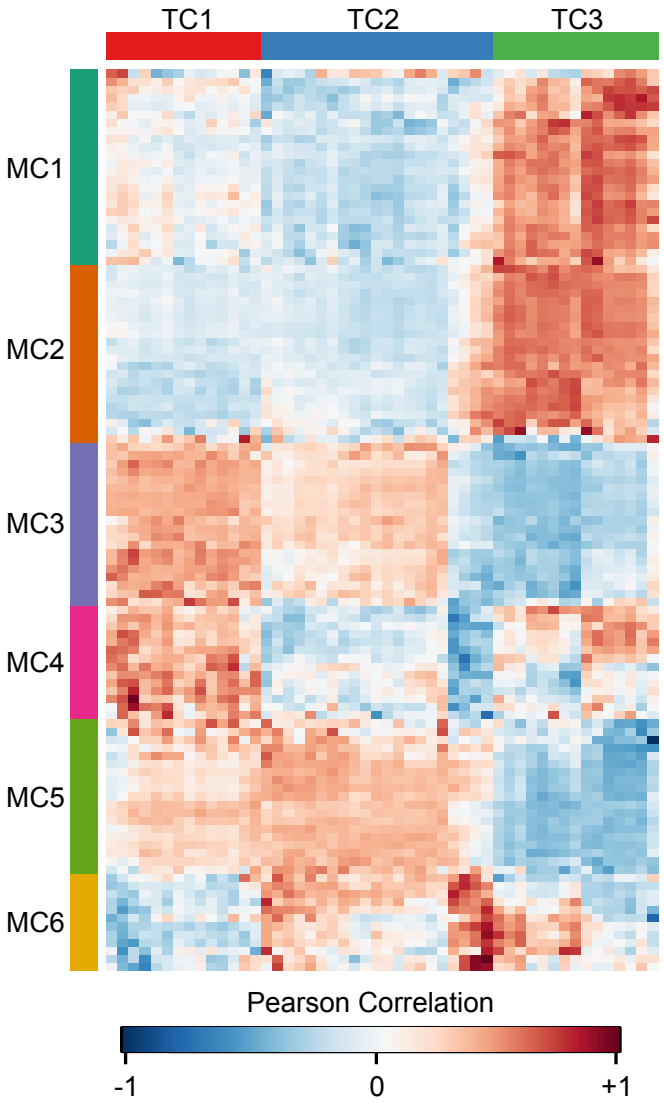

Figure 2-7. Heatmap of the correlation between the groupings of metabolites identified by ANOVA to have some significant change (TCs) and a filtered set of all detected known compounds (MCs). More intense red color indicates the abundance patterns between two compounds in all collected samples are more positively correlated; more intense blue color indicates a negatively correlated abundance pattern. TC1 and TC2 have similar patterns of corre- lations across all known compounds, whereas TC3 displays a unique pattern of correlation. Almost all the unknown compounds that are highly abundant in WT and significantly reduced in ΔkaiC can be found in TC3. Thus, TC3 may give metabolic context to the possible placement of these unknown com- pounds in metabolism.

Clusters, this pattern is very different from TC3's across the same clusters (**Figure 2-7**). TC1 and TC2 correlate positively with MC3 and MC5, and negatively with MC1 and MC2, whereas TC3 has the opposite pattern in that it correlates negatively with MC3 and MC5, and positively with MC1 and MC2 (**Figure 2-7**). The compounds that make up MC3 and MC5 are strongly enriched for roles in primary metabolic pathways such as: Starch and Sucrose Metabolism ($p = 9.95e-7$), the Pentose Phosphate Pathway ($p = 2.20e-6$), Branched Chain Amino Acid Biosynthesis ($p = 3.26e-3$), and Purine Metabolism ($p = 9.99e-4$) (**Supplementary Figure 2-S3**). Thus, TC1 and TC2 represent groupings of metabolites that increase together with primary metabolic activity including sugar phosphates, nucleotides, and amino acids. This pattern is clearly evident in TC1, as this cluster contains many of the primary metabolites that increase in both strains after a dark-to-light transition (**Table 2-3**). In contrast, the compounds that make up MC1 and MC2 are enriched for roles in secondary metabolic pathways such as: Fatty Acid Biosynthesis ($p = 1.96e-3$) and Glycerolipid Metabolism ($p=5.97e-3$) (**Supplementary Figure 2-S3**). MC1 and MC2 also contain a number of benzoate compounds that have been previously detected in cyanobacteria, including benzoic acid and 4-hydroxybenzoate (4HB) [38] (**Supplementary Figure 2-S4 and Supplementary Data Set 2-S2**). Recent work has shown that plastoquinone biosynthesis in cyanobacteria utilizes 4HB as an intermediate [39, 40]. Indeed, the benzoate compounds in MC1 and MC2

correlate negatively with the aromatic amino acids, which are consumed in plastoquinone biosynthesis (**Supplementary Figure 2-S4**). Thus, it is likely MC1 and MC2 are also enriched in compounds with roles in biosynthesis of plastoquinone or other quinone-like molecules. Overall, our correlation analysis suggests that unknown compounds elevated in Δ*kaiC* are primarily located in TC2 and likely function in primary metabolic pathways or increase during their activation. In contrast, the unknown compounds elevated in WT, which are exclusively found in TC3, likely function in secondary metabolic roles associated with lipid, glycerolipid, and possibly quinone biosynthesis.

2.4 Discussion

Prior to this work very limited data were available on the diurnal metabolism of *S. elongatus*, and no study had attempted to de-couple the influences of the circadian clock and dark-to-light transitions on metabolism when cells are grown in a diurnal cycle. Our major conclusions from the collected data are: (i) The output from the core oscillator is dispensable for the degradation of carbon at night in a diel cycle; (ii) KaiC output inhibits RpaA, which serves to block activation of nighttime metabolic processes in the morning; and (iii) The importance of the circadian oscillator with respect to metabolism is primarily to modulate the balance between the Calvin Cycle and the OPPP under diurnal growth conditions. The data are consistent with a model in which the clock serves to negatively regulate RpaA activity and

hence Class 1 gene expression in the morning. A decrease in inhibitory oscillator output over the day would allow RpaA to activate Class 1 genes closer to dusk. This model agrees with data from Paddock et al. suggesting that maximum output activity from the circadian oscillator occurs when KaiC is in the KaiC-pST (KaiC-ET) phosphostate, which is most abundant at dawn [19]. The question remains as to what metabolic processes are driven by RpaA that are important for LD viability. Inactivation of a number of RpaA targets, such as *zwf* and *gnd* in the OPPP, also causes an LD sensitivity phenotype. However, it is unclear where carbon flows at night in *S. elongtatus*, and why these pathways are so critical for survival under these conditions. Our data suggest that normal KaiC output activity primarily affects metabolic processes that occur in the morning, as the largest differences between the WT and *ΔkaiC* strains in both glycogen kinetics and global metabolite partitioning are seen at this time.

The *ΔkaiC* mutant accumulates larger pools of glycogen precursors and primary carbon metabolites early in the day period (**Figure 2-3A and 2-6B**). However, gene expression data from LL conditions show that relative to WT, the *ΔkaiC* mutant has significantly higher morning expression of transcripts involved in glycogen and carbon catabolism [21]. Under diurnal growth conditions it is likely that multiple factors influence the flow of carbon in *S. elongatus* including transcription, allosteric regulation of enzymes, and stoichiometric ratios of metabolites. Upon entering a morning period, when

glycogen stores are low and photosynthesis is active, glycogen levels may not be strongly influenced by transcript levels from catabolism genes, and instead reflect changes in other connected metabolic processes and allosteric regulation of glycogen biosynthetic enzymes. Indeed, GlgC is allosterically activated by the photosynthetic product 3-phosphoglycerate and a reducing cellular environment [29, 41]. Alternatively, when cells enter a dark period, glycogen content is high, and GlgC is allosterically inactive. Under these conditions transcriptional activation by RpaA and availability of degradative transcripts is a primary driving factor in glycogen catabolism. Activation of the OPPP in the morning by RpaA may in fact increase the availability of precursors for glycogen biosynthesis during a time when GlgC is strongly activated.

Other transcriptional changes in the *ΔkaiC* strain may also indirectly affect the regulatory protein CP12, a master regulator of the Calvin Cycle conserved between cyanobacteria and plants [36, 42]. Re-examining the transcriptomics data from LL reveals that two of the most highly up-regulated genes in a *ΔkaiC* mutant are the pyridine nucleotide transhydrogenase subunits A and B (*pntA* and *pntB*), which are also known RpaA targets [17, 21]. Products of these genes allow the interconversion of NADP(H) to NAD(H), and their overexpression may lower the normally high NADP(H)/NAD(H) ratio present during active photosynthesis. In *S. elongatus* low NADP(H)/NAD(H) levels activate CP12, which causes a shift from the

reductive (Calvin Cycle) to oxidative Pentose Phosphate Pathway [36]. In *S. elongatus* inactivation of CP12 resulted in decreased OPPP activity, in which a decrease in cellular fructose-6-phosphate could be directly detected [36]. Additionally, in tobacco plants more active CP12 was associated with more starch, soluble sugars (including sucrose), and amino acids [43]. The metabolic shifts observed in a *ΔkaiC* mutant in the morning mirror those seen when CP12 is active, including increased levels of fructose-6-phosphate, sucrose, nucleotides, and amino acids (**Figure 2-6B and 2-6C**). In contrast, the repression of CP12 in tobacco resulted in accumulation of complex insoluble metabolites such as protein and cell wall components [43]. In WT *S. elongatus* we observe increased abundance of unknowns that correlate strongly with compounds involved in fatty acid and glycerolipid biosynthesis, and both of these biosynthetic pathways would be important for cell wall and membrane biosynthesis in cyanobacteria. Thus, clock control may be important for regulating a shift between Calvin cycle activity and OPPP activity.

These data suggest a model in which KaiC output activity is important for inhibiting RpaA-driven OPPP activity in the morning. Inhibition of OPPP and other primary metabolic pathways frees up carbon such that it can be used in secondary biosynthetic processes. When inhibition of RpaA is relieved it can activate its targets (including *pntA* and *pntB*) such that a lowering of the NADP(H)/NAD(H) ratio and activation of CP12 occurs. The

strong correlation in WT samples of elevated unknown compounds with metabolites that participate in plastoquinone biosynthesis suggests that inhibition of primary metabolism by the clock in the morning may be important for this process (**Supplementary Figure 2-S4**). Accumulation of plastoquinone in the morning would not only support photosynthesis through the day period, but also would be important for its known role in resetting the circadian clock [44]. The influence of the clock on accumulation of these compounds may represent a metabolic feedback loop in which the oscillator output is important for the biosynthesis of compounds that reinforce the correct oscillator timing in LD. In fact, both circadian control over starch metabolism, and metabolic feedback to circadian timing have been previously observed in plants [45, 46]. Thus, there is already some precedent for the existence of circadian timing reinforcement by metabolism in photosynthetic organisms.

Overall, this study highlights the importance of understanding the interaction of the circadian clock with light/dark transitions to gain insights into diurnal physiology and metabolism under day-night cycles. Some aspects of metabolism may be heavily dependent on the circadian clock while others integrate both circadian influences and light availability. The expansion of mass spectral libraries and metabolic networks in photosynthetic organisms will be highly beneficial in determining the response to both internal circadian control and the external environment.

2.5 Materials and Methods

2.5.1 Cyanobacterial Strains, Media, and Culture Conditions

All strains were constructed in the *Synechococcus elongatus* PCC 7942 WT strain archived as AMC06 in our laboratory. Strains were constructed using standard procedures for cyanobacterial transformation [47], and are described in **Table 2-4**. All gene disruptions were validated by PCR of native loci. For all experiments pre-cultures were first prepared by transferring 3 ml of stationary phase culture into 100 ml flasks of fresh BG-11 medium [48] with appropriate antibiotics (5μg/ml Kanamycin or 2μg/ml combination Streptomycin/Spectinomycin). Pre-cultures were grown for 3-4 days at 30°C, 150 RPM shaking, and 150 μE m^{-2} s^{-1} constant light.

For all glycogen tracking and metabolomics experiments the pre-cultures were used to inoculate Phenometrics ePBR v1.1 photobioreactors (Phenometrics Inc.). Polycarbonate bioreactor vessels were inoculated to a volume of 400 ml, OD_{750} = 0.1 in medium that contained appropriate antibiotics. For all experiments temperature was maintained at 30°C, 0.2 μm filtered air was sparged at a rate of 50 ml/min, and light intensity was 150 μE m^{-2} s^{-1}, provided from the top of the culture, whenever lights were on. Controlled airflow was important for reproducibility of glycogen levels. After inoculation all cultures were allowed to grow in LL until OD_{750} = 0.3. Cells were then maintained turbidostatically at this density for the duration of the

experiments. For all strains, with the exception of the dark-sensitive strains Δ*rpaA* and KaiC-ET, circadian rhythms were entrained by growth in a 12:12 LD cycle for 3 days prior to release into experimental conditions and sampling. Dark-sensitive strains were maintained in LL prior to sampling periods.

For testing LD sensitivity pre-cultures were initially diluted to OD_{750} = 0.2, and subsequently serially diluted 1:5 in fresh BG-11 medium 5 times. Drops of 4 ul from each dilution were plated on solid BG-11 medium with appropriate antibiotics and 1 mM $Na_2S_2O_3$. Plates were placed at 30 °C/150 μE m^{-2} s^{-1} constant light for 24 h and subsequently transferred to 30 °C/150 μE m^{-2} s^{-1} constant light 12:12 LD for 5-7 days.

2.5.2 KEGG Pathway Analysis

The KEGG pathways syf00030 (pentose phosphate pathway), syf00710 (carbon fixation in photosynthetic organisms), and syf00010 (glycolysis and gluconeogenesis) were cross-referenced for shared and unshared metabolic reactions. Peak circadian expression of genes that control metabolic pathway reactions was determined by data from Vijayan et al. [10]. The number of dawn- or dusk-peaking genes unique to each pathway was compared to expected numbers of dawn- or dusk peaking genes in a random sample of genes and p-values were calculated using Fisher's Exact Test.

2.5.3 Glycogen Extraction and Analysis

For glycogen assay 10 ml of culture (OD_{750}~0.3) was collected and placed on ice. Cells were collected by centrifugation for 10 min at 5000 RPM and 4 °C. The supernatant fraction was discarded and pellets were frozen at -80 °C. Glycogen was extracted using methods modified from Ernst et al. [49]. Specifically, a solution of 50 µl of sterile water and 200 µl of KOH (30% w/v) was used to resuspend cell pellets, which were then placed at 100 °C for 1.5 h. Glycogen was precipitated from extracts by adding 1 ml of 100% EtOH, and placing extracts on ice for 1 h. Precipitated glycogen was collected by centrifugation. Supernatant was discarded and extracted glycogen was washed two times with 1 ml of 100% ethanol. Extracts were dried in a speed-vac (Labconco Cat#7810010) for 15 min at 60 °C. Extracted glycogen was resuspended in 500 µl of 25 mM Sodium Acetate buffer (pH = 5) and stored over night at 4°C prior to assay. To quantify glycogen 200 µl of each sample as well as purified glycogen standards (250, 200, 150, 100, 50, 25, 0 µg/ml) were mixed with 5 µl (5.5U) of amyloglucosidase (Sigma #10115) and incubated at 37 °C for 1 h. Glucose in the resulting digest was determined by mixing 10 µl of digested glycogen with 190 µl of a solution containing 0.5 U glucose oxidase/0.1U peroxidase (Sigma Cat#G3660), 50 µM Amplex Red (Cayman Chemical Cat#10010469), and 25 mM sodium acetate (pH = 5). Reactions were incubated for 45 min at 23°C and absorbance at 540 nm was

determined with a Tecan Infinite M200 plate reader. Unknown glycogen content was determined by comparison to purified standards and background glucose content was determined by assay of samples untreated with amyloglucosidase.

2.5.4 Glycogen Kinetic Analysis

Glycogen accumulation was modeled using the LOESS algorithm for local fitting with default parameters in the R plotting package ggplot2 [50]. Accumulation rates for early and late time points were modeled using the linear modeling function in the base R statistical package [51]. Glycogen degradation was modeled as a first order decay process using the following mathematical expression: $\mathrm{G}_T = (1 - G_{T12})^{(-\lambda \times T)} + G_{T12}$

Glycogen values (G_T) at the indicated time points (T) were provided to the model. The model was solved for the degradation rate constant (λ) and terminal glycogen content (G_{T12}) using the non-linear least squares function in the base R statistical package [51]. Errors indicated for all modeled coefficients and graphs is presented as values encompassing the 95% confidence interval of the data [52]. All graphics were produced using the R plotting package ggplot2 [50].

2.5.5 Metabolomics and Data Analysis

Strains for metabolomics analysis were grown in photobioreactors as described above. At sampling time points 40 ml of culture was collected over ice in a 50 ml conical tube (n=3 for all samples). Cells were immediately collected by centrifugation for 10 min at 5000 RPM and −10°C. Cell pellets were rapidly frozen in liquid nitrogen and placed at −80°C prior to analysis. During sampling, the glycogen content of cells was tracked and confirmed to be similar to accumulation behavior observed in Fig. 3A. Cell pellets were shipped on dry ice to the West Coast Metabolomics Center at UC Davis for subsequent analysis. Metabolite extraction, derivatization, and analysis by GC-TOF-MS are described in previous publications by Fiehn, et al. [34, 53]. Metabolites were identified from MS spectra using the BinBase algorithm [34].

Raw abundance data for all known and unknown metabolites, consisting of unique ion peak heights, were analyzed with MetaboAnalyst [54]. Principal Component Analysis (PCA) was applied to raw data as a quality control measure to observe sample replicate groupings (**Supplementary Figure 2-S5**). Raw data were subsequently filtered using interquartile range (IQR) to remove metabolites that showed very little variability over all samples. Filtered data were plotted using Log_2 normalization (**Supplementary Figure 2-S6**). A mixture of univariate and multivariate statistics were then applied to investigate changes between genotypes and through dark-to-light transitions. PLS-DA was applied using

default settings, and was cross-validated using a maximum of two components (permutation $P<0.01$). Differences in mean abundance between metabolites in different samples was assessed with ANOVA, and significance was determined using Tukey's HSD with a threshold of $P<0.05$. To build the correlation matrix, metabolites identified as statistically significant by ANOVA were compared to all known metabolites present in the IQR filtered set. Correlation between metabolites was calculated using Pearson's correlation statistic (r). Metabolite correlations were clustered with hierarchical clustering using Pearson correlation for the distance measure and average linkage for leaf ordering (Multiple Array Viewer v10.2). Cluster groupings were selected by eye and KEGG pathway enrichment analysis was conducted on clusters using MBRole [55] with a false discovery rate of 5% ($q<0.5$).

2.6 Acknowledgements

We thank Ryan Simkovsky and Mark Paddock for helpful discussions that improved the manuscript. Additionally we thank Anish Pal and Emily Effener for assistance in sample collection and strain maintenance. This work was supported by a grant from the National Science Foundation (MCB1244108). S.D. was supported in part by the National Institute of Health Cell and Molecular Genetics training grant (T32GM007240).

Chapter 2 is a reprint of Diamond, S., Jun, D., Rubin, B. E., & Golden, S. S. (2015). The circadian oscillator in *Synechococcus elongatus* controls

metabolite partitioning during diurnal growth. *Pnas*, *112*(15), E1916–25. http://doi.org/10.1073/pnas.1504576112. The dissertation author was the primary author of this publication

2.7 Supplementary Figures and Tables

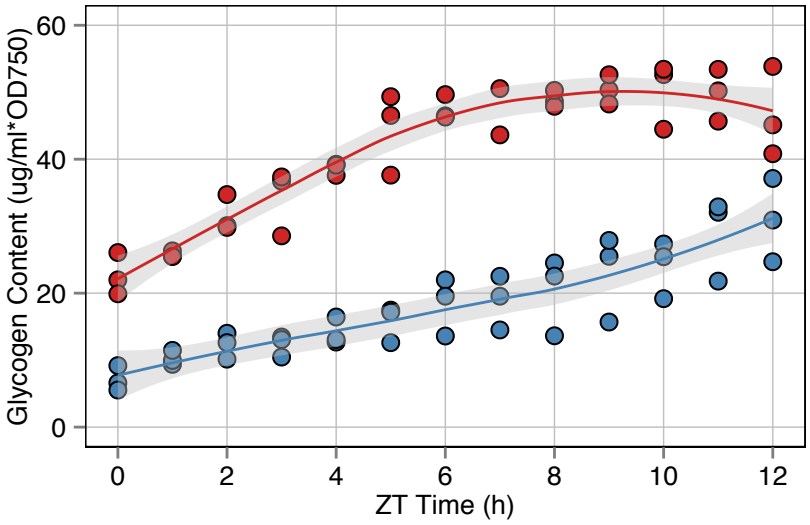

Supplementary Figure 2-S1. Total glycogen content in WT and ΔkaiC measured during the 12-h light period, as cells entered a light period following a dark period (Figure 2-3A). Best-fit curves were calculated for WT (blue line) and ΔkaiC (red line) cells using LOESS regression. The gray shaded area indicates the 95% CI for the regression line. Glycogen content was normalized to cell density based on OD at 750 nm. Sampling for each strain was conducted in triplicate. ZT, zeitgeber time.

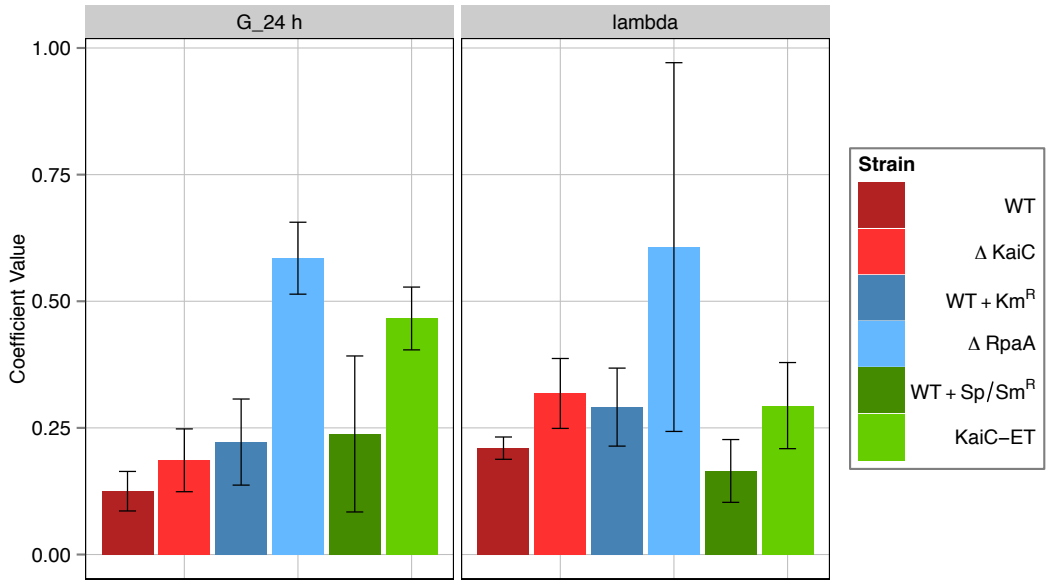

Supplementary Figure 2-S2. Graphical representation of coefficients calculated from glycogen degradation rate data; in Figure 2-4A–C and presented in the main text. The coefficient being compared is indicated at the top of the graph. Error bars indicate the 95% CI of the coefficient fit.

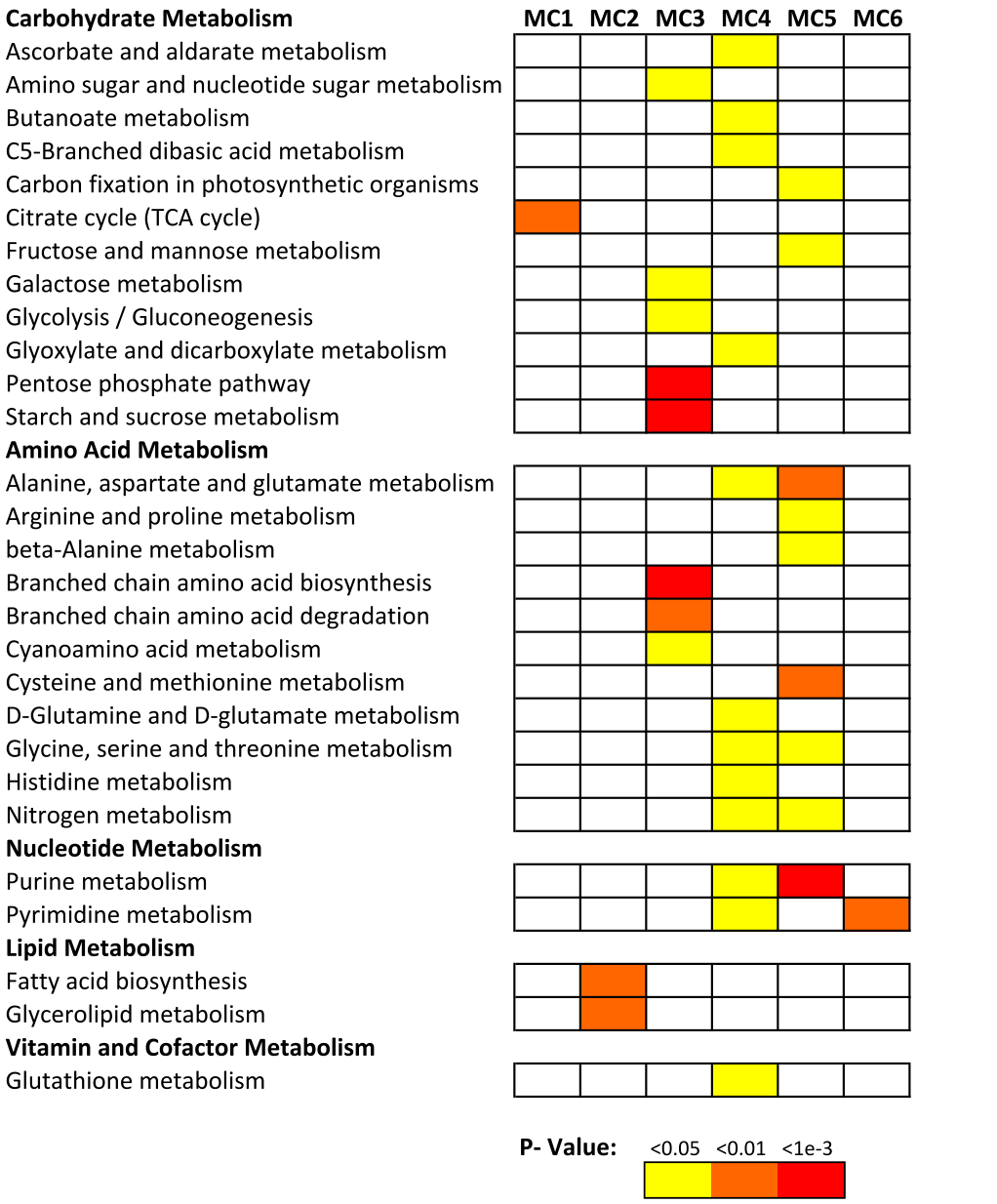

Supplementary Figure 2-S3. KEGG functional category analysis of MCs from the heatmap in Figure 2-7. Enrichment of compounds in a KEGG category was calculated using the online web server MBRole (43). A colored box indicates the presence of an enriched KEGG category in a given MC. The color of the box represents the FDR-corrected P value for that functional category.

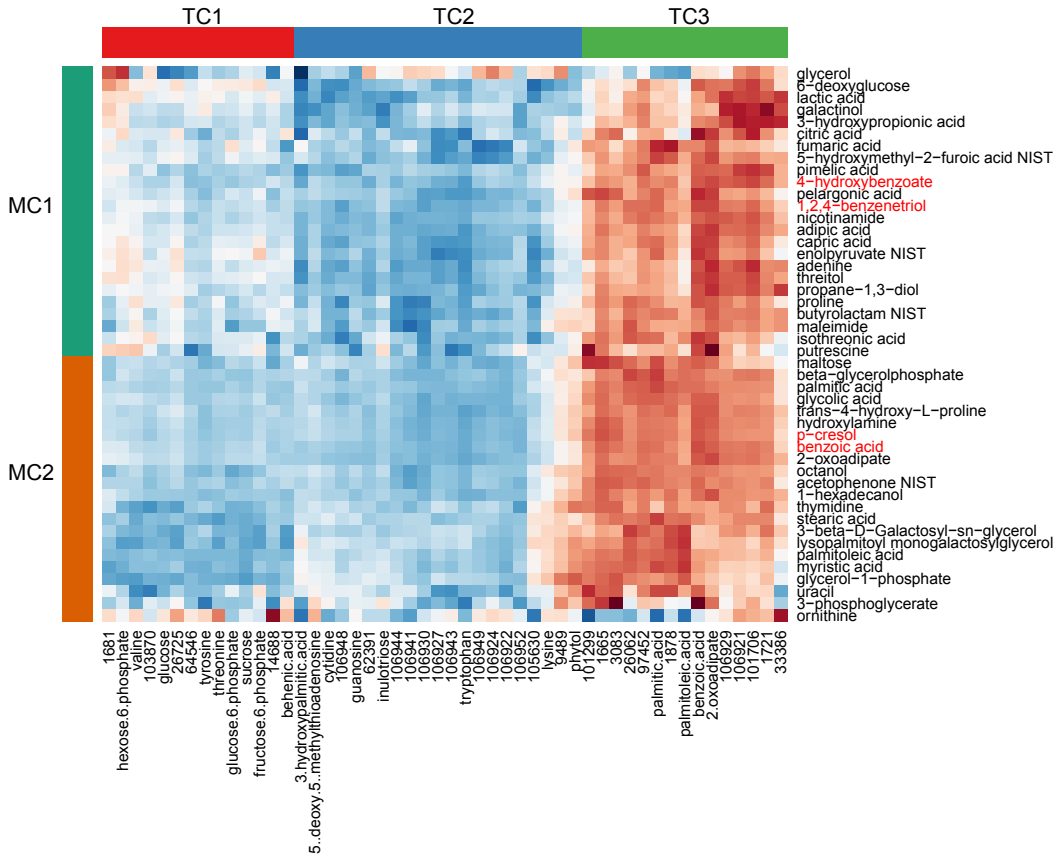

Supplementary Figure 2-S4. Enlarged area of heatmap from Figure 2-7 where compound names are visible for TC1, TC2, TC3, MC1, and MC2. This figure highlights the strong correlation of TC3 with the metabolites found in MC1 and MC2. Compounds highlighted in red are known to or may contribute to plastoquinone biosynthesis in cyanobacteria. A number of compounds present likely are used for extracellular matrix biosynthesis also.

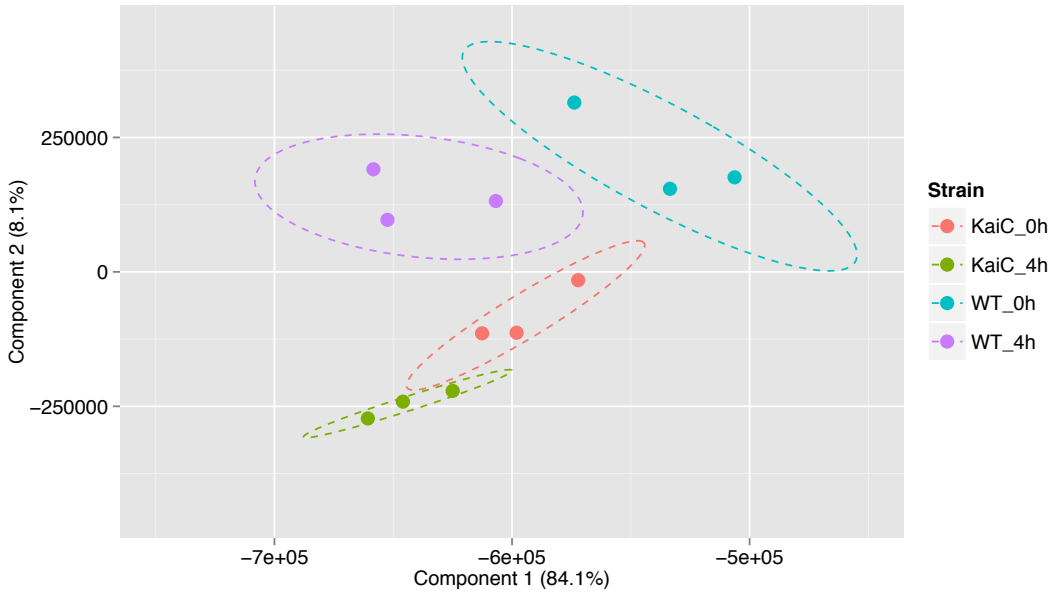

Supplementary Figure 2-S5. Plot of components 1 and 2 derived from PCA performed on raw metabolite abundance data before any subsequent analysis. The first two components describe 92.2% of the variability observed in the data, and the samples group strongly based on their biological replicates. Ellipses indicate the 95% CI of sample groupings.

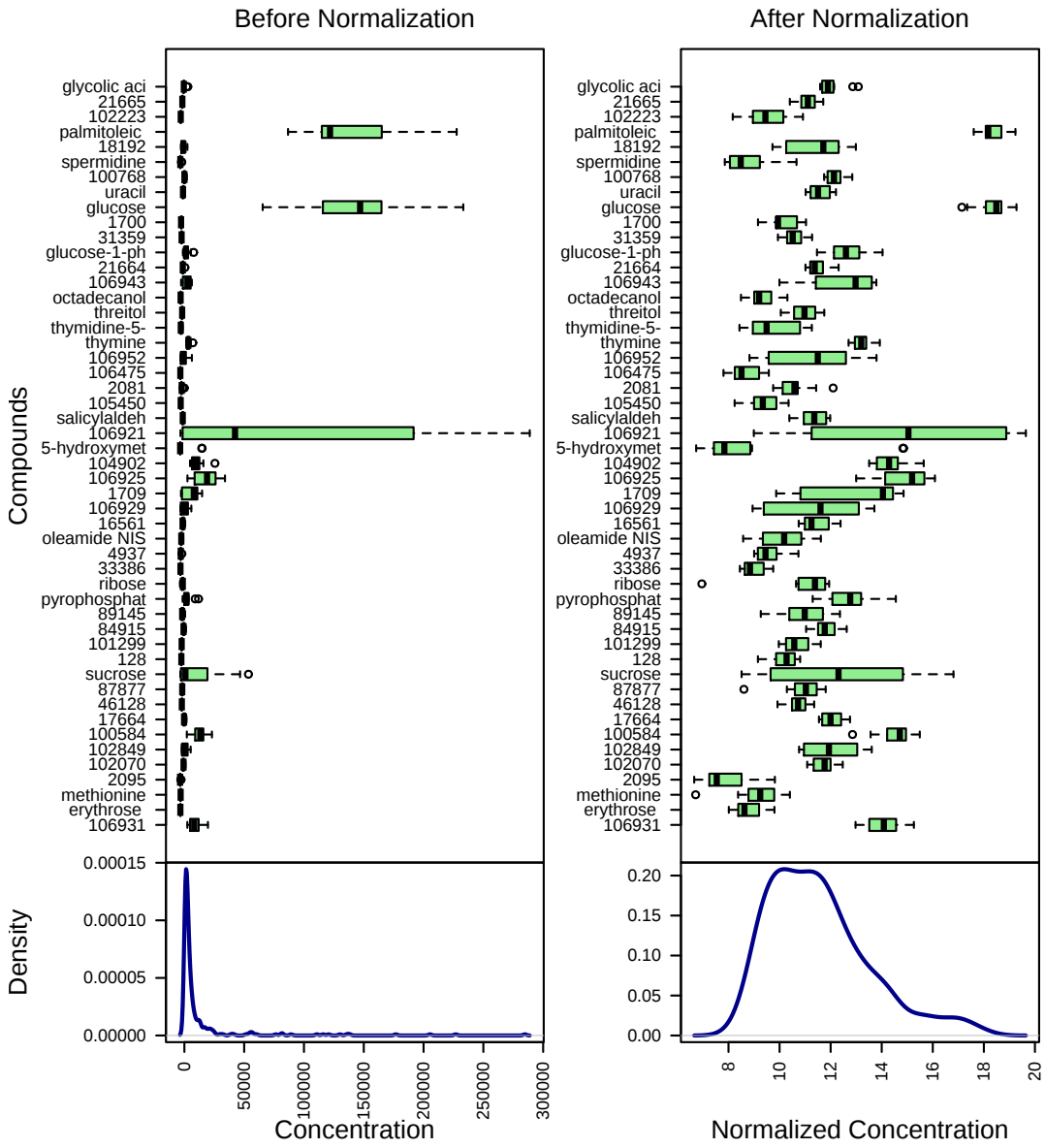

Supplementary Figure 2-S6. The effect of log2 normalization on raw metabolite abundance before analysis. (Left panel) Before normalization the overall concentration distribution of the dataset is strongly skewed toward extreme values. (Right panel) After log2 normalization the distribution of compound concentrations much more closely re- sembles a normal probability distribution and is suitable for parametric statistical analysis such as ANOVA.

Table 2-1. Metabolites with Significant Changes Between 0 h and 4 h

Compound	WT FC*	ΔKaiC FC*	Significant†
Valine	2.83	2.41	Both
Tyrosine	2.01	1.83	Both
Threonine	1.71	1.59	Both
Sucrose	14.14	22.32	Both
Phytol	0.66	0.71	Both
Palmitoleic acid	0.63	0.72	Both
Lysine	0.60	0.16	KaiC
Hexose-6-phosphate	1.90	1.98	Both
Glucose-6-phosphate	2.12	4.04	Both
Glucose	1.87	1.42	WT
Fructose-6-phosphate	1.83	4.08	KaiC
106943	3.00	1.00	WT
106922	1.85	1.16	WT
106921	2.56	0.39	KaiC
103870	2.29	1.78	WT
101299	0.51	0.97	WT
97452	0.67	0.79	WT
64546	2.32	1.55	WT
33386	1.58	0.85	WT
26725	1.83	1.42	WT
14688	2.10	1.06	WT
9489	0.77	0.57	KaiC
1878	0.52	0.69	WT
1681	1.72	2.33	Both
1665	0.61	0.77	WT

* Fold change values are reported without Log2 normalization

† Strains named had a significant fold change p-value <.05

Table 2-2. Metabolites with Significant Difference in Abundance at 4 h.
Compounds in bold are unknowns that were particularly elevated in the WT strain.

Compound	WT_4h*	WT† Rank	KaiC_4h*	ΔKaiC† Rank	High‡ Strain
Tryptophan	12.45	90	14.61	27	KaiC
Sucrose	12.76	71	15.44	19	KaiC
Inulotriose	8.54	308	10.03	226	KaiC
Guanosine	12.59	83	13.26	55	KaiC
Glucose-6-Phosphate	10.69	182	12.16	98	KaiC
Fructose-6-Phosphate	9.73	246	11.15	154	KaiC
Cytidine	9.37	265	10.45	197	KaiC
3-Hydroxypalmitic Acid	8.99	290	10.48	193	KaiC
106952	10.60	191	12.84	67	KaiC
106948	10.67	185	12.11	102	KaiC
106944	9.16	281	12.13	100	KaiC
106941	10.65	187	14.31	29	KaiC
106929	12.86	67	9.46	260	WT
106927	12.58	84	13.48	51	KaiC
106921	**17.93**	**3**	**10.21**	**219**	**WT**
101706	**14.94**	**23**	**9.51**	**256**	**WT**
97452	12.51	87	11.57	129	WT
62391	11.82	117	12.57	77	KaiC
33386	9.72	247	8.89	290	WT
26062	13.39	56	11.58	128	WT
1721	**17.53**	**6**	**10.58**	**187**	**WT**

* Log_2 normalized abundance value at 4 h time point
† Rank of metabolite's abundance at 4 h among the 325 identified metabolites
‡ Strain with the highest overall abundance of the compound at the 4 h time points

Table 2-3. Detailed Information on Each Target Cluster

Compound	Time*	Abundance†
Target Cluster 1		
Valine	Both	-
Tyrosine	Both	-
Threonine	Both	-
Sucrose	Both	Elevated
Hexose-6-phosphate	Both	-
Glucose-6-phosphate	Both	Elevated
Glucose	WT	-
Fructose-6-phosphate	KaiC	Elevated
Behenic acid	-	-
103870	WT	-
64546	WT	-
26725	WT	-
14688	WT	-
1681	Both	-
Target Cluster 2		
Tryptophan	-	Elevated
Phytol	Both	-
Lysine	KaiC	-
Inulotriose	-	Elevated
Guanosine	-	Elevated
Cytidine	-	Elevated
5'-methylthioadenosine	-	-
3-hydroxypalmitic acid	-	Elevated
106952	-	Elevated
106949	-	-
106948	-	Elevated
106944	-	Elevated
106943	WT	-
106941	-	Elevated
106930	-	-
106927	-	Elevated
106924	-	-
106922	WT	-
105630	-	-
62391	-	Elevated
9489	KaiC	-

Table 2-3. Detailed Information on Each Target Cluster (Continued)

Compound	Time*	Abundance†
Target Cluster 3		
Palmitoleic acid	Both	-
Palmitic acid	-	-
Benzoic acid	-	-
2-oxoadipate	-	-
106929	-	Depressed
106921	KaiC	Depressed
101706	-	Depressed
101299	WT	-
97452	WT	Depressed
33386	WT	Depressed
26062	-	Depressed
3083	-	-
1878	WT	-
1721	-	Depressed
1665	WT	-

* Strain in which a metabolite changed from 0h to 4h

† Significantly elevated or depressed in Δk*aiC* relative to WT at 4 h

Table 2-4. Cyanobacterial Strains Used in this Study

Strain	Genetic Background	Antibiotic*	Source
WT	AMC 06	None	Lab Collection
WT^{KmR}	AMC 06 transformed with pAM1579	Km	Lab Collection
WT^{SpSmR}	AMC 06 transformed with pAM1303	SpSm	Lab Collection
Δ*kaiC* (AMC704)	Δ*kaiC* in-frame deletion in AMC541	Cm	[1]
KaiC-ET	AMC 704 transformed with pAM4685	SpSmCm	[2]
Δ*rpaA*	AMC06 transformed with pAM4420	Km	Lab Collection
AMC541	AMC06 with P_{kaiB}-*luc* reporter in NS2	Cm	Lab Collection

*Antibiotics not applied to Δ*kaiC* strain

1. Ditty JL (2005) Stability of the Synechococcus elongatus PCC 7942 circadian clock under directed anti-phase expression of the kai genes. *Microbiology* 151:2605–2613.

2. Paddock ML, Boyd JS, Adin DM, Golden SS (2013) Active output state of the Synechococcus Kai circadian oscillator. *Proc Natl Acad Sci USA*.

2.7 References

1. Deng MD, Coleman JR: **Ethanol synthesis by genetic engineering in cyanobacteria.** *Applied and Environmental Microbiology* 1999, **65**:523–528.

2. Atsumi S, Higashide W, Liao JC: **Direct photosynthetic recycling of carbon dioxide to isobutyraldehyde**. *Nature Biotechnology* 2009, **27**:1177–1180.

3. Schirmer A, Rude MA, Li X, Popova E, del Cardayre SB: **Microbial biosynthesis of alkanes.** *Science* 2010, **329**:559–562.

4. Kruse O, Ben Hankamer: **Microalgal hydrogen production**. *Current Opinion in Biotechnology* 2010, **21**:238–243.

5. Wijffels RH, Kruse O, Hellingwerf KJ: **Potential of industrial biotechnology with cyanobacteria and eukaryotic microalgae**. *Current Opinion in Biotechnology* 2013, **24**:405–413.

6. Guo J, Nguyen AY, Dai Z, Su D, Gaffrey MJ, Moore RJ, Jacobs JM, Monroe ME, Smith RD, Koppenaal DW, Pakrasi HB, Qian W-J: **Proteome-wide Light/Dark Modulation of Thiol Oxidation in Cyanobacteria Revealed by Quantitative Site-Specific Redox Proteomics.** *Mol Cell Proteomics* 2014, **13**:3270–3285.

7. Vermaas WF: **Photosynthesis and Respiration in Cyanobacteria**. 2001:1–7.

8. Dong G, Kim Y-I, Golden SS: **Simplicity and complexity in the cyanobacterial circadian clock mechanism**. *Current Opinion in Genetics & Development* 2010, **20**:619–625.

9. Yang Q, Pando BF, Dong G, Golden SS, van Oudenaarden A: **Circadian Gating of the Cell Cycle Revealed in Single Cyanobacterial Cells**. *Science* 2010, **327**:1522–1526.

10. Vijayan V, Zuzow R, O'Shea EK: **Oscillations in supercoiling drive circadian gene expression in cyanobacteria**. *Proc Natl Acad Sci USA* 2009, **106**:22564–22568.

11. Mackey SR, Golden SS, Ditty JL: **The Itty-Bitty Time Machine**. In *Advances in Genetics*. *Volume 74*. Elsevier; 2011:13–53.

12. Ivleva NB, Gao T, LiWang AC, Golden SS: **Quinone sensing by the**

circadian input kinase of the cyanobacterial circadian clock. *Proc Natl Acad Sci USA* 2006, **103**:17468–17473.

13. Wood TL, Bridwell-Rabb J, Kim Y-I, Gao T, Chang Y-G, LiWang A, Barondeau DP, Golden SS: **The KaiA protein of the cyanobacterial circadian oscillator is modulated by a redox-active cofactor.** *Proc Natl Acad Sci USA* 2010, **107**:5804–5809.

14. Rust MJ, Golden SS, O'Shea EK: **Light-Driven Changes in Energy Metabolism Directly Entrain the Cyanobacterial Circadian Oscillator**. *Science* 2011, **331**:220–223.

15. Pattanayak GK, Phong C, Rust MJ: **Rhythms in Energy Storage Control the Ability of the Cyanobacterial Circadian Clock to Reset**. *Current Biology* 2014:1–5.

16. Takai N, Nakajima M, Oyama T, Kito R, Sugita C, Sugita M, Kondo T, Iwasaki H: **A KaiC-associating SasA-RpaA two-component regulatory system as a major circadian timing mediator in cyanobacteria.** *Proc Natl Acad Sci USA* 2006, **103**:12109–12114.

17. Markson JS, Piechura JR, Puszynska AM, O'Shea EK: **Circadian Control of Global Gene Expression by the Cyanobacterial Master Regulator RpaA**. *Cell* 2013, **155**:1396–1408.

18. Johnson CH, Golden SS: **Circadian programs in cyanobacteria: Adaptiveness and Mechanism**. *Annual Review of Microbiology* 1999:1–22.

19. Paddock ML, Boyd JS, Adin DM, Golden SS: **Active output state of the Synechococcus Kai circadian oscillator.** *Proc Natl Acad Sci USA* 2013.

20. Taniguchi Y, Katayama M, Ito R, Takai N, Kondo T, Oyama T: **labA: a novel gene required for negative feedback regulation of the cyanobacterial circadian clock protein KaiC.** *Genes & Development* 2007, **21**:60–70.

21. Ito H, Mutsuda M, Murayama Y, Tomita J, Hosokawa N, Terauchi K, Sugita C, Sugita M, Kondo T, Iwasaki H: **Cyanobacterial daily life with Kai-based circadian and diurnal genome-wide transcriptional control in Synechococcus elongatus**. *Proc Natl Acad Sci USA* 2009, **106**:14168–14173.

22. Stöckel J, Jacobs JM, Elvitigala TR, Liberton M, Welsh EA, Polpitiya AD, Gritsenko MA, Nicora CD, Koppenaal DW, Smith RD, Pakrasi HB: **Diurnal rhythms result in significant changes in the cellular protein complement**

in the cyanobacterium Cyanothece 51142. *PLoS ONE* 2011, **6**:e16680.

23. Guerreiro ACL, Benevento M, Lehmann R, van Breukelen B, Post H, Giansanti P, Altelaar AFM, Axmann IM, Heck AJR: **Daily rhythms in the cyanobacterium Synechococcus elongatus probed by high-resolution mass spectrometry based proteomics reveals a small-defined set of cyclic proteins.** *Mol Cell Proteomics* 2014.

24. Reinbothe C, Bakkouri El M, Buhr F, Muraki N, Nomata J, Kurisu G, Fujita Y, Reinbothe S: **Chlorophyll biosynthesis: spotlight on protochlorophyllide reduction**. *Trends in Plant Science* 2010, **15**:614–624.

25. Hosokawa N, Hatakeyama TS, Kojima T, Kikuchi Y, Ito H, Iwasaki H: **Circadian transcriptional regulation by the posttranslational oscillator without de novo clock gene expression in Synechococcus**. *Proc Natl Acad Sci USA* 2011, **108**:15396–15401.

26. Yang C, Hua Q, Shimizu K: **Integration of the information from gene expression and metabolic fluxes for the analysis of the regulatory mechanisms in Synechocystis.** *Appl Microbiol Biotechnol* 2002, **58**:813–822.

27. Osanai T, Kanesaki Y, Nakano T, Takahashi H, Asayama M, Shirai M, Kanehisa M, Suzuki I, Murata N, Tanaka K: **Positive regulation of sugar catabolic pathways in the cyanobacterium Synechocystis sp. PCC 6803 by the group 2 sigma factor sigE.** *J Biol Chem* 2005, **280**:30653–30659.

28. Suzuki E, Umeda K, Nihei S, Moriya K, Ohkawa H, Fujiwara S, Tsuzuki M, Nakamura Y: **Role of the GlgX protein in glycogen metabolism of the cyanobacterium, Synechococcus elongatus PCC 7942**. *Biochimica et Biophysica Acta (BBA) - General Subjects* 2007, **1770**:763–773.

29. Díaz-Troya S, López-Maury L, Sánchez-Riego AM, Roldán M, Florencio FJ: **Redox regulation of glycogen biosynthesis in the cyanobacterium Synechocystis sp. PCC 6803: analysis of the AGP and glycogen synthases.** *Mol Plant* 2014, **7**:87–100.

30. Grundel M, Scheunemann R, Lockau W, Zilliges Y: **Impaired glycogen synthesis causes metabolic overflow reactions and affects stress responses in the cyanobacterium Synechocystis sp. PCC 6803**. *Microbiology* 2012, **158**:3032–3043.

31. Scanlan DJ, Sundaram S, Newman J, Mann NH, Carr NG: **Characterization of a zwf mutant of Synechococcus sp. strain PCC 7942.** *J Bacteriol* 1995, **177**:2550–2553.

32. Doolittle WF, Singer RA: **Mutational analysis of dark endogenous metabolism in the blue-green bacterium Anacystis nidulans.** *J Bacteriol* 1974, **119**:677–683.

33. Boyd JS, Bordowitz JR, Bree AC, Golden SS: **An allele of the crm gene blocks cyanobacterial circadian rhythms.** *Proc Natl Acad Sci USA* 2013, **110**:13950–13955.

34. Fiehn O, Garvey WT, Newman JW, Lok KH, Hoppel CL, Adams SH: **Plasma Metabolomic Profiles Reflective of Glucose Homeostasis in Non-Diabetic and Type 2 Diabetic Obese African-American Women**. *PLoS ONE* 2010, **5**:e15234.

35. Maitra S, Yan J: **Principle component analysis and partial least squares: two dimension reduction techniques for regression**. *Applying Multivariate Statistical Models* 2008, **79**.

36. Tamoi M, Miyazaki T, Fukamizo T, Shigeoka S: **The Calvin cycle in cyanobacteria is regulated by CP12 via the NAD(H)/NADP(H) ratio under light/dark conditions**. *The Plant Journal* 2005, **42**:504–513.

37. Tikunov Y: **A Novel Approach for Nontargeted Data Analysis for Metabolomics. Large-Scale Profiling of Tomato Fruit Volatiles**. *PLANT PHYSIOLOGY* 2005, **139**:1125–1137.

38. Schwarz D, Nodop A, Huge J, Purfurst S, Forchhammer K, Michel KP, Bauwe H, Kopka J, Hagemann M: **Metabolic and Transcriptomic Phenotyping of Inorganic Carbon Acclimation in the Cyanobacterium Synechococcus elongatus PCC 7942**. *PLANT PHYSIOLOGY* 2011, **155**:1640–1655.

39. Pfaff C, Glindemann N, Gruber J, Frentzen M, Sadre R: **Chorismate Pyruvate-Lyase and 4-Hydroxy-3-solanesylbenzoate Decarboxylase Are Required for Plastoquinone Biosynthesis in the Cyanobacterium Synechocystis sp. PCC6803**. *Journal of Biological Chemistry* 2014, **289**:2675–2686.

40. Sadre R, Pfaff C, Buchkremer S: **Plastoquinone-9 biosynthesis in cyanobacteria differs from that in plants and involves a novel 4-hydroxybenzoate solanesyltransferase**. *Biochem J* 2012, **442**:621–629.

41. Ballicora MA, Iglesias AA, Preiss J: **ADP-Glucose Pyrophosphorylase, a Regulatory Enzyme for Bacterial Glycogen Synthesis**. *Microbiology and Molecular …* 2003.

42. Gontero B, Maberly SC: **An intrinsically disordered protein, CP12: jack of all trades and master of the Calvin cycle**. *Biochem Soc Trans* 2012, **40**:995–999.

43. Howard TP, Fryer MJ, Singh P, Metodiev M, Lytovchenko A, Obata T, Fernie AR, Kruger NJ, Quick WP, Lloyd JC, Raines CA: **Antisense Suppression of the Small Chloroplast Protein CP12 in Tobacco Alters Carbon Partitioning and Severely Restricts Growth**. *PLANT PHYSIOLOGY* 2011, **157**:620–631.

44. Kim Y-I, Vinyard DJ, Ananyev GM, Dismukes GC, Golden SS: **Oxidized quinones signal onset of darkness directly to the cyanobacterial circadian oscillator.** *Proc Natl Acad Sci USA* 2012, **109**:17765–17769.

45. Haydon MJ, Mielczarek O, Robertson FC, Hubbard KE, Webb AAR: **Photosynthetic entrainment of the Arabidopsis thaliana circadian clock**. *Nature* 2013, **502**:689–692.

46. Streb S, Zeeman SC: **Starch Metabolism in Arabidopsis**. *arbo* 2012, **10**:e0160.

47. Clerico EM, Ditty JL, Golden SS: **Specialized techniques for site-directed mutagenesis in cyanobacteria.** *Methods Mol Biol* 2007, **362**:155–171.

48. Xu Y, Mori T, Johnson CH: **Cyanobacterial circadian clockwork: roles of KaiA, KaiB and the kaiBC promoter in regulating KaiC.** *EMBO J* 2003, **22**:2117–2126.

49. Ernst A, Kirschenlohr H, Diez J, Böger P: **Glycogen content and nitrogenase activity in Anabaena variabilis**. *Arch Microbiol* 1984, **140**:120–125.

50. *Ggplot2: Elegant Graphics for Data Analysis*. New York, NY: Springer Science & Business Media; 2009.

51. R Core Team: *R: a Language and Environment for Statistical Computing*. Vienna, Austria; 2014:1–3604.

52. R Core Team: **R: A Language and Environment for Statistical Computing**. 2013:1–3604.

53. Fiehn O, Wohlgemuth G, Scholz M, Kind T, Lee DY, Lu Y, Moon S, Nikolau B: **Quality control for plant metabolomics: reporting MSI-compliant studies**. *The Plant Journal* 2008, **53**:691–704.

54. Xia J, Wishart DS: **Metabolomic data processing, analysis, and interpretation using MetaboAnalyst.** *Curr Protoc Bioinformatics* 2011, **Chapter 14**:Unit 14.10.

55. Chagoyen M, Pazos F: **MBRole: enrichment analysis of metabolomic data**. *Bioinformatics* 2011, **27**:730–731.

56. Ditty JL: **Stability of the Synechococcus elongatus PCC 7942 circadian clock under directed anti-phase expression of the kai genes**. *Microbiology* 2005, **151**:2605–2613.

Chapter 3

Keeping the Balance: The Cyanobacterial Circadian Response Regulator RpaA is Critical for Metabolic Stability at Night

3.1 Abstract

Cyanobacteria are the only bacterial phylum that has a fully functional circadian clock, and research suggests that the clock has direct effects on fitness and metabolism under natural diurnal conditions. However, the mechanism by which clock output affects metabolism is poorly studied, and data on the circadian control of metabolism under diurnal conditions are lacking. Here we use the model cyanobacterium, *Synechococcus elongatus* PCC7942, to demonstrate that the circadian response regulator RpaA is critical for regulation of global metabolic and redox stability during the day and night periods of diurnal growth. Deletion of *rpaA* leads to excess reactive oxygen species (ROS) generation during the day period, which can not be detoxified due to an inability of the mutant to activate primary reductant producing pathways at night. This also indicates that clock mediated RpaA activity is required to activate metabolic networks important for reductant generation at night, and reductant production at night is critical for maintaining metabolic stability in WT cells. Additionally, we identified secondary site

mutations and specific growth conditions in a Δ*rpaA* mutant background that can suppress diurnal lethality, and the suppressive mechanisms identified are suggest that metabolic and redox imbalance drives diurnal lethality in *rpaA* mutants. These results provide a mechanistic connection of the clock to metabolism under diurnal growth, and shed light on the enduring mystery of LD lethality in *rpaA* mutants.

3.2 Introduction

Cyanobacteria are both central agents of global carbon and nitrogen cycles, and promising platforms for renewable chemicals, fuels, and nutraceuticals [1-3]. Understanding the control mechanisms that govern the flow of carbon and nitrogen through these organisms is crucial for predicting their behavior in natural environments as well as for improving engineering strategies. Although the basic pathways for carbon and nitrogen metabolism, and their regulation, are well understood in heterotrophic bacteria, recent work has shown that cyanobacteria exhibit a number of deviations in core metabolic pathways [4-6]. Additionally, metabolic control mechanisms in cyanobacteria evolved to be compatible with photoautotrophic metabolism, and the dramatic changes that are imposed on those pathways by predictable daily light-dark (LD) cycles. Examples include the preference for the photosynthetically derived reductant NADPH over NADP in many metabolic processes [7, 8], light-dependent redox responsiveness for many metabolic

enzymes [9-12], and a circadian clock that drives 24 h transcriptional rhythms in most genes [13, 14]. Circadian control is a particularly unique aspect, as cyanobacteria are the only bacterial group known to have circadian clocks [14], and there is evidence that redox regulatory systems in cyanobacteria have a circadian component [15]. Overall, generating a more complete picture of metabolic regulation in cyanobacteria will need to take into account how regulatory mechanisms integrate into the natural diurnal growth conditions under which these organisms evolved.

The many metabolic and almost all circadian studies on cyanobacteria have used constant light growth conditions [16-19]. However, an increasing number of studies have investigated the integrative effects of metabolic control mechanisms in the context of LD growth [9, 20-22]. Recent work from our laboratory has shown that a functional circadian clock is important for controlling carbon metabolism in *Synechococcus elongatus* PCC7942 as cells transition from the dark into the light under diurnal growth [23]. In particular, it was shown that in the morning the clock represses the activity of the conserved circadian transcriptional regulator, RpaA (regulator of phycobilisome-association A), which normally activates night metabolic processes [19, 23]. In this study we continue to investigate how circadian regulation affects metabolism at LD transitions, focusing on the metabolic importance of RpaA activity as *S. elongatus* cells transition from light into darkness.

Synechococcus species are among the largest bacterial contributors to global primary production [24], and *S. elongatus* in particular has been successfully engineered to produce a variety of useful industrial products [2, 25-27]. *S. elongatus* is also genetically tractable [28], is the focus of a wide array of genetic tools [29], and is the most well studied model for bacterial circadian clocks [14, 30]. The circadian clock in *S. elongatus* is comprised of a core oscillator formed by the proteins KaiA, KaiB, and KaiC, with the phosphorylation state of KaiC over a 24-h period conferring the timing of the clock mechanism [14]. The oscillator relays timing information to the SasA-RpaA two component output pathway, in which RpaA is a transcription factor that binds 170 known downstream gene targets [19, 31]. Recent work has shown that the oscillator represses the activity of RpaA in the morning, and that this repression is relieved throughout the day such that RpaA reaches its peak activity at dusk [19, 23, 32]. This temporal activity pattern, and the fact that RpaA strongly activates nighttime metabolic genes, suggests that it plays an important role in metabolic control at night. Indeed, one of the original observations noted in the *S. elongatus* circadian literature is that inactivation of the core oscillator genes (*kaiA, kaiB,* and *kaiC*) has no major effect on growth rate or viability under LD cycles, but the inactivation of either *sasA* or *rpaA* significantly attenuates viability under LD growth conditions [31, 33]. While the transcriptional targets of RpaA have been well characterized, and it is clear that LD conditions are lethal to *rpaA*-null mutants, the mechanism of

cell death and type of metabolic and physiological changes that occur under these conditions have not been explored.

Under diurnal growth conditions *S. elongatus* performs biosynthetic metabolism and photosynthesis during the day with excess fixed carbon stored as the branched chain glucose polymer glycogen [23]. As cells enter a dark period glycogen is rapidly degraded via the oxidative pentose phosphate pathway (OPPP), which serves as the primary source of energy and reducing power (NADPH) at night [34, 35]. The OPPP shares many reactions with the Calvin Cycle, and the transition from photosynthetic to oxidative metabolism occurs through both transcriptional and redox-regulated steps [36-38]. In particular, the Calvin Cycle enzymes Gap2 (glyceraldehyde-3-phosphate dehydrogenase 2) and Prk (phosphoribulokinase) are controlled by a widely conserved regulatory mechanism in which inhibition occurs through complex formation with the protein CP12 in a redox-controlled and light-dependent manner [36, 39]. Also, prior to entering the dark, RpaA transcriptionally activates a number of genes for sugar catabolic pathway enzymes including: *glgP* (glycogen phosphorylase), *gap1* (glyceraldehyde-3-phosphate dehydrogenase 1), *opcA* (OxPP cycle protein A), and the OPPP rate-limiting enzyme *zwf* (glucose-6-phosphate dehydrogenase) [19]. In *rpaA* mutants glycogen degradation is strongly attenuated, which reflects an inability to activate these sugar catabolic pathways [23]. Thus, a transition into darkness requires both redox-regulated and RpaA-mediated metabolic regulatory

steps. Due to its direct control over the OPPP, RpaA likely exerts a strong influence over both energy generation and redox state at night.

In this study we investigate how inactivation of *rpaA* affects metabolism and physiology as *S. elongatus* transitions into darkness, and over the night period. We initially performed physiological characterization on WT and a *ΔrpaA* mutant by looking at cell viability and pigment changes over a 12-h dark period. Subsequently we used untargeted metabolic profiling to investigate how loss of RpaA affects the abundance of primary metabolites at time points after cells enter the dark. Finally, we determined both secondary site mutations and physiological growth conditions that suppress cell death in the *ΔrpaA* mutant under LD growth, and correlated these data with metabolomics, gene expression, and measurements of global oxidative stress. We present a model in which RpaA acts as a critical transcriptional regulator in the activation of reductant-producing pathways at night to maintain strict metabolic stability. In the absence of *rpaA* a cascade of negative metabolic and regulatory events is allowed to transpire that severely alters cellular metabolic state and leads to rapid cell death. These results directly connect the conserved cyanobacterial circadian output pathway to the maintenance of metabolic stability under diurnal growth conditions. Also, this work serves as a framework for understanding why carbon degradation and reductant production at night is important for survival in non-diazotrophic cyanobacteria.

3.3 Results

3.3.1 Stress-Related Pigmentation Changes and Rapid Cell Death the Δ*rpaA* Mutant

It is clear that *ΔrpaA* strains do not grow under LD conditions, but very little characterization of cellular physiology has been performed immediately after dark exposure [23, 40]. We initially characterized the *ΔrpaA* strain by examining changes in cell viability and overall pigmentation as cells entered the dark. WT and *ΔrpaA* were sampled from a turbidity-controlled photobioreactor immediately before entry into the dark (ZT12) and at intervals thereafter. We conducted viable cell counts and acquired absorbance spectra of whole cells from 400-750 nm to detect changes in pigmentation. Prior to dark exposure, the Δ*rpaA* strain had significantly elevated absorbance at 440 nm and 680 nm relative to WT (**Figure 3-1A**). This signal indicates increased carotenoid and chlorophyll absorbance. However, when the Δ*rpaA* strain was exposed to darkness a rapid change in absorbance occurred beginning after 1-2 h and reaching a maximum around 8 h. While WT cells showed no significant change in their absorbance spectrum, the Δ*rpaA* mutant had a significant decrease in absorbance at 630 nm and a further increase in absorbance at 440 nm (**Figure 3-1B and Supplementary Figure 3-S1A**). The decrease in absorbance at 630 nm indicates a loss of phycobilisomes-specific pigmentation, and is a classic chlorosis response to nutrient

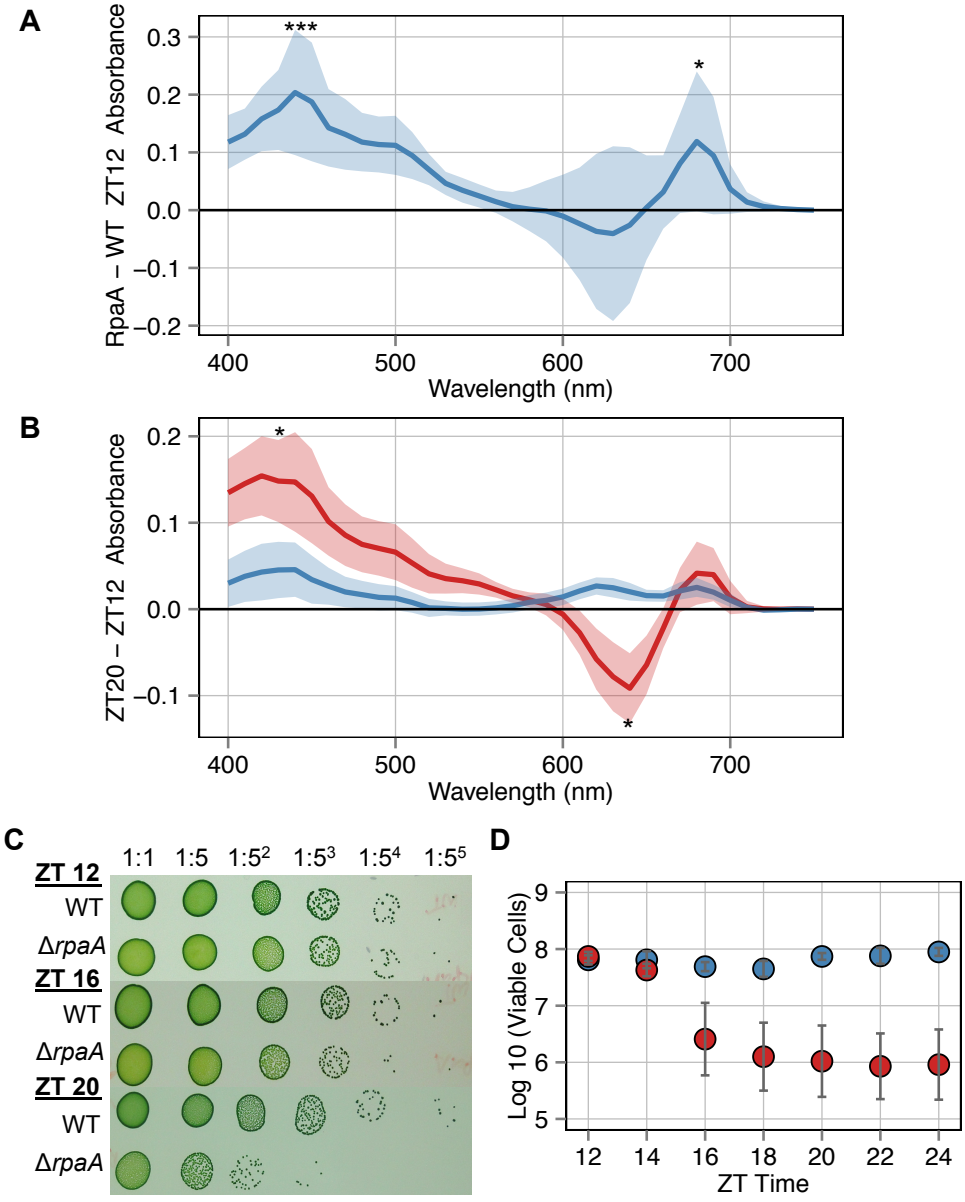

Figure 3-1. Absorbance and viaibility data from WT and the Δ*rpaA* mutant. (A) Mean subtracted absorbance value showing the absorbance difference between WT and the Δ*rpaA* mutant at ZT12 (0 h darkness). Shaded area indicates STDV of mean (n = 8; * $p < 0.05$, *** $p < 0.001$). **(B)** Mean subtracted absorbance values for WT (blue) and the Δ*rpaA* mutant (red) showing the change in absorbance from ZT12 (0 h darkness) to ZT20 (8 h darkness). Δ*rpaA* shows significant changes while WT does not. Shaded area indicates STDV of mean (n = 8; * $p<0.05$). **(C)** Representative photograph of a dilution series used for viable cell counting, with time point collected indicated above strain. **(D)** Mean viable cells counted after WT (blue) and the Δ*rpaA* mutant (red) entered the dark. Error bars indicate SEM. Significance calculated using student's t-test (n = 4; * $p<0.05$).

imbalance and stress in cyanobacteria, particularly nitrogen deprivation [41]. Additionally, the increase at 440 nm was not accompanied by an increase in chlorophyll absorbance, suggesting that this change is solely related to carotenoid accumulation, another known response to stress [42]. The differences in pigmentation observed between WT and *ΔrpaA* indicate that prior to entering darkness the *ΔrpaA* mutant is likely under high cellular stress, which further increases after a dark transition and is accompanied by a classic nutrient deprivation response.

During the measurement of absorbance, separate samples were also collected and serially plated to examine the number of viable cells (colony forming units) present in the culture. Samples taken immediately before dark exposure (ZT12) show that similar numbers of cells are present for each strain (**Figure 3-1C and 3-1D**). After 4 h of dark exposure (ZT16) a slight but quantifiable and reproducible decrease in cell number was evident for the Δ*rpaA* strain with no corresponding decrease for WT (**Figure 3-1C and 3-1D**). After 6-8 h of exposure (ZT18-20) a 10-fold decrease in the number of viable Δ*rpaA* cells was observed with no corresponding decrease in WT (**Figure 3-1C and 3-1D**). This change in viability was also reflected in optical density measurements collected from photobioreactors during the experiment. When Δ*rpaA* strains entered the 12h dark period they showed a sharp drop in optical density that did not recover during the following light period (**Supplementary Figure 3-S1B**). These data indicate that the Δ*rpaA* mutant

incurs rapid cell death after entering the dark. Taken together, the speed of the cell death response, the rapid changes in pigment absorbance, and an inability to regain viability in constant light (LL), support an active mechanism that drives cell death in LD, as opposed to simply being unable to reproduce under these conditions.

3.3.2 Analysis of Temporal Metabolic Changes in the Δ*rpaA* Mutant

Attenuated glycogen degradation in the Δ*rpaA* mutant [23], strong RpaA regulation of carbon catabolic pathways [19], and the classic nutrient deprivation chlorosis response we observed, suggests broad changes in central carbon and nitrogen metabolism likely occur in Δ*rpaA* cells after a light-to-dark transition. To characterize primary carbon and nitrogen metabolites in WT and Δ*rpaA* at the transition, we applied untargeted gas chromatography time-of-flight mass spectrometry (GC-TOF-MS) to samples collected from turbidity-controlled photobioreactors under 12:12 LD growth. Samples were collected directly prior to the dark transition (ZT12) and at 1 h, 2 h, 4 h, and 6 h thereafter. A total of 114 known compounds were identified and measured. Raw data and additional compound metadata including full mass spectra are provided in (**Supplementary Data Set 3-S1**). Dramatic differences were found in many metabolites that require NADPH for their biosynthesis, suggesting RpaA-driven reductant production at night is critically important to keep metabolite levels stable. Additionally, an unusual

accumulation of lipids and purine nucleotides in the Δ*rpaA* mutant may indicate that OPPP derived reductant is an important input for enzymatic redox-regulation at night. Finally, the detection of stress associated metabolites in the initial time point (ZT12) suggests that RpaA also plays a roll in mitigating cellular stress during the day.

3.3.2.1 Metabolite Levels in ΔrpaA Before Entering Dark Indicate Stress and OPPP Depression

Even before entering the dark (ZT12), compounds that are strong indicators of stress and OPPP depression were significantly different between WT and the Δ*rpaA* mutant (**Figure 3-2A and Supplementary Data Set 3-S1**). Polyamines were highly elevated in Δ*rpaA* with spermidine and putrescine increased 48.8-fold and 4.5-fold, respectively (**Figure 3-2A**). Accumulation of polyamines is a known general stress response in cyanobacteria [43]. Also, the level of adenosine monophosphate (AMP) was highly elevated in *ΔrpaA* relative to WT (29.7-fold), which may indicate that the stress condition affecting *ΔrpaA* is directly impacting its ability to generate energy (**Figure 3-2A**). The OPPP, although primarily active at night, is known to also be slightly active during the late-day period [44]. During this time the pathway can be used to produce phosphoribosyl pyrophosphate (PRPP) for nucleotide biosynthesis, and previous work has shown that OPPP activity is positively correlated with levels of glycolytic metabolites and sucrose [23, 36].

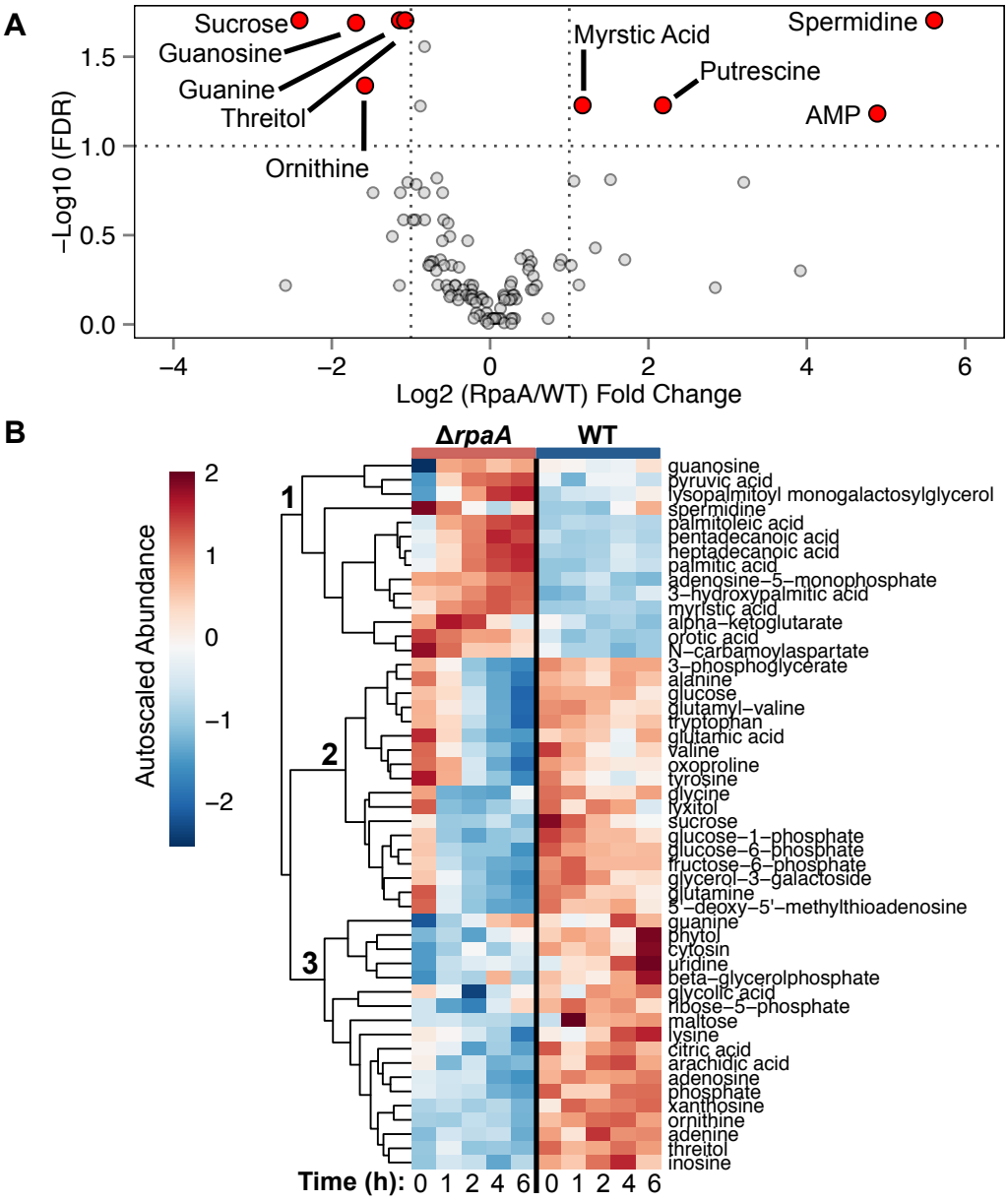

Figure 3-2. Summary of metabolites that differ significantly in the WT and Δ*rpaA* mutant strains. (A) Volcano plot of metabolites with significant differences between strains at ZT12 (0 h darkness). Dotted lines indicate required thresholds for significance, and red dots indicate metabolites with significant differences (n = 4 for WT and n = 5 for Δ*rpaA*). **(B)** Heatmap showing the autoscaled abundance of all metabolites where a significant difference was detected between WT and the Δ*rpaA* mutant over the time course by two-way ANOVA and Tukey's HSD (n = 4 for WT; n = 5 for Δ*rpaA*; $p < 0.05$). Metabolite clusters are indicated by numbers on the hierarchical clustering tree, and sampling time points are indicated at the bottom of the heatmap. Autoscaling represents a Z-score difference from the mean value of the metabolite across all time points.

Indeed the nucleotide metabolites guanine and guanosine were significantly less abundant in *ΔrpaA*, -2.2-fold and -3.2-fold respectively, relative to WT (**Figure 3-2A**). Sucrose was also observed to be less abundant in *ΔrpaA* by -5.3-fold. These changes are in agreement with depressed OPPP activity, and are consistent with RpaA being an important regulator of OPPP. Overall, the changes observed further support RpaA's regulatory control over the OPPP, and indicate that RpaA likely has other, less known, functions during the day. Clearly without RpaA there are strong indications of cellular stress and low energy status even before cells enter the dark.

3.3.2.2 WT Maintains Strict Metabolic Stability at Night Which is Lost in ΔrpaA

Over the first half of the dark period a large number of metabolite differences rapidly formed between WT and the *ΔrpaA* mutant. Using 2-way ANOVA we identified 50 compounds with significant differences in abundance patterns over the time course (**Figure 3-2B and Supplementary Data Set 3-S2**). To supplement our univariate statistics we also applied a multivariate modeling method, partial least squares discriminate analysis (PLS-DA), which allowed us to identify the top 25 metabolites that discriminate between WT and *ΔrpaA* samples. Additionally, we used PLS-DA to visualize and statistically test the overall similarity of sample groups based on the most discriminating metabolites (**Figure 3-3A**). One of the most striking observations from both analysis methods was the overall stability of

metabolite levels in WT relative to the *ΔrpaA* mutant (**Figure 3-2B and 3-3A**). Based on previous data showing significant flux through glycogen degradation and the OPPP at night[23, 44, 45], we had expected that WT cells would show some significant metabolic changes downstream of the OPPP. However, the data indicate that WT maintains a relatively strict level of stability across metabolites, while the *ΔrpaA* mutant exhibits broad and unusual metabolic changes.

Metabolites in the 1st and 2nd clusters of the heatmap show large changes over time in *ΔrpaA,* with metabolites in these clusters showing strong increases or decreases respectively (**Figure 3-2B**). In WT cells the corresponding metabolites show very gradual or no changes in abundance (**Figure 3-2B**). This effect is also highly pronounced in the plot of PLS-DA components 1 and 2 (**Figure 3-3A**). Component 1 discriminates very well between the two sample genotypes, and component 2 discriminates based on sampling time (**Figure 3-3A**). For the *ΔrpaA* mutant there is a clear separation across component 2 as the samples progress through time, with temporally close samples showing more similarity to each other than temporally distant samples (**Figure 3-3A**). This pattern is absent in the WT samples and the 95% confidence interval ellipses for all WT sample groups overlap indicating there are not major differences between these samples through the time course (**Figure 3-3A**). Thus, PLS-DA indicates that *ΔrpaA* samples are both different from WT samples and changing though time, while

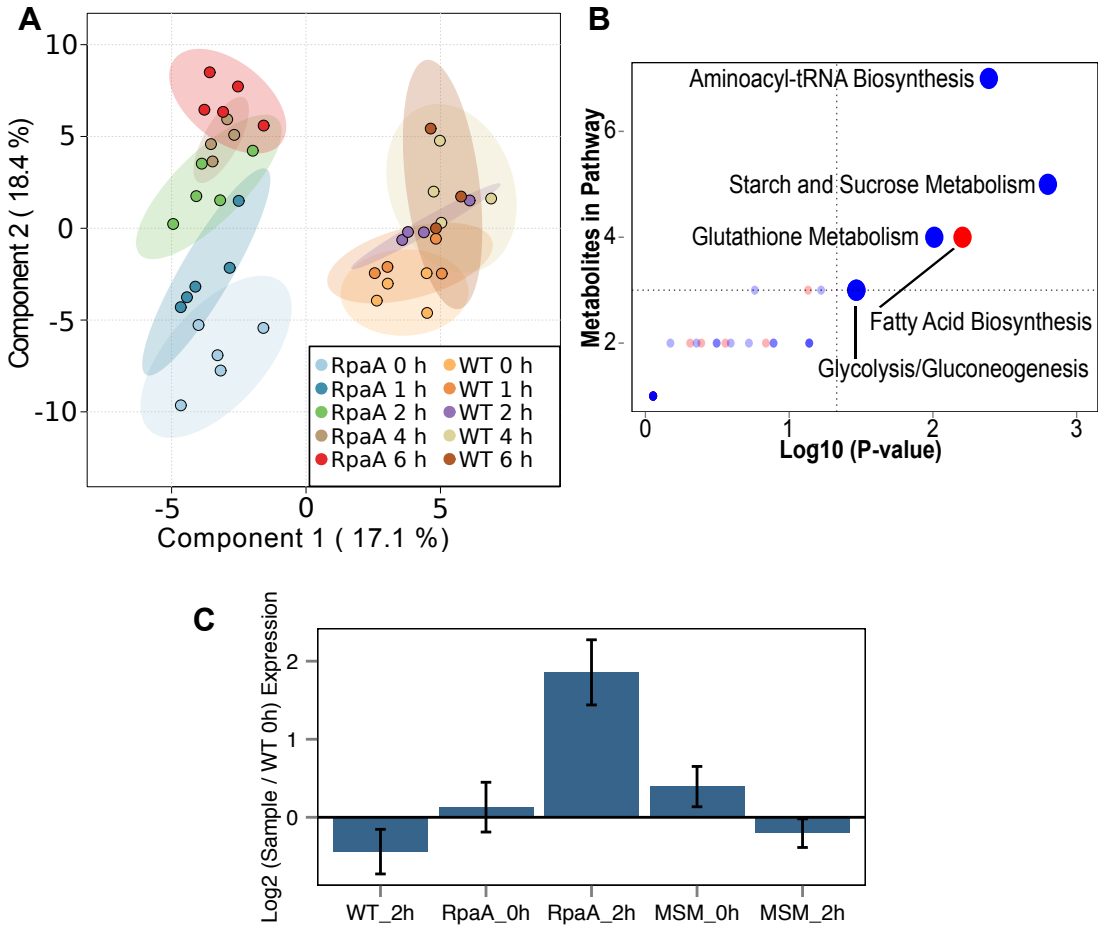

Figure 3-3. Multivariate modeling, KEGG category analysis, and qRT-PCR data from WT and Δ*rpaA* mutant strains. (A) Plot of PLS-DA components 1 and 2 for all metabolomics samples. Components 1 and 2 account for 35.5% of the variance in the dataset, and are significant predictors of class membership (**Supplementary Figure 3-10C**). Ellipses indicate the 95% CI of each grouping of samples on the plot, and overlaps indicate an inability to statistically distinguish groups via the PLS-DA model. **(B)** Plot of KEGG metabolic categories that were identified as enriched in heatmap clusters 1 (red) and 2 (blue). The x-axis indicates the number of metabolites detected in the respective pathway. Dotted lines indicate thresholds required for significance, and large dot size indicates a significant enrichment in the indicated category as calculated by Fisher's Exact Test ($p < 0.05$). **(C)** Relative expression levels of the *glnN* transcript at ZT12 (0 h darkness) and ZT14 (2 h darkness) as measured by qRT-PCR. Values presented relative to WT at ZT12 (0 h). Error bars indicate SEM. Significance calculated using one-way ANOVA and Tukey's HSD (n = 3; * $p<0.05$, ** $p<0.01$).

WT samples do not exhibit a large time related change. Additionally, this pattern is conserved in unsupervised principal component analysis (PCA) of the samples (**Supplementary Figure 3-S2A**), and a search of up to 5 PLS-DA components did not indicate any component that specifically separates WT samples based on time (**Supplementary Figure 3-S2B**). Thus, ANOVA, PLS-DA, and PCA indicate that WT cells maintain a rather high level of metabolic stability in the early night period, which is lost in *ΔrpaA* mutants.

3.3.2.3 Metabolic Changes in ΔrpaA Indicate Severe Reductant and Regulatory Imbalances

To determine whether compounds within specific metabolic pathways show conserved temporal changes we performed KEGG pathway enrichment analysis on heatmap clusters 1 and 2 (**Figure 3-2B and 3-3B**). The results of our analysis indicated that three major patterns of metabolic change occur in the *ΔrpaA* mutant: (1) Metabolites connected to glycolysis, the OPPP, and pathways that require a significant NADPH input show very rapid and large decreases in abundance; (2) Metabolic indicators of C/N imbalance and low energy status significantly increase; (3) Metabolites who's abundance may be directly impacted by cellular redox status increase later in the night. Overall these changes indicate that after transition into the dark the *ΔrpaA* mutant suffers a severe reductant deficit, which may subsequently influence the enzymatic regulation of metabolic flux later in the night period.

Cluster 2, which contains compounds that decrease in *ΔrpaA*, shows significant enrichment in starch and sucrose metabolism (p = 0.002), tRNA biosynthesis (p = 0.004), glutathione metabolism (p = 0.008), glycolysis (p = 0.036), and nitrogen metabolism (p = 0.036) (**Figure 3-3B**). In agreement with attenuated OPPP activity and glycogen degradation in *ΔrpaA*, the compounds sucrose, glucose-1-phosphate (G1P), glucose-6-phosphate (G6P), and fructose-6-phosphate (F6P) all show a precipitous drop in abundance as soon as *ΔrpaA* cells enter the dark period (**Figure 3-2B**). WT cells also show decreases in these metabolites over time, which is expected as glycogen is utilized, but the decrease is much more gradual (**Figure 3-2B**). Also, WT cells show an increase of F6P at the 1 h time point after dark, which is an indicator of OPPP activation in these cells as they enter the dark phase [36]. A large number of amino acids show strong decreases in the *ΔrpaA* mutant, as reflected by enrichment of the tRNA biosynthesis and nitrogen metabolism pathways (**Figure 3-2B and 3-3B**). In particular we see that both glutamine and glutamic acid, the primary nitrogen donors, show large decreases in *ΔrpaA* mutants. This supports the hypothesis of a reductant deficit, as without reducing power to biosynthesize these amino acids from alpha-ketoglutarate (AKG), there should be a global decrease in amino acid pools with a corresponding increase in AKG as the residual carbon flows down through glycolysis.

In addition to its participation in nitrogen assimilation, glutamine participates in the glutathione biosynthetic pathway along with oxoproline, glycine, and glutamyl-valine [46], which all show large decreases in *ΔrpaA* mutants (**Figure 3-2B**). Glutathione biosynthesis is important for signaling, modulating redox state, and counteracting reactive oxygen species (ROS) in cyanobacteria and its regeneration requires NADPH as a reductant [42, 47, 48]. However, glutathione has never been directly implicated in LD survival. Thus, we produced mutants in two critical genes for glutathione biosynthesis *gshA* and *gshB*, and tested these strains for LD sensitivity. Growth was attenuated in the *gshB* mutant specifically under LD conditions (**Supplementary Figure 3-S3C**). To show that glutathione is specifically important in LD survival versus other ROS scavenging systems [42] we also inactivated the gene for catalase (*katG*), which showed no growth attenuation under LD conditions (**Supplementary Figure 3-S3C**). Thus, not only do we see the expected decrease in metabolites involved in the OPPP and glycolysis, we also see a number of downstream indications that *ΔrpaA* cells are severely reductant stressed. The implication of glutathione metabolism in LD sensitivity further reinforces the importance of reductant balance and redox regulation for LD survival.

In cluster 1, which contains compounds that increase in *ΔrpaA*, there was a significant enrichment of compounds participating in fatty acid biosynthesis ($p = 0.007$) (**Figure 3-3B**). Fatty acids were not significantly

elevated prior to entering the dark period (**Figure 3-2A**), however later in the time course (between 2-6 h) palmitic acid, palmitoleic acid, and myristic acid all show very large increases in abundance in *ΔrpaA* mutants (**Figure 3-2B**). Additionally, there are large increases in the metabolically connected compounds pyruvate, 3-hydroxypalmitic acid, which is a component of lipid A [49]**,** and the membrane glycerolipid monogalactosyl monoacylglycerol (MGMG) (**Figure 3-2B**). The *ΔrpaA* mutant also exhibits a large transient increase in α-ketoglutarate (AKG) 1 h after entering into the dark, which is agreement with an inability to biosynthesize amino acids (**Figure 3-2B and Supplementary Figure 3-S3A**). Finally, AMP becomes further elevated over the night period. AKG and AMP are particularly important indicators of C/N balance and energy status respectively, and these metabolites are classified as two of the most important discriminates between WT and *ΔrpaA* by the PLS-DA model (**Figure 3-3A and Supplementary Figure 3-S3B**)**.** In cyanobacteria elevated AKG is the primary signal for nitrogen deprivation, and activation of this system results in a coordinated transcriptional response with the subsequent degradation of phycobilisomes [50, 51]. The observed AKG elevation in *ΔrpaA* mutants temporally correlates with the rapid decrease in phycobilisome absorbance at 630 nm we observed in *ΔrpaA* mutants after 2 h in the dark (**Figure 3-1B**). Overall, it is interesting that we observe a buildup of AKG, AMP, and fatty acids together, as these metabolic networks are not directly linked by a known regulatory mechanism. The

combined elevation of these metabolites may be driven by the overall status of the cell as a reductant and energy poor environment.

An overall lower abundance of compounds involved in purine and pyrimidine biosynthesis may also indicate insufficient reducing power and OPPP activity in *ΔrpaA* mutants (**Figure 3-2B**). However, guanine and guanosine increase in their abundance dramatically over the time course (**Figure 3-2B**). Both guanine and guanosine are produced directly from GMP via independent enzymatic reactions [46]. However, unlike most biosynthetic reactions that consume reducing power, the biosynthesis of GMP from its precursor IMP results in the net formation of one NADH. Additionally, the movement of GMP to guanine results in the regeneration of the OPPP-derived intermediate PRPP, which is critical for many biosynthetic processes [46]. Thus, cellular conditions where reductant and OPPP intermediates are limiting may specifically drive metabolic movement towards guanine and its metabolites.

In summary, WT cells show very few metabolic changes for the first 6 h in the dark, with only small changes that indicate the activation of carbon degradation and the OPPP. However, when *ΔrpaA* mutants enter the dark we observe large and rapid decreases in both OPPP metabolites, and downstream compounds that require reducing power for their biosynthesis. Further, there are large elevations of fatty acid compounds in the late night period, and unusual nucleotide biosynthetic activity that may be driven by a

lack of reducing power and OPPP metabolites. In particular, the inability to provide reduced glutathione will affect the ability of the cell to deal with oxidative stress, modify the activity of metabolic enzymes via glutathionylation [42, 48], and has a demonstrated negative impact on LD survival (**Supplementary Figure 3-S3C**). Finally, we see an increase in both AKG and AMP, which are global indicators of C/N imbalance and low energy status respectively. Taken together, the data indicate that WT cells maintain a high level of metabolic stability in the dark, while *ΔrpaA* mutants experience a severe metabolic imbalance likely driven by a reductant deficit.

3.3.2.4 ΔrpaA Mutants Activate a Nitrogen Starvation Transcriptional Response

The elevated AKG and chlorosis observed in the *ΔrpaA* mutant suggest that these cells are activating a nitrogen-deprivation response after the dark transition. However, chlorosis can occur under a variety of stress conditions that may not be directly related to AKG elevation [41]. To determine if elevated AKG is accompanied by a transcriptional response linked to nitrogen deprivation we tracked transcript levels of *glnN* (glutamine synthase), a primary target of this response, before and 2 h after WT and *ΔrpaA* mutants entered the dark [51]. WT showed a slight decrease in *glnN* transcript levels after the dark transition; however, at the same time the *ΔrpaA* mutant showed a roughly 4-fold increase in *glnN* transcript levels (**Figure 3-3C**). Thus, the observed chlorosis response in the *ΔrpaA* mutant is likely the

result of an AKG-driven nitrogen-starvation transcriptional response rather than other stress factors.

3.3.2.5 Metabolite Abundance is Correlated Based on Global Redox and Energy Indicators

In our analysis a number of metabolites increase/decrease together despite the fact that they do not have a known shared regulatory mechanism. To investigate the hypothesis that metabolic shifts at night are coupled to the redox and energy state of the overall cellular environment we produced a correlation network that evaluated the empirical interdependencies of metabolite abundances across the combined data from WT and *ΔrpaA*. In this way we could infer coordinated regulation among metabolites that do not belonging to a common biochemical pathway [52, 53]. The full result of our analysis shows that two distinct groups of positively correlated metabolites exist, and correlations generally group based on the reductant and energy inputs necessary for a metabolite's biosynthesis rather than its biochemical proximity to other metabolites (**Supplementary Figure 3-S4**). Thus, we took a subset of this data and examined only statistically significant correlations between all compounds and four indicator metabolites: F6P, G6P, AMP, and AKG. These metabolites are good indicators for OPPP activity, cellular energy status, and global carbon/nitrogen balance [46, 51] (**Figure 3-4**).

The OPPP metabolites F6P and G6P show strong positive correlation with each other, primary carbon metabolites, and the nitrogen assimilatory

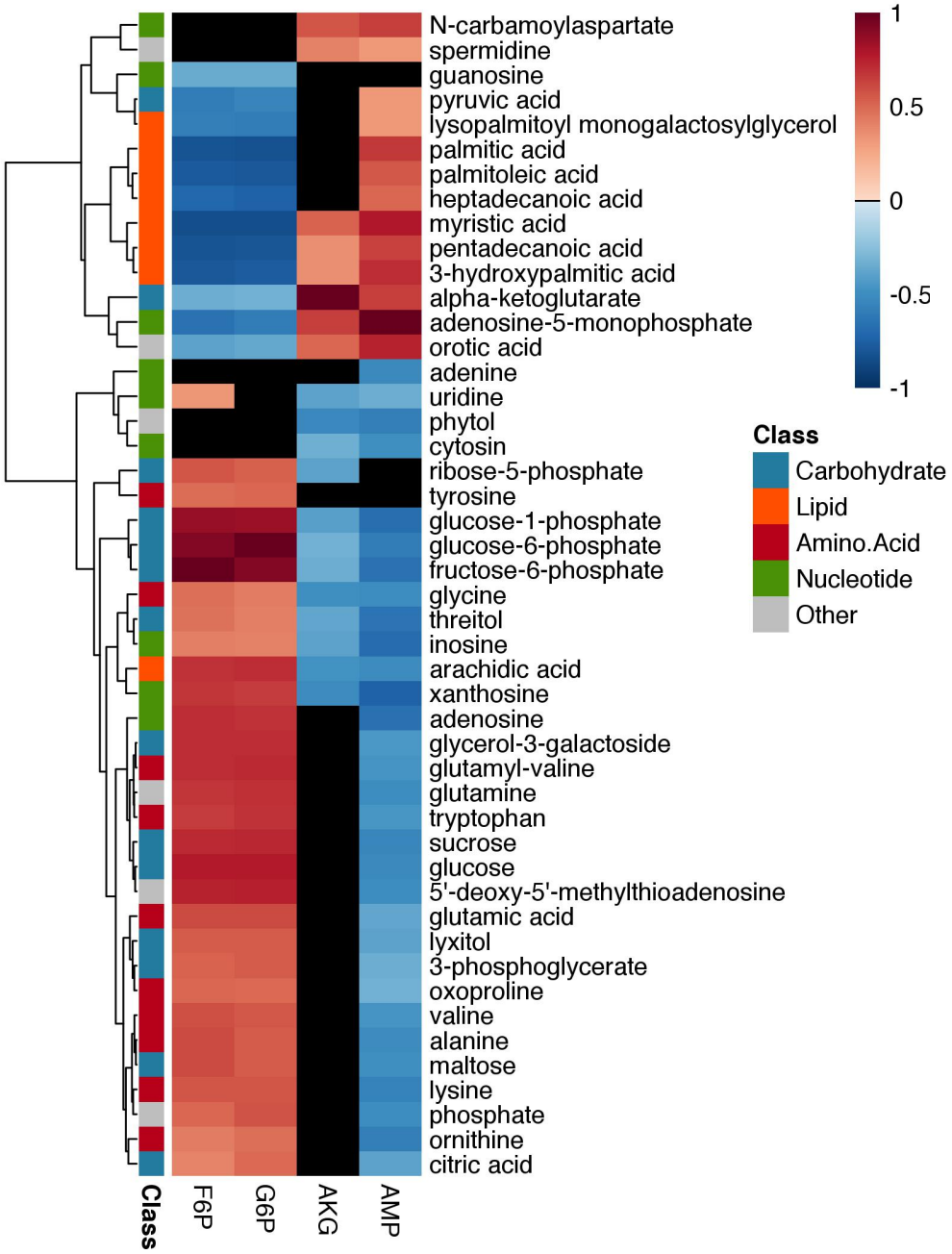

Figure 3-4. Heatmap of significant correlations between the indicator metabolites AMP, AKG, G6P, and F6P and all identified metabolites. Pearson's correlation coefficient (r) used to calculate correlation. Colored boxes to the right of clustering tree indicate metabolite class. Black boxes indicate that the calculated correlation did not pass the significance threshold. Significance calculated for individual correlations using a t-distribution and corrected for multiple testing using the method of Benjamini Hochberg (n = 43 per comparison; FDR < 0.05).

amino acids glutamine and glutamic acid (**Figure 3-4 and Supplementary Figure 3-S4**). Negative correlations with F6P and G6P are found for most fatty acids, AMP, AKG, and orotic acid a pyrimidine precursor that should accumulate when reducing power is lacking. Alternatively, AMP and AKG show a roughly opposite pattern of correlation to F6P and G6P. AMP and AKG are negatively correlated with most primary carbon metabolites, and show strong to moderate positive correlation with fatty acids (**Figure 3-4 and Supplementary Figure 3-S4**). These metabolites also have a strong positive correlation with orotic acid and another pyrimidine precursor N-carbamoylaspartate. Finally, AMP and AKG have strong positive correlations with each other.

Overall the correlation data suggest that the metabolic changes we observe in the *ΔrpaA* mutant are tightly coupled to global cellular energy status and redox state. Interestingly, while the transcriptional regulatory mechanisms that control fatty acid biosynthesis in cyanobacteria are poorly understood, we see that their increased abundance is strongly correlated with indicators of low energy status and reductant availability. Recent work has shown that fatty acid recycling increases dramatically and is important for growth under high-light conditions [54]. Thus, a change in cellular redox state may act as a signal for fatty acid turnover. Indeed, many enzymes in cyanobacteria are directly redox modified [9-11], and the high degree of correlation seen with cellular indicators of energy and nitrogen status

suggests that a large portion of the metabolic change occurring in *ΔrpaA* mutants may be driven by the specific cellular redox and metabolic environment rather than a coordinated transcriptional program.

3.3.3 Interventions That Suppress the ΔRpaA LD Lethality Phenotype Support Reductant Imbalance as a Hypothesis for Cell Death

To better understand the mechanism behind the phenotypic and metabolic responses we observed in the *ΔrpaA* mutant, we searched for compensatory interventions that would re-balance the system to suppress LD lethality. We found that secondary site mutations in metabolic genes and changes in growth condition light intensity suppressed sensitivity of *ΔrpaA* cells to LD conditions. The data strongly implicate cellular redox state and carbon/nitrogen imbalance as principal factors that drive *ΔrpaA* LD lethality.

3.3.3.1 Suppression of ΔrpaA LD Lethality by Secondary Site Mutagenesis

Observation of *ΔrpaA* mutants revealed that older cultures accumulate cells with the ability to grow under normally restrictive LD conditions (**Supplementary Figure 3-S5A**). These cells still maintained fully segregated deletions at the *rpaA* locus; thus, it was surmised that they have accumulated compensatory changes at secondary genetic loci. To investigate the types of mutations that could suppress *ΔrpaA* LD lethality, we mutagenized a freshly constructed *ΔrpaA* mutant with ethyl methanesulfonate (EMS). Both EMS

exposed and unexposed *ΔrpaA* cells were then incubated under a restrictive LD growth condition, after which hundreds of colonies with a wide degree of coloration and morphology appeared exclusively on the plate from the mutagenized sample (**Supplementary Figure 3-S5B**). We isolated 20 colonies, confirmed that all maintained fully segregated deletions at the *rpaA* locus (**Supplementary Figure 3-S5C**), and performed full genome re-sequencing on each. Comparison of the mutagenized genomes to both a WT control and the *ΔrpaA* parent strain revealed a total of 63 single nucleotide changes across all strains with an average of 3.15±1.2 new mutations per strain. Subsequently we filtered the mutations (see methods) and identified a subset of 56 that we categorized as “high confidence” for having a biological effect. Full data on all mutagenized strains and their associated mutations can be found in (**Supplementary Data Set 3-S3)**.

Of the high confidence mutations, 47% occurred in genes that code for metabolic enzymes (**Supplementary Data Set 3-S3**). A KEGG category enrichment analysis (**Figure 3-5A and Supplementary Data Set 3-S2**) identified enrichment for mutations in biosynthesis of purines (FDR = 2.8e-4), valine, leucine, and isoleucine (VLI) (FDR = 8.3e-4), pantothenate and CoA (FDR = 8.4e-4), global amino acids (FDR = 2.8e-4), and aminoacyl-tRNAs (FDR = 0.01) (**Figure 3-5A**). Thus, the vast majority of mutations were detected in nitrogen-utilizing metabolic pathways. Within these pathways we detected multiple independent mutations that affect the same biochemical

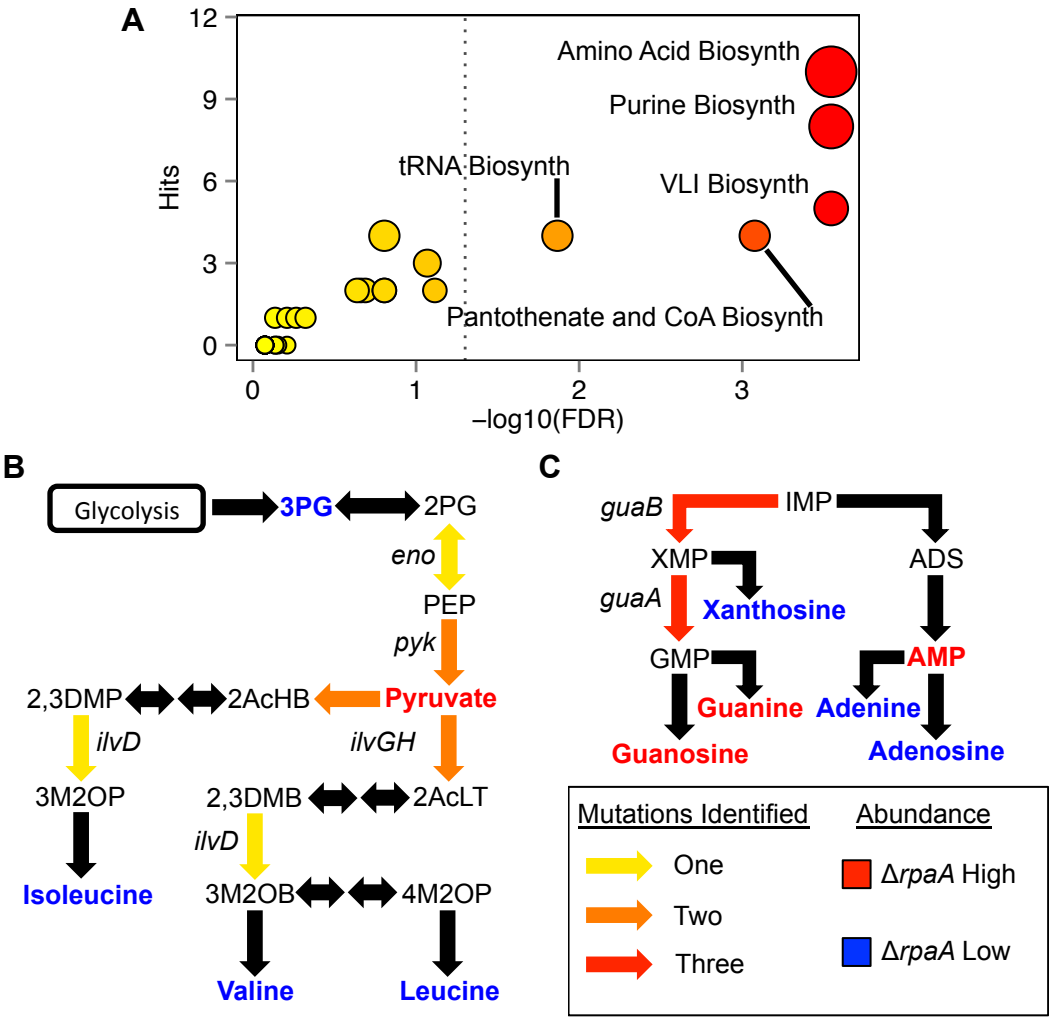

Figure 3-5. Summary of Δ*rpaA* suppressor mutant KEGG functional categories and metabolic pathway topology of mutated genes. (A) Plot of KEGG metabolic categories that were enriched in the gene set carrying "high confidence" suppressor mutations. The x-axis indicates the number of times a specific KEGG pathway was matched to genes in the set. Size of dots scales from small to big with increasing numbers of KEGG category matches, and color of dots scales from yellow to red with increasing significance. Dotted line indicates threshold required for significance. Significance calculated using the binomial distribution and corrected for multiple testing using the method of Benjamini Hochberg (FDR < 0.05). (B and C) Sub-pathway diagrams of VLI biosynthesis **(B)** and purine nucleotide biosynthesis **(C)** indicating locations of Δ*rpaA* suppressor mutations, and average abundance of compounds in the Δ*rpaA* strain relative to WT over the metabolomics time course (**Figure 3-2B**). Genes were named for reactions where a suppressing mutation was identified, and colors are detailed in the key.

step (**Figure 3-5B and 3-5C**), such as independent point mutations in *ilvG* and *ilvH* (the acetolactate synthase catalytic and regulatory subunits), the rate-limiting step of the VLI pathway (**Figure 3-5B**) [55]. We also found two independent point mutations in *pyk* (pyruvate kinase), which produces pyruvate, the substrate of *ilvGH* (**Figure 3-5B**) [46]. The effects within purine metabolism were even more striking, with three independent point mutations in *guaA* (GMP synthase), and three in *guaB* (inosine-5-monophosphate dehydrogenase) (**Figure 3-5C**). Interestingly, GuaA and GuaB participate in the steps directly responsible for guanine and guanosine biosynthesis, which is significantly elevated when the *ΔrpaA* mutant enters the dark (**Figure 3-2B and 3-5C**). In addition to VLI biosynthesis, a large number of mutations were found across a broad range of amino acid biosynthetic and tRNA-loading pathways (**Figure 3-5A and Supplementary Figure 3-S6**), suggesting that a general slow down of amino acid biosynthesis and utilization can suppress LD sensitivity in an *ΔrpaA* background.

3.3.3.2 Blocking VLI Biosynthesis Suppresses LD Lethality in ΔrpaA

Because the suppressed *ΔrpaA* strains each contained multiple EMS generated mutations, we wanted to confirm that an affected pathways identified by enrichment analysis was truly responsible for the suppression of LD lethality. We investigated the LD suppression mechanism via VLI biosynthesis using the herbicide metsulfuron methyl (MSM), which is a potent

and specific inhibitor of IlvGH [6, 56]. Treatment of *ΔrpaA* with MSM under LD growth revealed that this inhibitor could suppress cell death of *ΔrpaA* in these conditions on solid (100 nM MSM) and in liquid (25 μM MSM) medium (**Figure 3-6A, and Supplementary Figure 3-S7A**). Additionally, *ΔrpaA* cells treated with MSM did not become chlorotic in the dark (**Figure 3-6B and 3-1B**), or up-regulate the nitrogen deprivation response gene *glnN* (**Figure 3-3C**). Thus, one of the enriched pathways identified by genetic suppression is responsible for rescue of LD growth in *ΔrpaA*.

3.3.3.3 Suppression of VLI Biosynthesis Lowers Phycobilisome Content

Strains that carry VLI pathway mutations have a strong yellow color (**Supplementary Figure 3-S7B**). Absorbance scans taken prior to genomic DNA extraction for sequencing revealed that these strains have a decreased phycobilisome to chlorophyll ratio (630 nm/680 nm) relative to WT ($p < 0.01$) (**Table 3-1**). To investigate if pigmentation changes are the direct result of blocking VLI biosynthesis we incubated WT and *ΔrpaA* cells with MSM in the light for 12h and compared whole cell absorbance spectra of treated and untreated cells. The results showed that suppression of IlvGH activity by MSM results in a similar yellowing of cells. WT treated with MSM were decreased in all three pigment absorption maxima: 440 nm, 630 nm, and 680 nm ($p < 0.05$), with 630 nm showing the largest difference (**Figure 3-6C**); treated *ΔrpaA* cells also showed a significant decrease at 630 nm ($p < 0.05$)

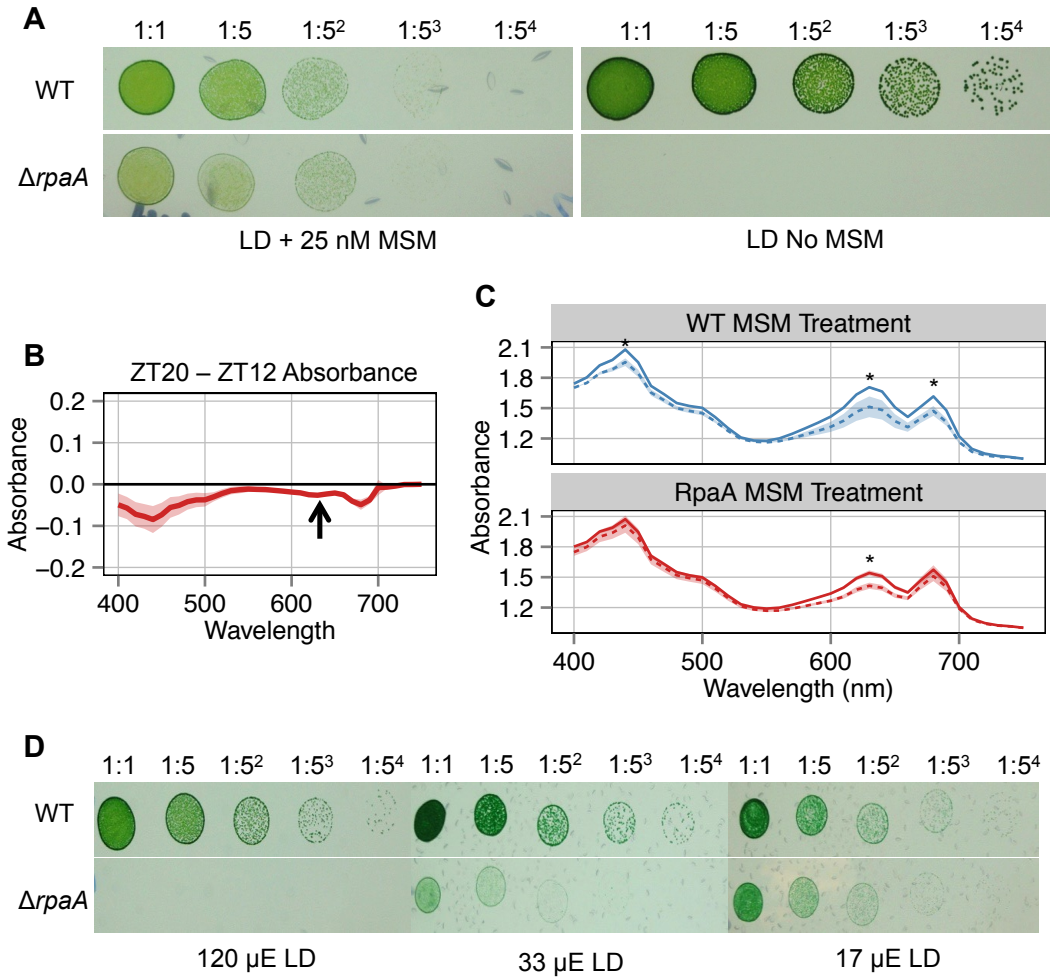

Figure 3-6. Summary of data on MSM and light intensity-mediated suppression of the Δ*rpaA* LD lethality phenotype. (A) Representative photo of dilution series of WT and Δ*rpaA* cells treated (left panel) and not treated (right panel) with 100 nM MSM (n = 6 biological replications of experiment). Pictured cells were grown under a 12:12 light-dark cycle with a light intensity of 120 $\mu E*m^{-2}*s^{-1}$. **(B)** Mean subtracted absorbance value of Δ*rpaA* cells treated with 25 µM MSM at ZT0 showing the absorbance difference from ZT12 (0 h darkness) to ZT 20 (8 h darkness). Shaded region indicates STDV of mean, and black arrow points to change in absorbance at 630 nm highlighting no significant change. Significance calculated using Student's t-test for absorbance at 440 nm, 630 nm, and 680 nm, and no significant change was observed (n = 3). **(C)** Mean absorbance values of WT (blue) and Δ*rpaA* (red) untreated (solid line) and treated (dotted line) with 25 µM MSM after 12 h of exposure in the light. Shaded area indicates SEM. MSM exposed cells show significantly lower absorption values at 440 nm, 630 nm, and 680 nm as calculated by a one-sided student's t-test (n = 3 for MSM treated samples and n = 4 for untreated samples; *p < 0.05). **(D)** Representative photo of dilution series of WT and Δ*rpaA* cells grown in a 12:12 light-dark cycle with decreasing daytime light intensity (indicated below each panel). Two biological replicates were performed.

(**Figure 3-6C**). These findings are in agreement with a similar yellowing phenotype observed in *Synechocystis sp.* PCC6803 cells that carry *ilvG*-null mutations [6]. Thus, while MSM treated *ΔrpaA* cells do not show further phycobilisome bleaching at night (**Figure 3-6B**), they do show reductions in phycobilisome content directly after treatment during the day (**Figure 3-6C**). As phycobilisomes are the primary light collecting protein pigment in *S. elongatus,* the MSM mediated decrease at 630 nm represents a significant change in the ability of cells to collect light, and likely alters both photosynthetic output and cellular redox state [57, 58].

3.3.3.4 Decreasing Light Intensity Suppresses ΔrpaA LD Lethality

Seeing that one suppressive mechanism may decrease the ability of cells to collect light, we tested whether lowering the light intensity used during the day portion of an LD cycle could suppress *ΔrpaA* LD lethality. WT and *ΔrpaA* mutants were serially plated and incubated under 3 light intensities in LL and LD. At the highest light intensity tested (120 μE) we observed the expected *ΔrpaA* growth defect in LD (**Figure 3-6D**). However, at an intermediate light intensity (33μE) *ΔrpaA* mutants had slightly improved growth (**Figure 3-6D**). Finally, at the lowest light intensity (17μE) *ΔrpaA* mutants grew to almost WT levels (**Figure 3-6D**). Thus, lowering the light intensity during an LD cycle creates a permissive condition where *ΔrpaA* mutants can survive. This permissive LD growth was also observed when

ΔrpaA mutants were cultured in photobioreactors under low light intensities (**Supplementary Figure 3-S7C**). The results suggest that the suppressive mechanism behind inactivation of VLI biosynthesis may be at least in part related to a decreased ability of cells to absorb light energy.

3.3.4 Redox Stress is Associated with Cell Death in the *ΔrpaA* Mutant

The protective effects of MSM treatment (**Figure 3-6B**) and decreased light intensity (**Figure 3-6C**), are consistent with photosynthetically generated ROS as a destructive agent that could account for *ΔrpaA* LD phenotypes. *S. elongatus* maintains a strict cellular redox balance and controls ROS using multiple systems including: modulation of phycobilisome abundance, glutathione redox control, and enzymatic ROS scavenging [42, 59]. Our data show that glutathione metabolism in particular is important for survival in LD (**Supplementary Figure 3-S3C**), and metabolites in glutathione biosynthesis are significantly affected when the *ΔrpaA* mutant enters the dark (**Figure 3-3B**). Thus, we tracked total ROS in WT and *ΔrpaA* over a 24-h LD cycle (high light intensity) using the fluorescent marker 2',7'-dichlorodihydrofluorescein diacetate (H_2DCFDA), which has been used previously to quantify total cellular ROS load in cyanobacteria [60, 61]. Samples were taken every 2 h during the 12-h day period and every hour during the 12-h night period. Additionally, we assessed the impact on total ROS when MSM was added to

cultures over the same growth period, to determine if this suppressive mechanism affects ROS levels.

ROS levels were similar for all strains at the beginning of the 12-h day (**Figure 3-7**). ROS increased gradually in all strains through the first 6 h of the day. Subsequently, ROS levels rapidly increased in the *ΔrpaA* mutant, and by the end of the light period (ZT 12) were on average 3.5-fold higher than in the WT or MSM-treated *ΔrpaA* strain (**Figure 3-7**). Upon entering the dark all strains showed a rapid drop in ROS level within the first two hours (**Figure 3-7**). ROS continued to drop in WT and the MSM-treated *ΔrpaA* mutant throughout the night, reaching a level similar to the beginning of the previous day period. In contrast, the untreated *ΔrpaA* mutant maintained high static ROS levels after the first 2-3 h of darkness and even showed a slight increase in ROS late in the night period (**Figure 3-7**). Additionally, when we compared ROS levels back to data on cell viability (**Figure 3-1C**) we found a limited (n = 4) positive association between the level of ROS at ZT12 and the degree of cell death that occurs the *ΔrpaA* mutant (**Supplementary Figure 3-S8A**). Treatment of WT cells with MSM did not affect ROS levels over the time course (**Supplementary Figure 3-S8B**). Overall, the *ΔrpaA* mutant accumulates much higher levels of ROS under the restrictive light condition and has trouble clearing ROS over the night period. However, treatment with MSM alleviates the elevated ROS phenotype observed in *ΔrpaA*. We propose that the rapid lethal effect of darkness on an *ΔrpaA* mutant results from a

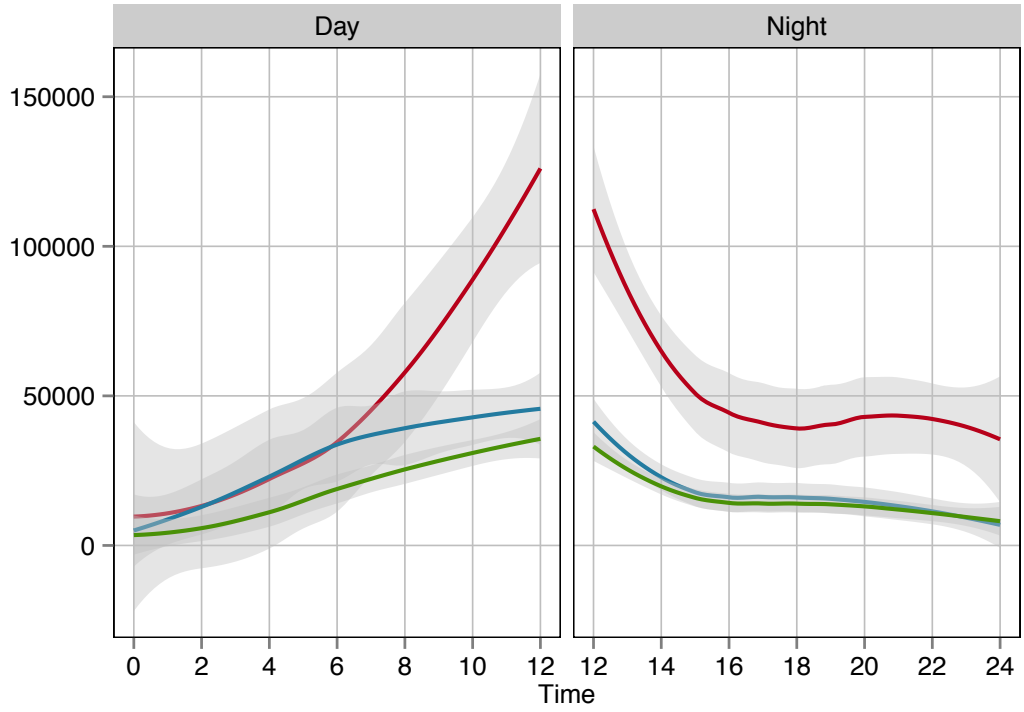

Figure 3-7. Plot of H_2DCFDA fluorescence over a 24 h 12:12 light-dark cycle indicating total cellular ROS in WT (blue), Δ*rpaA* (red), and Δ*rpaA* treated with 25 µM MSM (green). Curves shown are best-fit lines calculated using LOESS regression to all data points in a given sample; the grey shaded area indicates the 95% CI of the regression line (n = 21 data points for day samples; n = 42 data points for night samples). Day and night from the same experiment were split to more effectively fit regressions. Places were the confidence interval does not overlap indicate a statistically significant difference in the model.

failure to clear ROS that accumulates late in the day period. Detoxification of ROS at night places an additional strain on the reductant pool, which likely exacerbates the metabolic imbalances we observe in this strain.

3.4 Discussion

It is clear that RpaA is critical for activating carbon metabolism at night and for diurnal viability in *S. elongatus*. However, the overall metabolic and physiological importance of metabolism at night, and the mechanism behind LD lethality in *rpaA* mutants has been an open question. In this study, we present three main findings that provide a framework for understanding why carbon metabolism is important at night, and illustrate critical functions of RpaA during the day and night periods of diurnal growth: (1) Inactivation of *rpaA* affects cellular pigmentation and causes a significant buildup of ROS during the day period; (2) WT cells maintain strict metabolic stability at night while the *ΔrpaA* mutant shows changes indicative of a severe reductant deficit; (3) The *ΔrpaA* mutant fails to detoxify ROS accumulated during the day, which causes abnormal redox driven metabolic flux and directly contributes to dell death during the night period. Thus, circadian outputs play a key role in maintaining cellular redox balance, and this function is critical for metabolic stability and viability at night.

3.4.1 RpaA has Critical Functions During the Day Period for Diurnal Survival

One of the surprising findings from this study is that events during the day ultimately lead to rapid killing of the *ΔrpaA* mutant in the dark, as the mutant survives the night when the day-time light levels are low. This outcome was not anticipated because levels of light that lead to lethality in the dark, in an LD cycle, are well tolerated by the *ΔrpaA* mutant when it is grown under LL conditions. It is still unclear why *ΔrpaA* mutants accumulate high levels of ROS during the day. However, the period of most rapid ROS accumulation in the *ΔrpaA* mutant occurs during the last 6 h of the day, when RpaA would normally become phosphorylated and increase in its activity [62]. Regardless of source, the pigment absorbance, ROS, and metabolomics data indicate that once cells reach the light-to-dark transition the *ΔrpaA* mutant is already under a great deal of cellular redox stress, as indicated by increased carotenoids and high levels of spermidine and putrescine (**Figure 3-1A, 3-2A, and 3-7A**) [42, 43]. AMP is also highly elevated, which indicates that *ΔrpaA* may be having difficulty producing ATP. It is possible this deficit is a secondary effect of redox stress, as the ATP synthase subunits are known to be redox regulated [63].

We expect that the high redox stress observed prior to entering the dark period is a critical component of the LD lethality phenotype, and do in fact observe a limited positive association between the level of ROS prior to

the dark transition and the degree of cell death through the dark period (**Supplementary Figure 3-S8A**). Because MSM administration, which phenocopies the suppressor mutations found in the VLI biosynthesis pathway, both decreases phycobilisome absorbance (**Figure 3-6C**), and directly alleviates the ROS phenotype (**Figure 3-7**), the results are consistent with overstimulation of photosynthetic pathways as a source of ROS. Thus, contrary to our expectations, many of the suppressor mutations may assert their primary effect during the light period via depression of phycobilisome levels and attenuation of light absorption. Although our investigation focused on the mutations affecting the VLI biosynthetic pathway, strains that carry other mutations in amino acid and aminoacyl-tRNA biosynthesis also exhibit similarly depressed phycobilisome absorbance (**Supplementary Figure 3-S7B and Table 3-1**). As some of the most abundant proteins in cyanobacteria [21], phycobilisomes are expected to be affected significantly by amino acid limitation. In this way the cells would collect less light energy and reduce the generation of ROS. Also in agreement with this hypothesis, we identified two independent strains that carry mutations in the membrane transporter for magnesium (**Supplementary Data Set 3-S3**). Magnesium limitation causes a significant reduction in chlorophyll content and ribosome functionality in *S. elongatus* [64], which is consistent with both a reduction in protein biosynthesis and a mechanism that functions via attenuated light absorption.

The viability of the *ΔrpaA* mutant in LL, at a light intensity that generates high ROS, suggests that lethality in the dark results from cessation of ROS scavenging processes that protect cell in the light. It is likely that NADPH produced via photosynthesis can drive the ROS detoxification mechanisms necessary to maintain *ΔrpaA* cell viability. However, when the *ΔrpaA* mutant enters the dark under redox stress, they lack a source of NADPH due to an attenuated ability to degrade glycogen and activate the OPPP [19, 23]. Subsequently, we see a cascade of metabolic and physiological events that eventually leads to cell death.

3.4.2 Metabolic Changes at Night in ΔrpaA Indicate a Severe NADPH Deficit

The OPPP is the primary mechanism for sugar catabolism and NADPH generation at night, and RpaA is a strong activator of this pathway [19, 23, 38, 65]. Consistent with an inability to activate the OPPP, the first change that occurs when the *ΔrpaA* mutant enters the dark is the rapid depletion of soluble sugars (**Figure 3-2B**), particularly the OPPP indicator F6P[36], which can not be replenished by glycogen catabolism [23]. Without an operable OPPP, the primary pathway available to metabolize soluble carbon is glycolysis. Glycolysis will only produce NADH as a reducing equivalent, which is a poor electron source for ROS detoxifying processes [42], and will result in the excess buildup of downstream metabolites relative to the OPPP. This is due to the fact that the OPPP functions as a cycle at

night, recycling its inputs, as opposed to a linear pathway [44, 45]. Increased pyruvate and AKG in the *ΔrpaA* mutant are consistent with this hypothesis (**Figure 3-2B**).

AKG buildup normally results in its rapid conversion to glutamate via nitrogen assimilation, however this requires significant reducing power in the form of NADPH, as glutamine synthase and nitrate reductase are ferredoxin dependent enzymes that use NADPH exclusively in their oxidation/reduction cycle [66, 67]. Because glutamine and glutamate are the primary nitrogen donors in metabolism, the rapid depletion of many amino acid species in the *ΔrpaA* mutant, concurrent with AKG elevation (**Figure 3-2B**), is consistent with an NADPH deficit that precludes cells from performing AKG to glutamate biosynthesis. Additionally, because elevated AKG is a signal for nitrogen deprivation [51], we see an activation of the nitrogen deprivation transcriptional response (**Figure 3-3C**) and phycobilisome degradation (**Figure 3-1B**) soon after the *ΔrpaA* mutant enters the dark. Transcriptional activation of this system likely puts further strain on reductant pools in the *ΔrpaA* mutant. In fact, a known response of WT cells to darkness is to strongly up-regulate glutamine synthase inactivating factor (IF7) [68], suggesting that the activation of nitrogen assimilation is highly unfavorable at night.

We expect that the point ROS detoxification terminates in the *ΔrpaA* mutant (**Figure 3-7**) is concurrent with the exhaustion of its limited NADPH

pool, as NADPH is critical for ROS scavenging [42]. Consistent with this hypothesis chlorosis (**Figure 3-A2)**, AKG elevation (**Figure 3-2B and Supplementary Figure 3-S3A**), and the start of cell death **(Figure 3-1D**) occur at a similar time to the stagnation of ROS levels (**Figure 3-7**). Once the NADPH pool is depleted we see the termination of ROS scavenging and the emergence of more severe phenotypes. Thus, the primary mechanisms directly driving cell death likely occur between the 2-6h period after entering the dark, and cell viability rapidly drops off during this time.

3.4.3 Altered Redox State Drives Abnormal and Detrimental Metabolic Flux in ΔrpaA

Although it has been known for some time that protein redox modifications drive important metabolic shifts in cyanobacteria and plant chloroplasts [11, 36, 69, 70], recent work has shown that redox modifications are highly pervasive across all metabolic pathways in cyanobacteria, and that light-dark transitions drive global changes in the oxidation state of redox modified proteins [9, 10, 48]. Due to the fact that *S. elongatus* performs almost no *de novo* transcription at night [68], redox modifications on metabolic enzymes likely play a major role in dictating metabolic flux when cells are in the dark. We expect that some of the metabolic changes seen in the *ΔrpaA* mutant after the termination of ROS detoxification are directly driven by an inability of the mutant to further modulate cellular redox state.

Specifically in the case of lipids and purine nucleotides, there is evidence that accumulation of these metabolites can be driven by redox changes and may contribute directly to LD lethality.

Lipids are particularly sensitive to oxidative stress, and their turnover is important under redox stress conditions, as their oxidized species can further perpetuate oxidative damage [71]. It has been recently shown that the rate limiting enzyme of cyanobacterial lipid biosynthesis, FabH, undergoes light-dark dependent redox modification [9, 72], and separately that high light intensity can activate lipid recycling in *S. elongatus* [54]. Consistent with a redox driven mechanism, the largest increases in fatty acid abundance in the *ΔrpaA* mutant are temporally coincident with the termination of ROS detoxification (**Figure 3-2B and 3-7**). However, free fatty acids are uncommon in cyanobacteria as they are activated and recycled by AAS (Acyl-ACP synthetase) in an ATP dependent reaction [49]. This is important as high concentrations of free fatty acids cause detrimental phenotypes in *S. elongatus* [73]. Thus, under conditions where fatty acid turnover becomes active, any free fatty acids would normally be recycled. However, the buildup of free fatty acids in the *ΔrpaA* mutant likely indicates that ATP is not available to perform the AAS driven recycling reaction, which agrees with the positive correlation between fatty acids and AMP (**Figure 3-4 and Supplementary Figure 3-S4**). In fact the fatty acid profile of the *ΔrpaA* mutant is almost identical to that of an *aas*-null mutant where myristic acid,

palmitic acid, palmitoleic acid, 3-hydroxypalmitic acid, and MGMG all increase in abundance but steric acid does not (**Figure 3-2B**) [49, 54]. Thus oxidative stress in the *ΔrpaA* mutant may promote fatty acid turnover, but insufficient ATP precludes fatty acid activation. The accumulation of free fatty acids will negatively affect membrane integrity and elicit oxidative stress like responses [73, 74], which is consistent with the small increase in ROS noted in *ΔrpaA* mutants 8 h into the night period (**Figure 3-7**).

Most nucleotide species are far less abundant the *ΔrpaA* mutant (**Figure 3-2B**), as they require precursors derived from the OPPP. Thus, we expect that the accumulation of guanine and guanosine in the *ΔrpaA* mutant at night is highly detrimental, as it would deplete limited carbon and nitrogen precursors such as PRPP and glutamine (**Figure 3-2B**). This hypothesis is consistent with the identification of six independent mutations in the GMP biosynthetic pathway (**Figure 3-5C**). It is not fully clear why these nucleotide metabolites accumulate, but the buildup of guanine and guanosine from GMP is favorable to the production of GTP, as GTP synthesis requires ATP, which is likley unavailable in the *ΔrpaA* mutant. The enzymatic activity of GuaA and GuaB may also be directly affected by redox state, as they are modified by glutathionlaytion under oxidative conditions [48], and the enzymes leading from IMP to AMP are not [48]. Regardless of mechanism, the biosynthesis of guanine and guanosine likely depletes already limited carbon and nitrogen pools, and causes a detrimental effect in the *ΔrpaA* mutant at night.

3.4.4 Conclusions and Future Directions

The data presented here reinforce the growing connection between circadian clock outputs and metabolism, help explain the mechanism behind the LD lethality of the *ΔrpaA* mutant, and establish a framework for the importance of coordinated circadian regulation and redox balance during LD growth. We have shown that RpaA plays a critical role in ROS control and the maintenance of metabolic stability at night. These data support redox state as a major regulatory factor in the dark, which is not surprising considering the low level of *de novo* mRNA synthesis occurring in *S. elongatus* at night [68]. Although it is known that RpaA activates OPPP genes in the late day [19], these data support a model where transcriptional activation by RpaA is the primary driver of OPPP activity at night. Subsequently, the reductant derived from the OPPP at night serves to detoxify ROS generated during the day, and maintain metabolic stability.

The high levels of ROS accumulated in the *ΔrpaA* mutant during the day provide a unique insight into the daytime functions of RpaA, and should be further explored. In particular the pigmentation changes noted during LL growth of the *ΔrpaA* mutant (**Figure 3-1A**) suggest that core photosynthetic parameters are altered. Metrics such as photosystem efficiency, capacity, and oxygen evolution have not been well explored in the context of circadian rhythms. Additionally, it is very interesting that ROS levels in the *ΔrpaA* mutant consistently increase at a specific time of the day, as this mutant lacks

a clock output mechanism and does not exhibit transcriptional rhythms [19, 31]. This may indicate that non-circadian rhythmic processes, such as peroxiredoxin rhythms, are important for modulating ROS [15, 75]. This would be consistent with peroxiredoxins playing roles in oxidative stress mediated signaling [76]. Additionally, because ROS levels increase at the time RpaA would normally be most active [62], this may indicate that there is normally an interaction between circadian and non-circadian rhythmic processes at this time.

The importance of redox modifications across metabolism is a deeply unexplored area in cyanobacteria. The application of redox proteomics to an *ΔrpaA* mutant would likley provide a more complete understanding of why we see specific metabolic movement when the OPPP is inactive at night. Additionally, it is possible that not all redox stress is the same, and the redox stress encountered in a *ΔrpaA* mutant only affects a subset of proteins that have the capacity to be redox modified. Understanding how redox modifications affect metabolism, and how to manipulate them, also holds great promise for improving metabolic engineering efforts. One of the primary factors considered in cyanobacterial metabolic engineering strategies is reductant balance [1], as many engineered pathways will consume considerable amounts of reducing power. Understanding how redox imbalances affect cyanobacterial metabolism will be of crucial importance to advance the engineering of cyanobacteria grown under natural diurnal

conditions. Overall, the data presented here further link circadian output to metabolic and redox stability, and shed light on the long standing mystery of LD lethality in *S. elongatus rpaA* mutants.

3.5 Materials and Methods

3.5.1 Cyanobacterial Strains, Media, and Culture Conditions

The WT *S. elongatus* PCC7942 strain used in this study is archived as AMC06 in our laboratory. All *ΔrpaA* mutants were constructed in the AMC06 background with the plasmid pAM4420, previously used in our laboratory [40], using standard procedures for cyanobacterial transformation [28]. All *rpaA* gene disruptions were validated by PCR of native loci. For all experiments, pre-cultures were first prepared in 100 mL fresh BG-11 medium [77] as in Diamond, et al. [23].

For metabolomics experiments, pre-cultures were used to inoculate Phenometrics ePBR v1.1 photobioreactors (Phenometrics Inc.) at an initial density of OD_{750} = 0.1 in a total volume of 400 mL of BG-11 medium without antibiotics. Temperature was maintained at 30 °C, 0.2 μm, filtered air was sparged at a rate of 50 mL/min, and light intensity was either 150 $\mu E*m^{-2}*s^{-1}$ or 500 $\mu E*m^{-2}*s^{-1}$ provided from the top of the culture while lights were on. After inoculation, cultures were grown at a constant light intensity of 150 $\mu E*m^{-2}*s^{-1}$ until OD_{750} = 0.3. Cells were then maintained turbidostatically at

this density for the duration of the experiment. In the metabolomics experiment WT cells circadian rhythms were entrained by growth in a 12:12 LD at a light intensity of 150 $\mu E*m^{-2}*s^{-1}$ cycle for 1 d and subsequently at a light intensity of 500 $\mu E*m^{-2}*s^{-1}$ for 2 d before release into experimental conditions and sampling. The Δ*rpaA* strains were maintained in constant light at the same intensities of the WT strain prior to the sampling procedure (**Supplementary Figure 3-S9**).

For absorbance scanning, viable cell counts, qRT-PCR, MSM treatment absorbance measurements, and oxidative stress measurements pre-cultures were used to inoculate Phenometrics ePBR v1.1 photobioreactors at an initial density of OD_{750} = 0.2 in a total volume of 400 mL of BG-11 medium without antibiotics. Temperature, airflow rate, and light intensity settings were the same as above. For these experiments both WT and *ΔrpaA* mutants were maintained at a constant light intensity of 150 $\mu E*m^{-2}*s^{-1}$ for 1 d. Subsequently both strains were subjected to growth in a 12:12 LD cycle at a light intensity of 150 $\mu E*m^{-2}*s^{-1}$ for 2 d. Light intensity was then increased to 500 $\mu E*m^{-2}*s^{-1}$ over the final 12:12 LD period during which sampling took place.

For viable cell plating 200 µL of the indicated sample was serially diluted in fresh BG-11 medium without antibiotics 5 times using a 1:5 dilution ratio. For LD sensitivity testing samples were first all diluted to an OD_{750} = 0.2, and the same dilution scheme was then followed. Subsequently, 4 µL of each

sample was spotted on to solid BG-11 plates without antibiotics. It was found that the use of antibiotics under these conditions confounded the results of LD sensitivity testing. Plates for viable cell counting were incubated at 30 °C and 150 $\mu E*m^{-2}*s^{-1}$ constant light for 5-6 d before being photographed. Plates for LD sensitivity testing were plated in duplicate with one set being incubated at 30 °C and 150 $\mu E*m^{-2}*s^{-1}$ constant light for 5-6 d, and a second set being incubated at 30 °C and a 12:12 LD cycle with a light intensity of 150 $\mu E*m^{-2}*s^{-1}$ for 6-8 d before being photographed.

3.5.2 Whole Cell Absorbance Spectra Analysis

For all reported absorbance spectra, the absorbance between 400 – 750 nm was determined for 200 µL of the indicated sample using a Tecan Infinite M200 plate reader. Raw absorbance values were normalized to the within sample value of OD_{750}. Statistical analysis of particular absorbance values were conducted using the students t-test with a p-value < 0.05 being considered significant ($n \geq 3$).

3.5.3 Metabolomics and Data Analysis

Strains for metabolomics were grown in Photobioreactors as described above. Sampling at the indicated time points ($n = 5$ at each time point and for each genotype) before and after cells entered a dark period (**Supplementary Figure 3-S9**) was conducted identically to the methods used in Diamond, et

al. [23]. Metabolite extraction and analysis by GC-TOF-MS was conduced at the West Coast Metabolomics Center (WCMC) at the University of California, Davis using the methods described by Fiehn, et al. [78, 79].

Raw metabolite abundance data for known metabolites (**Supplementary Data Set 3-S1**) were analyzed using a combination of the online analysis platform MetaboAnalyst 3.0 [80], and the statistical package R [81]. Principal component analysis (PCA) was applied to $\log_2$ normalized and autoscaled data to detect outlying samples. Based on PCA, replicate A of the WT sample was removed from the dataset prior to statistical analysis (**Supplementary Figure 3-S10A**). Also, WT replicate C time T6 and *ΔrpaA* replicate C time T4 were removed before analysis due to problems during sample extraction reported by the WCMC.

To detect metabolites that changed between WT and *ΔrpaA* at the initial sampling time point (0 h) we used a t-test on $\log_2$ normalized data (FDR corrected p-value < 0.05) [82], and required significant metabolites to show a > 2-fold change between genotypes. To detect metabolites that changed between WT and *ΔrpaA* over the entire time course we applied two separate statistical methods to $\log_2$ normalized abundance data: 2-way ANOVA analysis (Tukeys HSD, $p < 0.05$), and a linear mixed effect model using genotype and time as fixed effects and allowing for each replicate and time of sampling to contribute random effects. Models produced using genotype as a fixed effect were compared to models produced without genotype as a fixed

effect using ANOVA, and p-values were corrected using the method of Benjamini and Hochberg [82] (pFDR < 0.05) Both methods produced almost identical lists of significant metabolites, thus we chose to use the output from 2-way ANOVA in our analysis. Hierarchical clustering of significant metabolites for heatmap ordering was performed using the R package pheatmap, with Euclidian distance and complete linkage for leaf ordering.

PLS-DA modeling was carried out on log_2 normalized and autoscaled data with genotype and time as class factors. Using leave-one-out cross-validation indicated that the PLS-DA model providing the most prediction accuracy utilized 2 components (**Supplementary Figure 3-S10B**). Subsequently, permutation testing confirmed that the ability of our PLS-DA model to correctly predict class membership based on the top 25 discriminating metabolites was statistically significant relative to a random permuted model (p = 0.008; n=1000) (**Supplementary Figure 3-S10C**).

Metabolite KEGG enrichment analysis was conducted using a custom written R script and the metabolic categories in (**Supplementary Data Set 3-S2**). Statistical overrepresentation was determined using fishers exact test. Due to the difficulty in achieving high statistical significance with the low numbers of tested metabolites, we did not apply a multiple testing correction to p-values, but required > 3 metabolites to be present in a pathway with a p-value < 0.05 to be considered significant.

Correlation between metabolites was calculated using Pearson's correlation statistic (r). Correlations of indicator metabolites was filtered based on statistical significance calculated using a students t distribution and corrected using the method of Benjamini and Hochberg [82] (pFDR < 0.05). Hierarchical clustering of correlations was performed identically to above.

3.5.4 qRT-PCR Analysis

For each respective cyanobacterial sample, 10 ml culture at an OD750 of 0.2-0.4 was collected and immediately placed on ice. The cultures were then centrifuged for 10 min at 4,000x g and -10°C. Pellets were then frozen at -80°C until extraction. Total RNA was extracted using the TriZol reagent (Life Technologies; Carlsbad, CA) and the Direct-zol RNA MiniPrep Kit (Zymo Research; Irvine, CA). Briefly, the frozen pellets were thaw on ice and resuspended thoroughly in 1ml of TriZol reagent. Cell suspensions were then transferred to 1.5-ml microcentrifuge tubes on ice, and cells were lysed by 5-10 cycles of vortexing for 30 sec at RT and then sitting for 30 sec on ice. Cell debris were pelleted by centrifuging at 16,000x g at room temperature for 5 min. After transferring the supernatant to an RNase-free 2-ml tube, 1 volume of 100% ethanol for every volume of TriZol (typically 1 ml) was added and mixed by pipetting up and down. Total RNA was isolated from the TriZol-ethanol mixture following the manual of the Direct-zol RNA MiniPrep Kit. The RNA quality was checked with agarose gel imaging (1% agarose, 0.5x TBE,

75 V/60 min), using 10,000x SYBR green II RNA gel stain (Lonza, Switzerland). The extracted RNA samples were treated with DNaseI (Thermo Scientific, USA) to remove contaminating gDNA. Cognate cDNA was synthesized with the SuperScript III First-Strand Synthesis System for RT-PCR (Life Technologies) following the kit manual. For qRT-PCR experiments, standard reactions in triplicates were set up with the Power SYBR Green PCR Master Mix (Life Technologies) and run on a StepOnePlus Real-Time PCR System (Life Technologies) following the instructions of the manufacturer. The qPCR results were calculated from triplicate experiments.

3.5.5 Mutagenesis and Identification of *ΔrpaA* Suppressing Mutations

Ethyl methanesulfonate (EMS) mutagenisis of fresh *ΔrpaA* mutant cyanobacterial strains was carried out as in Kondo, et al. [30]. Mutaganized cultures were resuspended in 5 mL BG-11 medium with appropriate antibiotics and incubated at 30 °C, using 150 RPM shaking, under 30 $\mu E*m^{-2}*s^{-1}$ constant light for 2 days. Subsequently 300 µL of mutaganized *ΔrpaA* cells (as well as appropriate controls) were plated on BG-11 plates with appropriate antibiotics. Plates were prepared in duplicate and one set was incubated at 30 °C and 150 $\mu E*m^{-2}*s^{-1}$ constant light for 15 d, with the second set being incubated at 30 °C and a 12:12 LD cycle with a light intensity of 150 $\mu E*m^{-2}*s^{-1}$ for 15 d. 40 colonies that formed on the 12:12 LD grown plate that contained EMS mutagenized *ΔrpaA* cells, were picked and patched onto BG-

11 plates with appropriate antibiotics and grown for a further 10 d at 30 °C and a 12:12 LD cycle with a light intensity of 150 $\mu E*m^{-2}*s^{-1}$ to confirm suppression of the LD death phenotype. Patches of surviving *ΔrpaA* EMS mutants were then transferred to 10 mL BG-11 medium and incubated at 30 °C, using 150 RPM shaking, with a 12:12 LD cycle and light intensity of 120 $\mu E*m^{-2}*s^{-1}$ for between 11-16 d. Absorbance scans were taken of all cultures as described above, and genomic DNA was extracted using standard methods [28]. Prior to sequencing genomic DNA, the disruption of *rpaA* in all strains was verified by PCR (**Supplementary Figure 3-S5C**).

Genomic library preparation for Illumina short read sequencing was performed using the NEBNext DNA library preparation kit (NEB #E6040S/L) with NEXTflex barcoded cDNA adaptors (BIOO Scientific #514104). Samples were run on an Illumina HiSeq2500 DNA sequencer at the University of California, Berkeley QB3 Genomics Sequencing Laboratory. Sequencing runs resulted in 50 bp reads with a median coverage depth of 45.7X per sample over the *S. elongatus* genome. However, for Samples 1.1, 1.25, and 2.3, (**Supplementary Data Set 3-S3**) genome re-sequencing was performed at Bio Applied Technologies Joint, Inc. using the Ion PGM system (Life Technologies) following the standard work flow illustrated in the manuals of the Life Technologies kits. Sequencing libraries were prepared with the Ion Xpress Plus Fragment Library Kit. In brief, 1 mg total gDNA was sheared into desired fragment size (200-400 bp) via enzymatic digestion, and then ligated

to specified sequencing adapters and/or barcode adapters. The sequencing templates were amplified from constructed libraries using the Ion OneTouch 2 System and the Ion PGM Hi-Q OT2 Kit. Amplified templates were processed with the Ion PGM Hi-Q Sequencing Kit and loaded on an Ion 316 Chip Kit v2 for sequencing on a Ion PGM system with 500 sequencing flows (200 bp reads). Reads from all sequencing methods were mapped against the *S. elongatus* genome (GenBank accession NC_007604) and the large plasmid pANL (GenBank accession AF441790), and polymorphisims were called using the program breseq [83]. Polymorphisims were filtered for "high confidence" mutations by removing all mutations that resulted in a high-use codon coding for the same amino acid. All mutations in non-coding regions were included in the "high confidence" set.

KEGG enrichment analysis of mutated genes was conducted using a custom written R script and the metabolic categories in (**Supplementary Data Set 3-S2**). Statistical overrepresentation was determined using the binomial test, and p-values were corrected using the method of Benjamini and Hochberg [82].

3.5.6 Quantification of Reactive Oxygen Species

ROS were quantified using the fluorescent marker H_2DCFDA (Life Technologies #D399). Briefly, 2 mL of photobioreactor grown (see above) culture was collected and split into 1 mL aliquots. H_2DCFDA was added to

one sample at a final concentration of 5 μM. Tubes were protected from light and shaken at 30 °C for 30 min. Following incubation, 200 μL of each tube was added to a separate well in a 96-well plate. Fluorescence was quantified at an Ex: 480 nm and an Em: 520 nm on a Tecan Infinite M200 plate reader with the gain manually set to 120. Fluorescence data was normalized to OD_{750} of each sample and untreated sample background fluorescence was then subtracted from treated sample fluorescence.

3.6 Acknowledgements

We thank all of the members of the Greenspan Lab, and the Berkeley QB3 Genomics Sequencing Laboratory, for their assistance with library preparation and sequencing. Additionally, we thank BATJ, Inc. for their collaboration in sequencing the remaining suppressor mutants after the initial sequencing effort. Also we would like to thank Mark Paddock for helpful discussion that improved the manuscript, and Anish Pal for assistance with sample collection and strain maintenance. This work was supported by National Science Foundation Grant MCB1244108. S.D. and B.R. were supported in part by National Institute of Health and Molecular Genetics Training Grant T32GM007240.

Chapter 3 is a manuscript in preparation for publication under the tentative citation: Diamond, S., Rubin, B. E., Shultzaberger, R. K., Chen, Y., Barber, C. D., & Golden, S. S. (2015). Keeping the Balance: The

Cyanobacterial Circadian Response Regulator RpaA is Critical for Metabolic Stability at Night. The dissertation author will be the primary author of this publication

3.7 Supplementary Figures and Tables

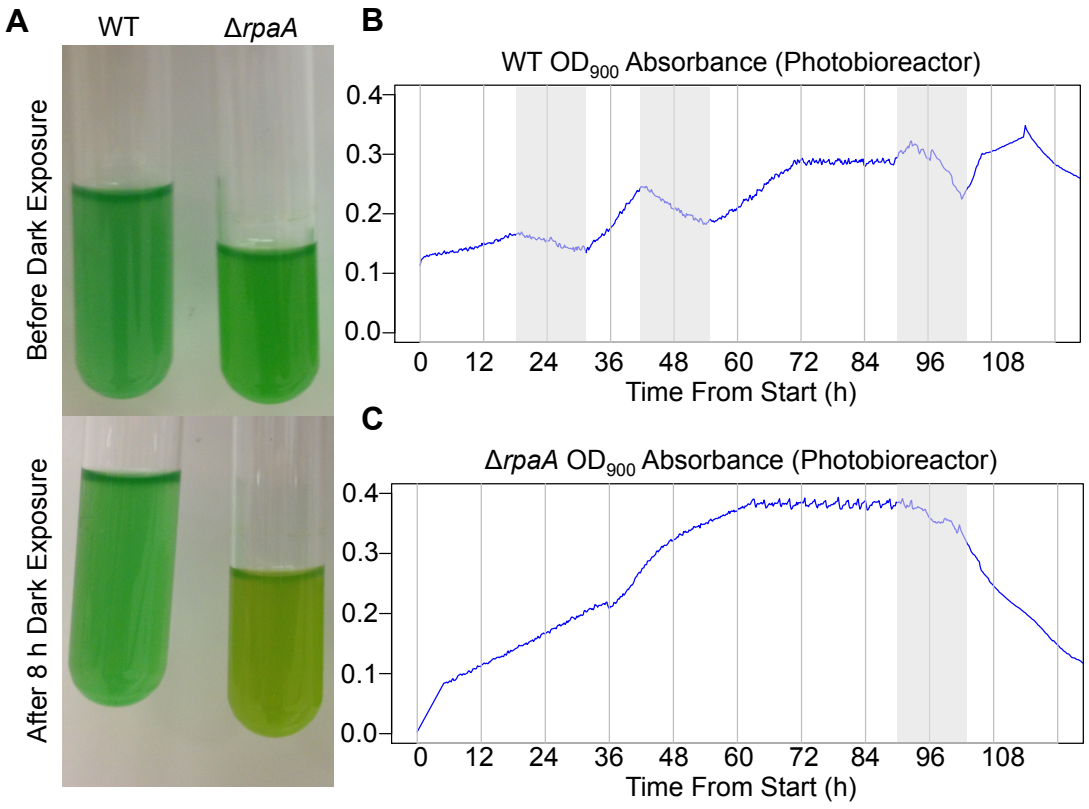

Supplementary Figure 3-S1. Summary of phenotypic effects of darkness on WT and the Δ*rpaA* mutant. (A) Representative photographs of WT and Δ*rpaA* before and after 8 h of darkness exposure. Significant chlorotic bleaching is evident in the Δ*rpaA* strain after incubation in darkness. **(B)** Representative data collected from photobioreactor's optical density sensor (900 nm absorbance) over the course of an experiment where WT and the Δ*rpaA* mutant were exposed to darkness. Time is given from the inoculation of photobioreactors, and grey bars indicate 12 h periods of darkness. The optical density of the Δ*rpaA* mutant can be seen to rapidly decrease after the 12 h dark period.

Supplementary Figure 3-S2 (On Following Page). Summary of PCA and PLS-DA performed on all samples in the metabolomics time course experiment. (A) Plot of PCA components 1 and 2 derived from log_2 atuoscaled metabolite abundance from all WT and Δ*rpaA* samples. Components 1 and 2 account for 38.8% of the variability in the dataset. The plot indicates that component 1 describes time-derived variance, while component 2 is not strongly associated with apparent variables. A similar pattern over time is present relative to that seen in PLS-DA analysis (**Fig. 3A**), where Δ*rpaA* shows global differences in samples collected at different time points, with temporally close time points being more similar than temporally distant time points. Also, WT samples do not show a significant difference over time. Ellipses indicate the 95% CI of each grouping of samples on the plot. **(B)** A matrix comparing the first 5 components derived from the PLS-DA model. The first 5 PLS-DA components describe 55.6% of the sample variance. This plot is provided to show that none of the first 5 PLS-DA components associate with time across WT samples. Thus, WT samples do not show any significant changes with time using this analysis technique.

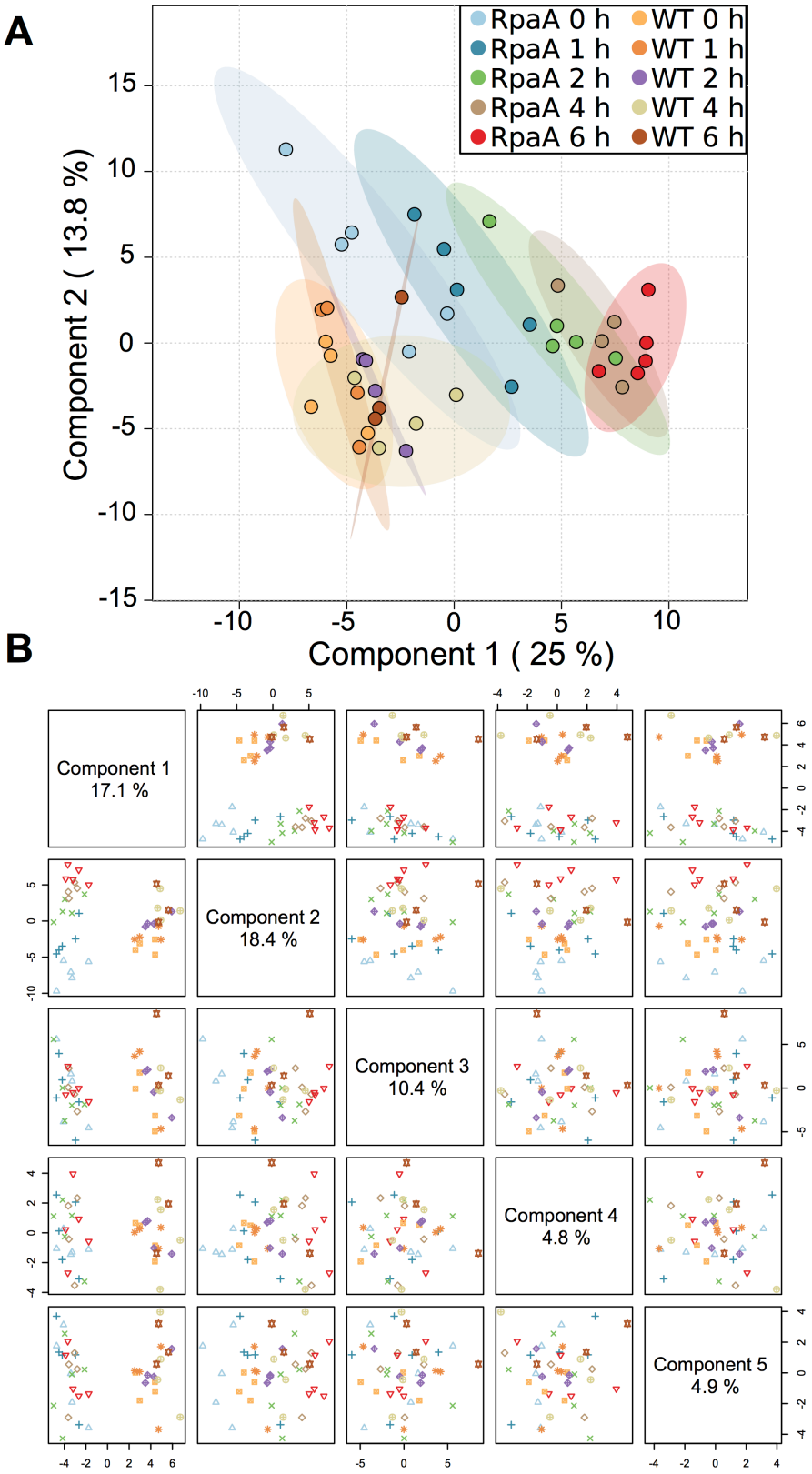
A
RpaA 0 h
RpaA 1 h
RpaA 2 h
RpaA 4 h
RpaA 6 h
WT 0 h
WT 1 h
WT 2 h
WT 4 h
WT 6 h
Component 2 (13.8 %)
Component 1 (25 %)
B
Component 1
17.1 %
Component 2
18.4 %
Component 3
10.4 %
Component 4
4.8 %
Component 5
4.9 %

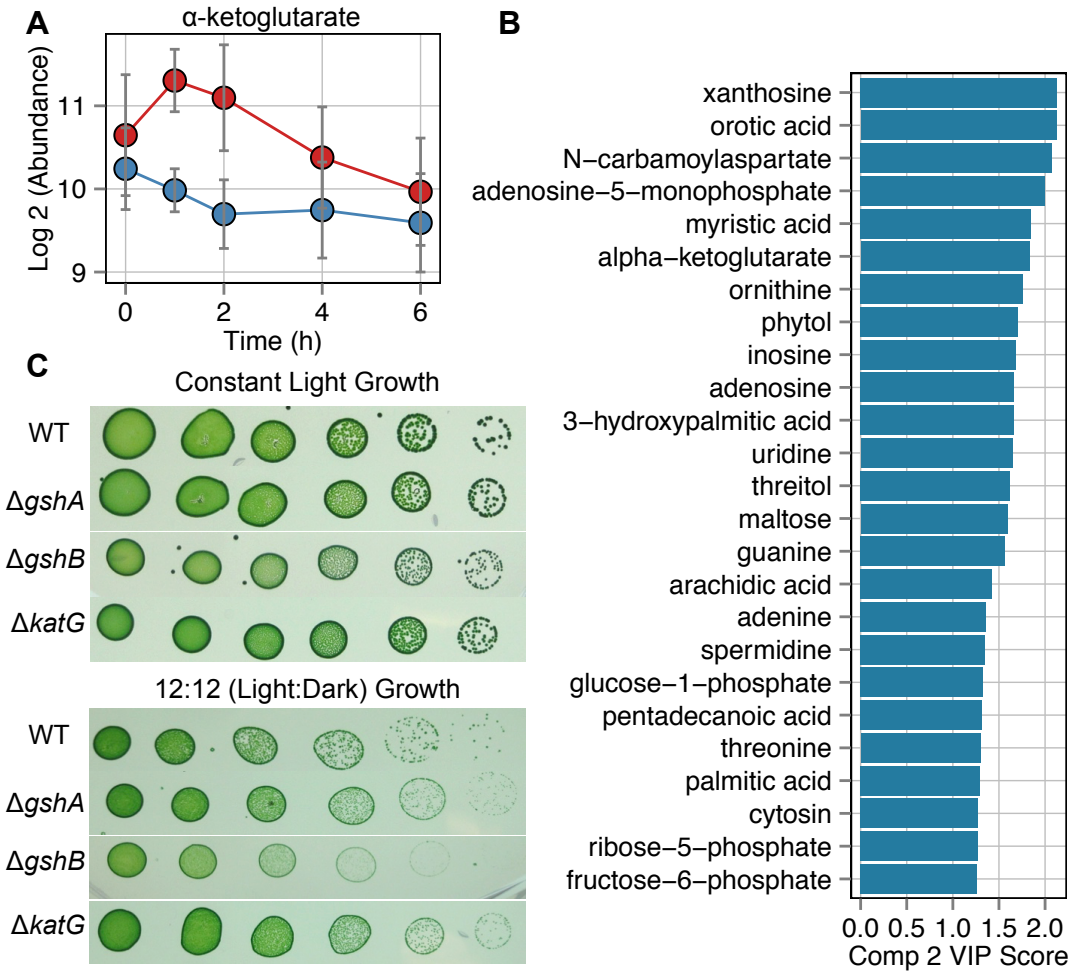

Supplementary Figure 3-S3. Supporting data for Δ*rpaA* metabolomics experiment. (A) A plot showing the average $\log_2$ α-ketoglutarate abundance in WT (blue) and the Δ*rpaA* mutant (red) over the metabolomics time course. Time in the dark is indicated on the x-axis in hours. In the Δ*rpaA* mutant an elevation of α-ketoglutarate can be seen in the first 2 h of the night period. Error bars indicate the STDV of the average (n = 4 for WT; n = 5 for Δ*rpaA*). **(B)** The variable importance in projection (VIP) scores for the top 25 metabolites affecting component 2 of the PLS-DA model. This number indicates the how strongly a metabolite differentiates between classes (ie: genotype and time point) modeled by PLS-DA component 2. Thus, these metabolites show a strong difference between WT and Δ*rpaA* over time. **(C)** Representative photo of dilution series of WT and *gshA, gshB*, and *katG* mutants grown under constant-light (top panel) and 12:12 light-dark (bottom panel) growth conditions. The data indicate that growth of the *gshB* mutant is attenuated specifically under LD growth.

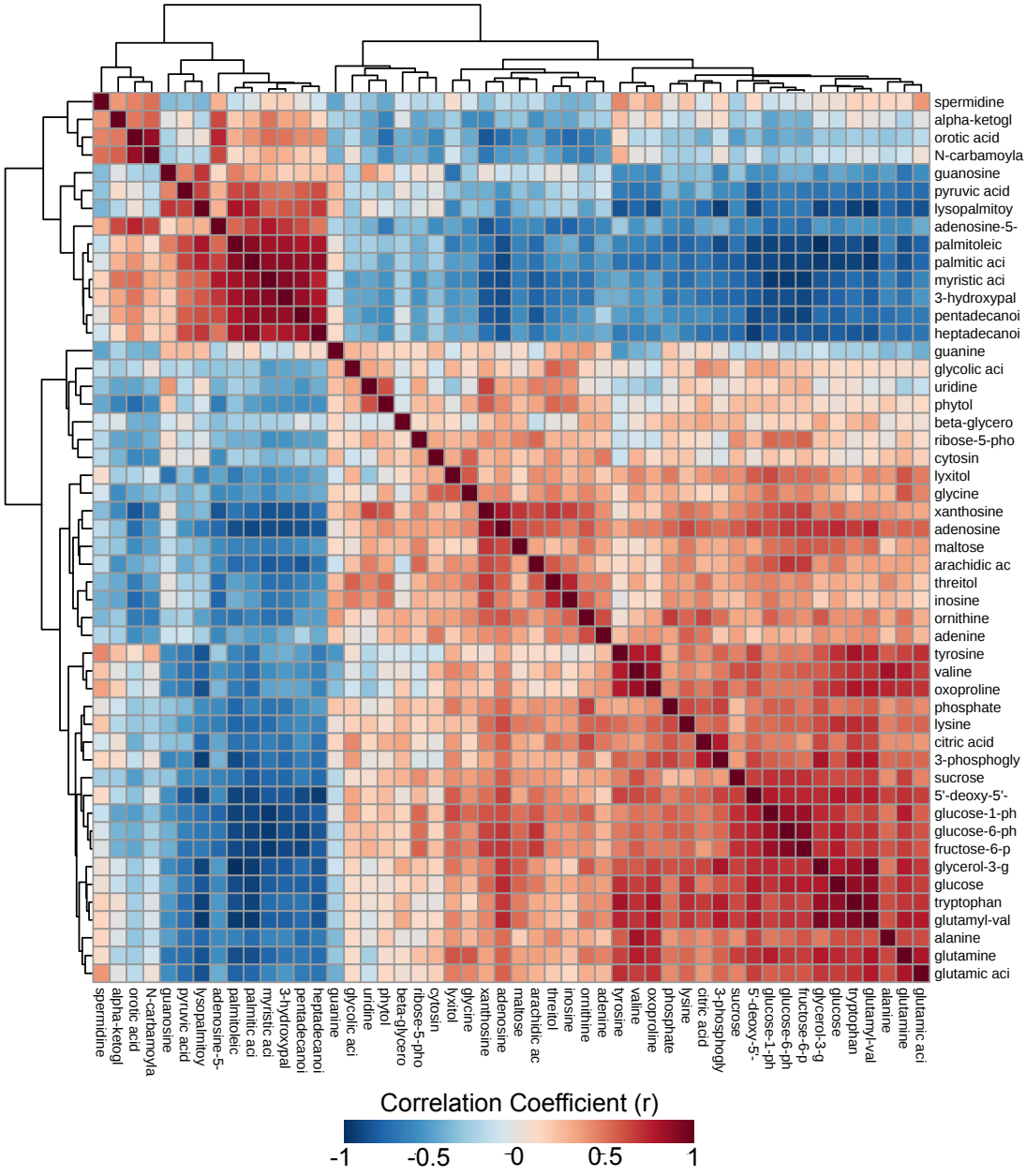

Supplementary Figure 3-S4. Heatmap of the Pearson's correlation (r) between log_2 abundances of all metabolites identified in our study. More intense red color indicates a stronger positive correlation while more intense blue color indicates a stronger negative correlation. Data in this plot were not filtered for statistical significance so that all correlations could be viewed. Hierarchical clustering was performed using the pheatmap package in R with Euclidian distance and complete linkage applied for leaf ordering. The data indicate that two major clusters of metabolites show strong positive correlations with each other while showing strong negative correlations with metabolites in the opposite cluster.

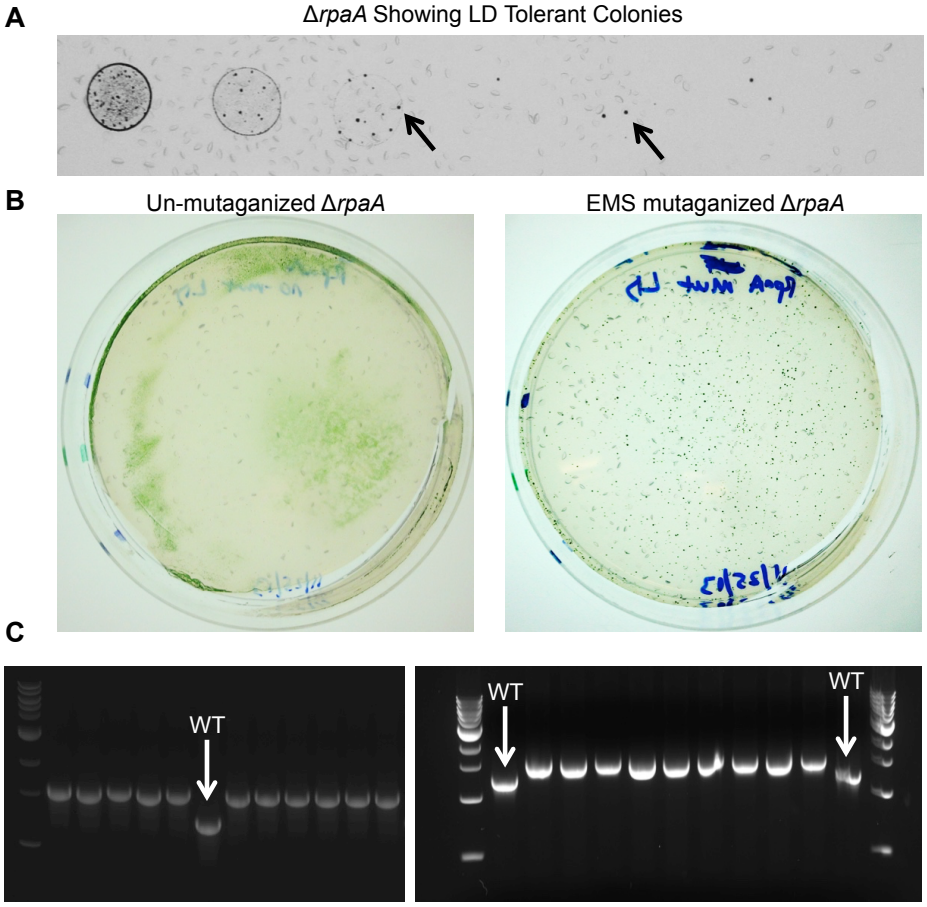

Supplementary Figure 3-S5. Supporting data for EMS mutagenesis of the *ΔrpaA* mutant. (A) A representative photo of an older *ΔrpaA* culture (> 2 months on bench top) that was plated as a serial dilution and grown in a 12:12 light-dark cycle. The black arrows indicate *ΔrpaA* colonies showing robust growth even under conditions that are lethal to *ΔrpaA* mutants. This representative photo shows how suppressing mutations occur naturally in a population of *ΔrpaA* mutants that can allow growth under normally restrictive LD conditions. **(B)** Photographs of plates after incubation in a 12:12 light-dark cycle for 15 d where EMS mutagenized and un-mutagenized *ΔrpaA* cell cultures were plated. The photographs show that hundreds of colonies form on the plate where EMS mutagenized *ΔrpaA* cells were plated, but do not form on the plate that received un-mutagenized cells. 20 of the colonies from the plate containing mutagenized cells were isolated for the genome re-sequencing study. **(C)** Result of PCR amplification of the *rpaA* gene locus from WT and *ΔrpaA* cells carrying secondary site genetic mutations. The recombination at the *rpaA* locus with the pAM4420 vector to produce the *ΔrpaA* strain results in an expected region size of 1.8 kb. Comparison to amplification from WT cells (white arrows) shows that all *ΔrpaA* strains tested in this study produce the expected amplicon size for a strain carrying a deletion mutation. Additionally no WT size bands are present in the *ΔrpaA* strains, indicating that the mutation is fully segregated.

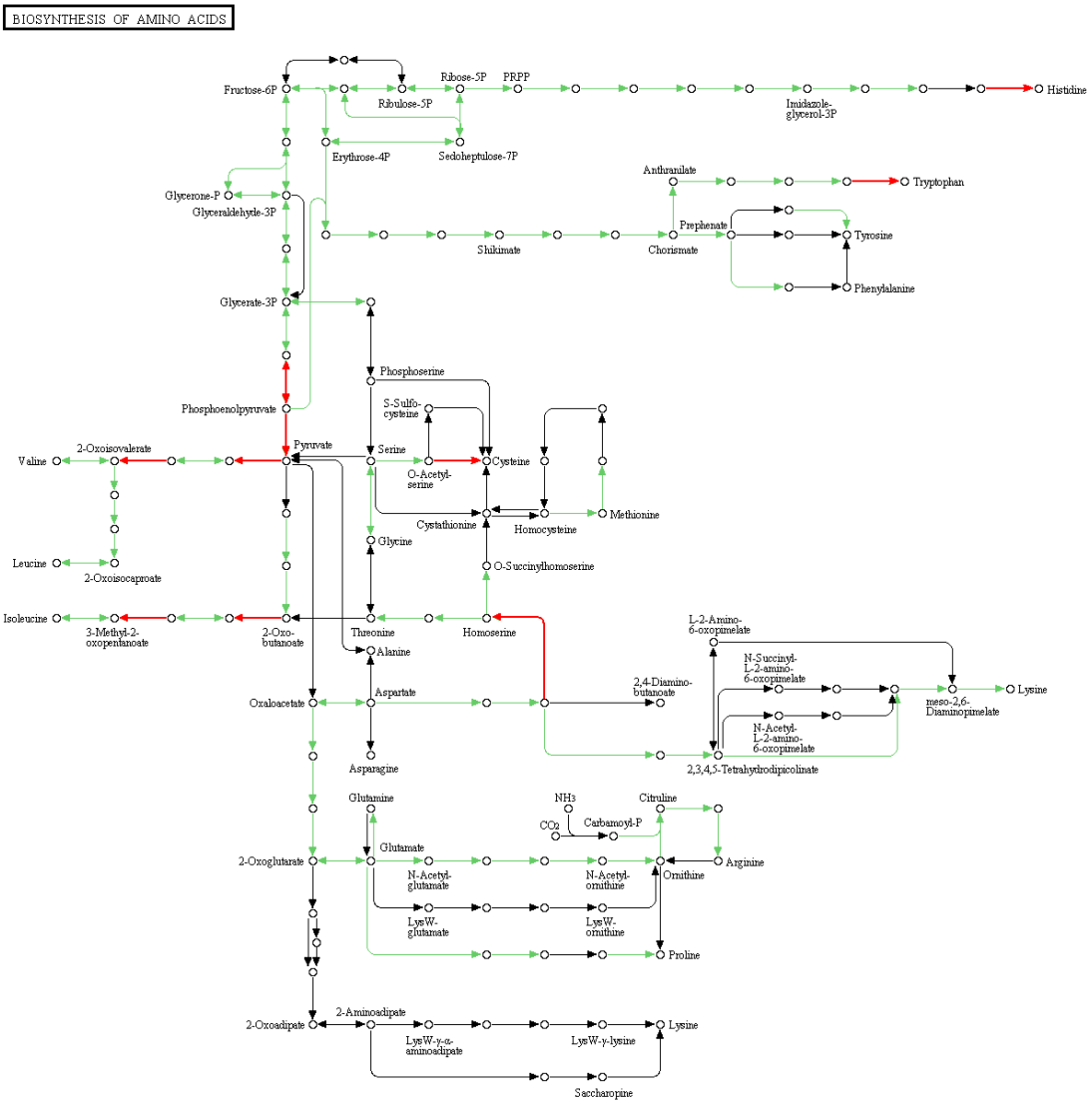

Supplementary Figure 3-S6. Overview of reactions in amino acid metabolism that were found to have at least one mutation during the screening of all *ΔrpaA* EMS mutagenized strains. Green arrows indicate reactions that are annotated in the KEGG database for *S. elongatus*. Red arrows indicate reactions where the corresponding gene was identified to carry a mutation in at least one or more suppressed *ΔrpaA* strains. Map produced using the gene to pathway mapping function on the KEGG tools portal.

Supplementary Figure 3-S7 (On Following Page). Supporting data for mechanisms that suppress LD lethality in that *ΔrpaA* mutant. (A) Representative data collected from photobioreactor's optical density sensor (900 nm absorbance) over the course of an experiment where Δ*rpaA* mutants were exposed to darkness and not treated (top panel) or treated (bottom panel) with MSM. Time starts at inoculation of photobioreactors, grey bars indicate 12 h periods of darkness, and light intensity during the light periods is noted with black text. The black arrow in the bottom panel indicates where 25 μM MSM was added to one culture. The data indicate that the Δ*rpaA* mutant receiving MSM was able to continue growth even after an LD cycle that was lethal to the Δ*rpaA* mutant not receiving MSM. **(B)** Photographs of EMS mutagenized Δ*rpaA* strains prior to genomic DNA extraction. Strains are organized by the type of mutation they were found to carry, and only strains with mutations that affected amino acid metabolism in some way are included. The pathway affected is indicated above each photograph set and the mutant number is indicated below the photo (**Sup Dataset S3**). The photos highlight the altered pigmentation that is present in these strains relative to WT cells **(C)** Representative data collected from photobioreactor's optical density sensor (900 nm absorbance) over the course of an experiment where an Δ*rpaA* mutant was exposed to increasing light intensity in a 12:12 light-dark cycle. Grey bars indicate 12h dark periods and the red trace indicates the light intensity at a given time. The data show how once light intensity is high enough, the dark period becomes lethal to the Δ*rpaA* mutant and there is no recovery of growth even when light is constantly provided.

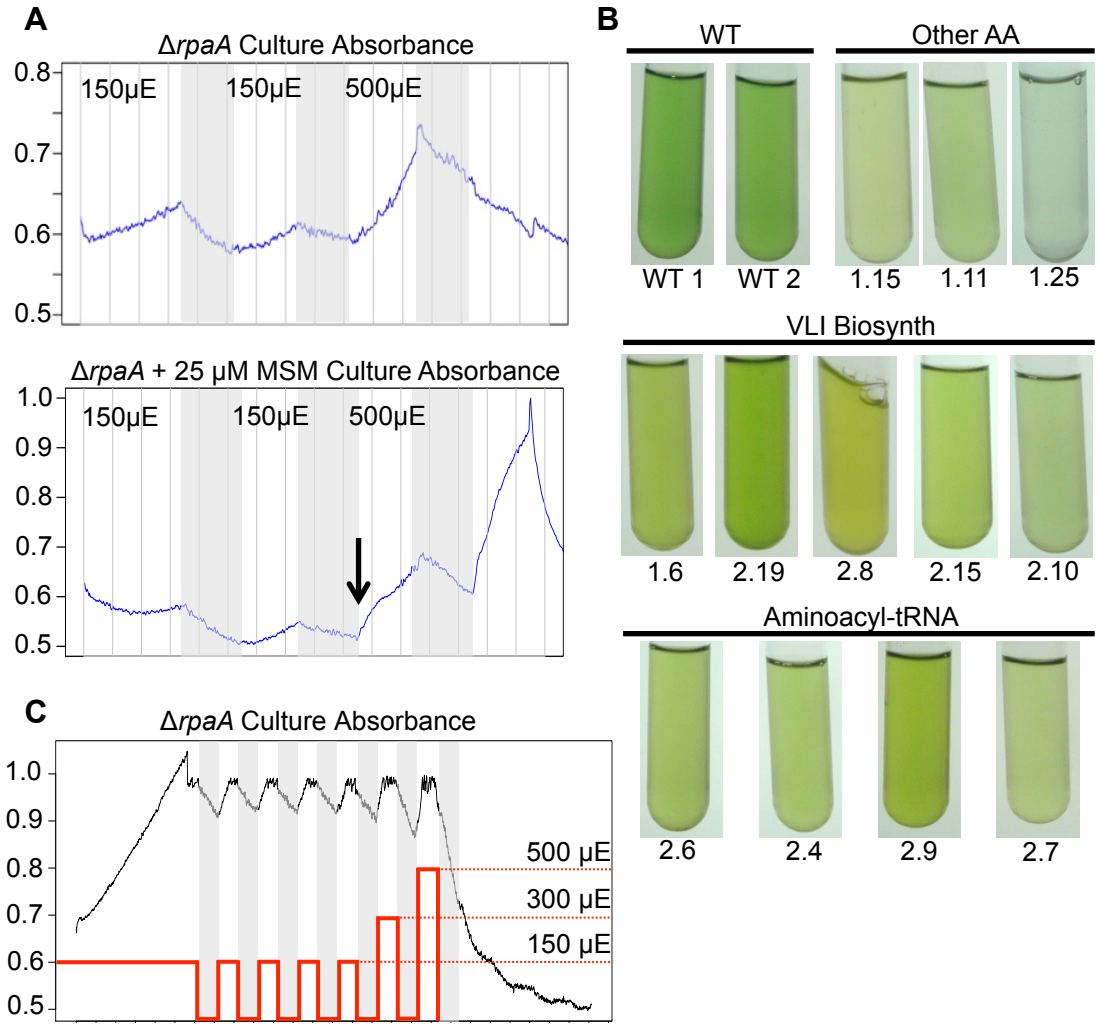
A
ΔrpaA Culture Absorbance
150μE
150μE
500μE
0.8
0.7
0.6
0.5
ΔrpaA + 25 μM MSM Culture Absorbance
150μE
150μE
500μE
1.0
0.9
0.8
0.7
0.6
0.5
B
WT
Other AA
WT 1
WT 2
1.15
1.11
1.25
VLI Biosynth
1.6
2.19
2.8
2.15
2.10
Aminoacyl-tRNA
2.6
2.4
2.9
2.7
C
ΔrpaA Culture Absorbance
500 μE
300 μE
150 μE
1.0
0.9
0.8
0.7
0.6
0.5

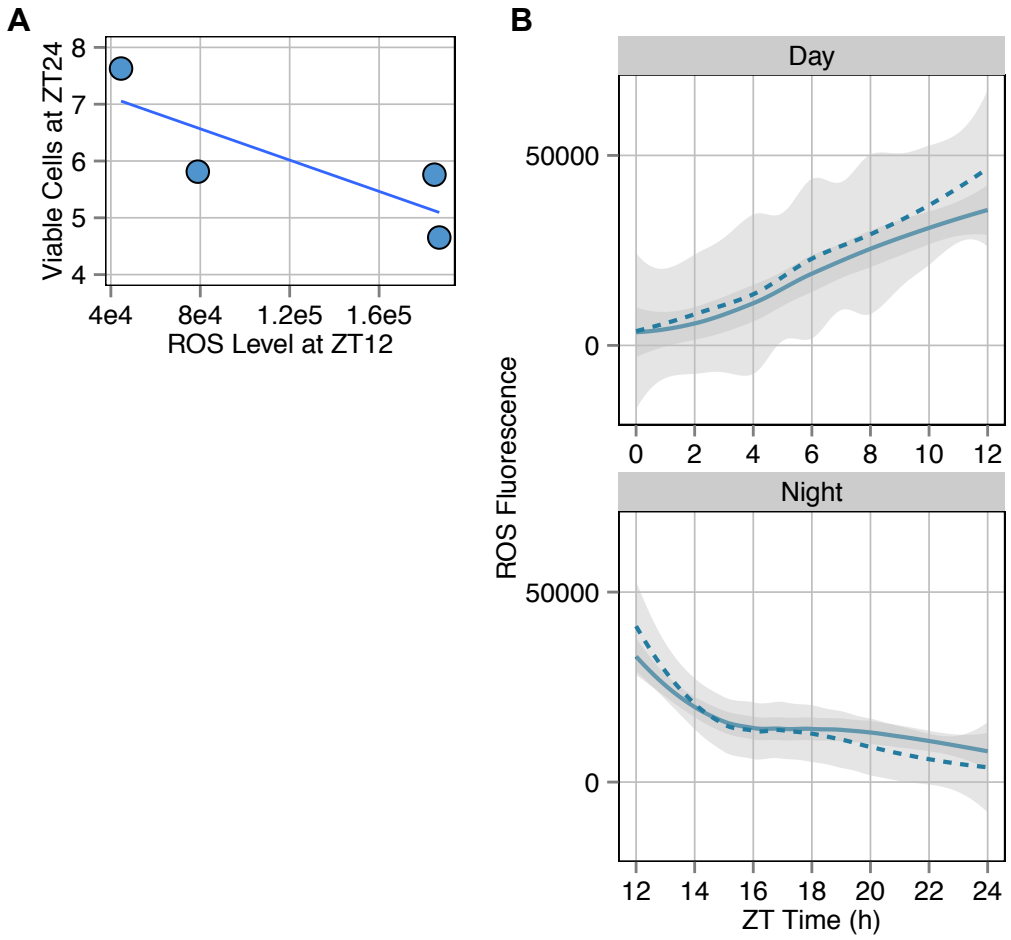

Supplementary Figure 3-S8. Supporting data for ROS tracking experiments and relationship to cell viability. (A) A graph depicting the relationship between H_2DCFDA fluorescence levels measured directly before the Δ*rpaA* mutant entered the dark (ZT12), and the number of viable cells that remained after a 12 h dark period (ZT24). The x-axis indicates arbitrary fluorescence units, and the y-axis indicate the colony forming units counted from dilution plating. The blue line is a linear regression fit to the data. Due to the low number of tests the data can not be considered statistically significant, but a negative trend is apparent. **(B)** Plot of H_2DCFDA fluorescence over a 24 h 12:12 light-dark cycle indicating total cellular ROS in WT untreated (solid line) and treated (dashed line) with 25 μM MSM. Curves shown are best-fit lines calculated using LOESS regression to all data points in a given sample; the grey shaded area indicates the 95% CI of the regression line (n = 21 data points for day samples; n = 42 data points for night samples). The data show that treatment of WT with 25 μM MSM does not significantly affect levels of ROS over the 24 h LD cycle.

Supplementary Figure 3-S9 (On Following Page). Diagram of the growth and sampling scheme used for experiments conducted in photobioreactors. Each box indicates a 12 h period with white boxes corresponding to periods of light and black boxes corresponding to periods of darkness. Where indicated, only the WT strain was exposed to darkness. Light intensity during each light period is indicated in black text within each white box. Times where samples were taken during the metabolomics experiment are indicated by pink arrows. Arrows correspond to time points ZT12 (0 h), ZT13 (1 h), ZT14 (2 h), ZT16 (4 h), and ZT18 (6 h) from left to right.

Metabolomics

All Other Experiments

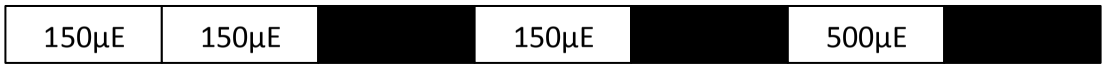

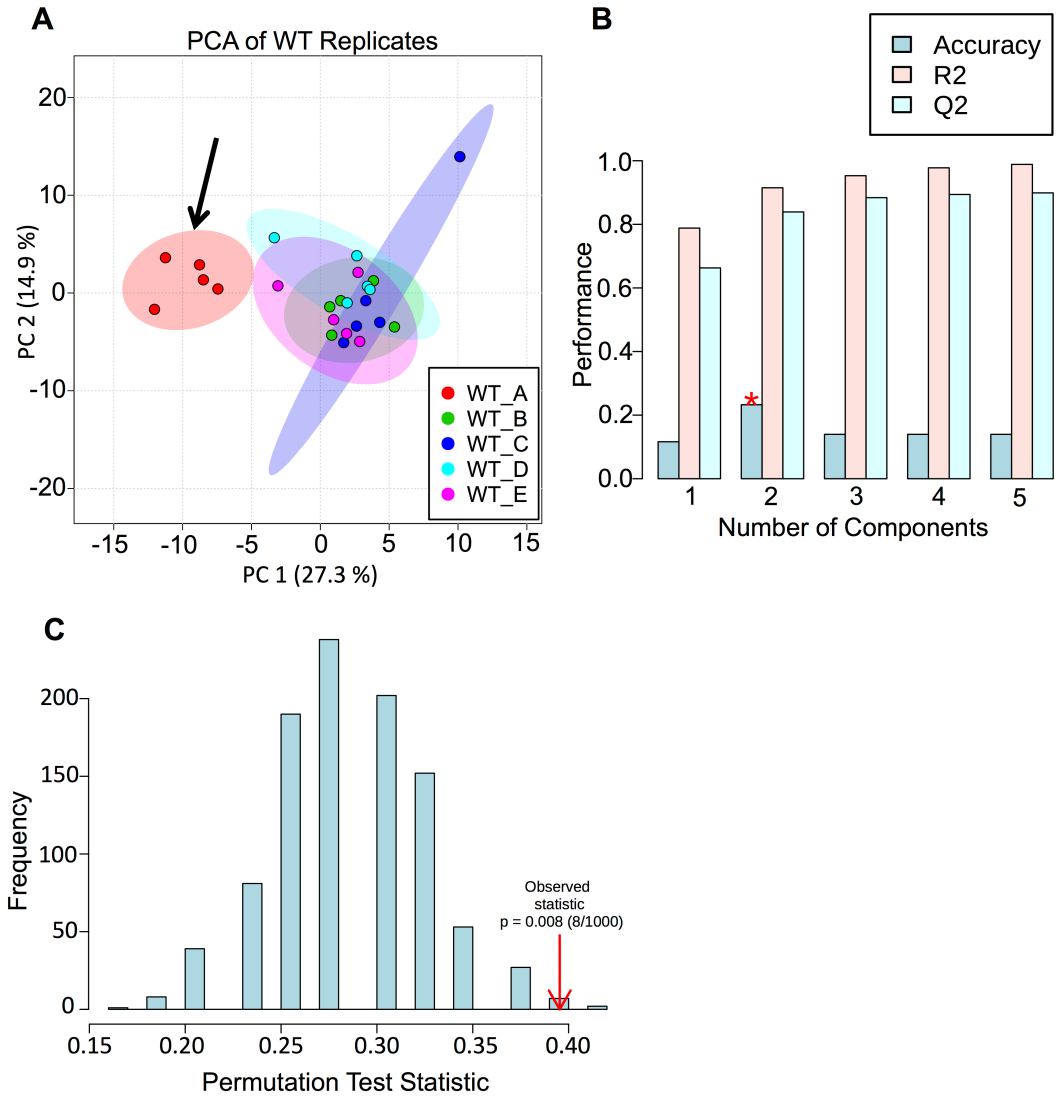

Supplementary Figure 3-S10. Supporting data for metabolomics statistical analysis. (A) Plot of PCA components 1 and 2 for log_2 autoscaled metabolite abundance data for all WT samples. Ellipses indicate the 95% CI for each sample group. The black arrow indicates all time points collected for WT biological replicate A. The statistically significant separation of the WT_A replicate indicates that this sample is an outlier relative to the other WT samples collected. **(B)** Plot showing result from LOOCV performed on the PLS-DA model. The red star indicates the accuracy of the model is highest when it includes only two components. Due to a high degree of variability in the data, which is typical of metabolomics datasets, we chose prediction accuracy as a metric to select a number of components over other metrics such as model fit (Q2). **(C)** Plot showing the results of accuracy permutation testing on the PLS-DA model. The red arrow indicates the test statistic .The data indicate that our PLS-DA model is significantly better at predicting class membership than a random model ($p < 0.01$; n=1000).

Table 3-1. Summary of pigment absorbance for *rpaA* suppressor mutants categorized by mutation type. Only mutants with a single metabolic mutation were included in the table.

EMS Mutant	Main Mutation	Color	630nm*	680nm*	Ratio	Ratio Avg	Ratio SD	TTEST (vs WT)
WT Controls								
WT_1	None	Green	1.478	1.574	0.939	0.951	0.016	1.000
WT_2	None	Green	1.442	1.527	0.944			
WT_3	None	Green	1.590	1.640	0.970			
Purine Biosynthesis								
1_9	guaA (0189)	Light Green	1.332	1.457	0.914	**Ratio Avg**	**Ratio SD**	**TTEST (vs WT)**
1_10	guaA (0189)	Light Green	1.280	1.276	1.004	0.976	0.057	0.493
1_3	guaB (1831)	Very Light Green	1.162	1.100	1.056			
1_1	guaB (1831)	Light Green	1.335	1.364	0.979			
2_3	guaA (0189)	Yellow Green	1.310	1.410	0.929			
VLI Biosynthesis								
1_6	pyk (0098)	Yellow Green	1.249	1.475	0.847	**Ratio Avg**	**Ratio SD**	**TTEST (vs WT)**
2_19	AHAS (0139)	Yellow Green	1.552	1.820	0.853	0.876	0.028	0.006
2_8	ilvD (0626)	Strong Yellow	1.259	1.376	0.915			
2_10	eno (0639)	Light Green	1.189	1.361	0.874			
2_15	ilvH (2434)	Yellow Green	1.334	1.496	0.892			
tRNA Related								
2_4	ileS (2437)	Yellow Green	1.410	1.748	0.807	**Ratio Avg**	**Ratio SD**	**TTEST (vs WT)**
2_6	glyQ (2457)	Yellow Green	1.350	1.520	0.889	0.860	0.039	0.014
2_7	tRNA-Arg (R0011)	Pale Yellow Green	1.325	1.488	0.890			
2_9	leuS (1920)	Strong Yellow Green	1.526	1.787	0.854			
Other Amino Acid Biosynthetic								
1_11	trpB (2143)	Pale Green	1.216	1.306	0.931	**Ratio Avg**	**Ratio SD**	**TTEST (vs WT)**
1_15	thrA (2090)	Pale Yellow	1.299	1.508	0.861	0.947	0.095	0.947
1_25	hisD (1519)	Pale Yellow/Clear	1.221	1.164	1.049			

3.7 References

1. Oliver J, Atsumi S: **Metabolic design for cyanobacterial chemical synthesis**. *Photosynth Res* 2014.

2. Ducat DC, Way JC, Silver PA: **Engineering cyanobacteria to generate high-value products**. *Trends in Biotechnology* 2011, **29**:95–103.

3. Bryant DA: **The beauty in small things revealed.** *Proc Natl Acad Sci USA* 2003, **100**:9647–9649.

4. Zhang S, Bryant DA: **Biochemical validation of the glyoxylate cycle in the cyanobacterium Chlorogloeopsis fritschii strain PCC 9212.** *Journal of Biological Chemistry* 2015.

5. Zhang S, Bryant DA: **The Tricarboxylic Acid Cycle in Cyanobacteria**. *Science* 2011, **334**:1551–1553.

6. Kouhen OM-E, Joset F: **Biosynthesis of the branched-chain amino acids in the cyanobacterium Synechocystis PCC6803: existence of compensatory pathways.** *Current Microbiology* 2002, **45**:94–98.

7. Yuan Z, Yin B, Wei D, Yuan Y-RA: **Structural basis for cofactor and substrate selection by cyanobacterium succinic semialdehyde dehydrogenase.** *J Struct Biol* 2013, **182**:125–135.

8. Gaston D, Roger AJ: **Functional divergence and convergent evolution in the plastid-targeted glyceraldehyde-3-phosphate dehydrogenases of diverse eukaryotic algae.** *PLoS ONE* 2013, **8**:e70396.

9. Guo J, Nguyen AY, Dai Z, Su D, Gaffrey MJ, Moore RJ, Jacobs JM, Monroe ME, Smith RD, Koppenaal DW, Pakrasi HB, Qian W-J: **Proteome-wide Light/Dark Modulation of Thiol Oxidation in Cyanobacteria Revealed by Quantitative Site-specific Redox Proteomics**. *Molecular & Cellular Proteomics* 2014, **13**:3270–3285.

10. Ansong C, Sadler NC, Hill EA, Lewis MP: **Characterization of protein redox dynamics induced during light-to-dark transitions and nutrient limitation in cyanobacteria**. *Frontiers in …* 2014.

11. Lindahl M, Kieselbach T: **Disulphide proteomes and interactions with thioredoxin on the track towards understanding redox regulation in chloroplasts and cyanobacteria.** *J Proteomics* 2009, **72**:416–438.

12. Schürmann P: **Redox signaling in the chloroplast: the**

ferredoxin/thioredoxin system. *Antioxid Redox Signal* 2003, **5**:69–78.

13. Vijayan V, Zuzow R, O'Shea EK: **Oscillations in supercoiling drive circadian gene expression in cyanobacteria**. *Proc Natl Acad Sci USA* 2009, **106**:22564–22568.

14. Mackey SR, Golden SS, Ditty JL: **The Itty-Bitty Time Machine**. In *Advances in Genetics*. *Volume 74*. Elsevier; 2011:13–53. [*Advances in Genetics*]

15. Edgar RS, Green EW, Zhao Y, van Ooijen G, Olmedo M, Qin X, Xu Y, Pan M, Valekunja UK, Feeney KA, Maywood ES, Hastings MH, Baliga NS, Merrow M, Millar AJ, Johnson CH, Kyriacou CP, O'Neill JS, Reddy AB: **Peroxiredoxins are conserved markers of circadian rhythms.** *Nature* 2012, **485**:459–464.

16. Schwarz D, Nodop A, Huge J, Purfurst S, Forchhammer K, Michel KP, Bauwe H, Kopka J, Hagemann M: **Metabolic and Transcriptomic Phenotyping of Inorganic Carbon Acclimation in the Cyanobacterium Synechococcus elongatus PCC 7942**. *PLANT PHYSIOLOGY* 2011, **155**:1640–1655.

17. Hickman JW, Kotovic KM, Miller C, Warrener P, Kaiser B, Jurista T, Budde M, Cross F, Roberts JM, Carleton M: **Glycogen synthesis is a required component of the nitrogen stress response in Synechococcus elongatus PCC 7942**. *Algal Research* 2013.

18. Knoop H, Zilliges Y, Lockau W, Steuer R: **The Metabolic Network of Synechocystis sp. PCC 6803: Systemic Properties of Autotrophic Growth**. *PLANT PHYSIOLOGY* 2010, **154**:410–422.

19. Markson JS, Piechura JR, Puszynska AM, O'Shea EK: **Circadian Control of Global Gene Expression by the Cyanobacterial Master Regulator RpaA**. *Cell* 2013, **155**:1396–1408.

20. Stöckel J, Jacobs JM, Elvitigala TR, Liberton M, Welsh EA, Polpitiya AD, Gritsenko MA, Nicora CD, Koppenaal DW, Smith RD, Pakrasi HB: **Diurnal rhythms result in significant changes in the cellular protein complement in the cyanobacterium Cyanothece 51142.** *PLoS ONE* 2011, **6**:e16680.

21. Guerreiro ACL, Benevento M, Lehmann R, van Breukelen B, Post H, Giansanti P, Altelaar AFM, Axmann IM, Heck AJR: **Daily rhythms in the cyanobacterium Synechococcus elongatus probed by high-resolution mass spectrometry based proteomics reveals a small-defined set of cyclic proteins.** *Mol Cell Proteomics* 2014.

22. Welkie D, Zhang X, Markillie ML, Taylor R, Orr G, Jacobs J, Bhide K, Thimmapuram J, Gritsenko M, Mitchell H, Smith RD, Sherman LA: **Transcriptomic and proteomic dynamics in the metabolism of a diazotrophic cyanobacterium, Cyanothece sp. PCC 7822 during a diurnal light–dark cycle**. *BMC Genomics* 2014, **15**:1185.

23. Diamond S, Jun D, Rubin BE, Golden SS: **The circadian oscillator in Synechococcus elongatus controls metabolite partitioning during diurnal growth.** *Proc Natl Acad Sci USA* 2015, **112**:E1916–25.

24. Pedrós-Alió C: **Genomics and marine microbial ecology.** *Int Microbiol* 2006, **9**:191–197.

25. Deng MD, Coleman JR: **Ethanol synthesis by genetic engineering in cyanobacteria.** *Applied and Environmental Microbiology* 1999, **65**:523–528.

26. Atsumi S, Higashide W, Liao JC: **Direct photosynthetic recycling of carbon dioxide to isobutyraldehyde**. *Nature Biotechnology* 2009, **27**:1177–1180.

27. Schirmer A, Rude MA, Li X, Popova E, del Cardayre SB: **Microbial biosynthesis of alkanes.** *Science* 2010, **329**:559–562.

28. Clerico EM, Ditty JL, Golden SS: **Specialized techniques for site-directed mutagenesis in cyanobacteria.** *Methods Mol Biol* 2007, **362**:155–171.

29. Taton A, Unglaub F, Wright NE, Zeng WY, Paz-Yepes J, Brahamsha B, Palenik B, Peterson TC, Haerizadeh F, Golden SS, Golden JW: **Broad-host-range vector system for synthetic biology and biotechnology in cyanobacteria.** *Nucleic Acids Res* 2014, **42**:e136.

30. Kondo T, Tsinoremas NF, Golden SS, Johnson CH, Kutsuna S, Ishiura M: **Circadian clock mutants of cyanobacteria.** *Science* 1994, **266**:1233–1236.

31. Takai N, Nakajima M, Oyama T, Kito R, Sugita C, Sugita M, Kondo T, Iwasaki H: **A KaiC-associating SasA-RpaA two-component regulatory system as a major circadian timing mediator in cyanobacteria.** *Proc Natl Acad Sci USA* 2006, **103**:12109–12114.

32. Paddock ML, Boyd JS, Adin DM, Golden SS: **Active output state of the Synechococcus Kai circadian oscillator.** *Proc Natl Acad Sci USA* 2013.

33. Iwasaki H, Williams SB, Kitayama Y, Ishiura M, Golden SS, Kondo T: **A KaiC-interacting sensory histidine kinase, SasA, necessary to sustain robust circadian oscillation in cyanobacteria**. *Cell* 2000, **101**:223–233.

34. Yang C, Hua Q, Shimizu K: **Integration of the information from gene expression and metabolic fluxes for the analysis of the regulatory mechanisms in Synechocystis.** *Appl Microbiol Biotechnol* 2002, **58**:813–822.

35. Osanai T, Azuma M, Tanaka K: **Sugar catabolism regulated by light- and nitrogen-status in the cyanobacterium Synechocystis sp. PCC 6803**. *Photochem Photobiol Sci* 2007, **6**:508.

36. Tamoi M, Miyazaki T, Fukamizo T, Shigeoka S: **The Calvin cycle in cyanobacteria is regulated by CP12 via the NAD(H)/NADP(H) ratio under light/dark conditions**. *The Plant Journal* 2005, **42**:504–513.

37. Wedel N, Soll J: **Evolutionary conserved light regulation of Calvin cycle activity by NADPH-mediated reversible phosphoribulokinase/CP12/ glyceraldehyde-3-phosphate dehydrogenase complex dissociation**. *Proceedings of the National Academy of …* 1998.

38. Waldbauer JR, Rodrigue S, Coleman ML, Chisholm SW: **Transcriptome and Proteome Dynamics of a Light-Dark Synchronized Bacterial Cell Cycle**. *PLoS ONE* 2012, **7**:e43432.

39. Gontero B, Maberly SC: **An intrinsically disordered protein, CP12: jack of all trades and master of the Calvin cycle**. *Biochem Soc Trans* 2012, **40**:995–999.

40. Boyd JS, Bordowitz JR, Bree AC, Golden SS: **An allele of the crm gene blocks cyanobacterial circadian rhythms.** *Proc Natl Acad Sci USA* 2013, **110**:13950–13955.

41. Collier JL, Grossman AR: **Chlorosis induced by nutrient deprivation in Synechococcus sp. strain PCC 7942: not all bleaching is the same.** *J Bacteriol* 1992, **174**:4718–4726.

42. Latifi A, Ruiz M, Zhang C-C: **Oxidative stress in cyanobacteria.** *FEMS Microbiology Reviews* 2009, **33**:258–278.

43. Aurora: **Polyamines in cyanobacteria: biosynthesis, transport and abiotic stress response**. 2011:1–10.

44. Young JD, Shastri AA, Stephanopoulos G, Morgan JA: **Mapping photoautotrophic metabolism with isotopically nonstationary 13C flux analysis**. *Metabolic Engineering* 2011, **13**:656–665.

45. Nakajima T, Kajihata S, Yoshikawa K, Matsuda F, Furusawa C, Hirasawa

T, Shimizu H: **Integrated Metabolic Flux and Omics Analysis of Synechocystis sp. PCC 6803 under Mixotrophic and Photoheterotrophic Conditions.** *Plant and Cell Physiology* 2014.

46. Kanehisa M, Goto S: **KEGG: kyoto encyclopedia of genes and genomes**. *Nucleic Acids Res* 2000, **28**:27–30.

47. Cameron JC, Pakrasi HB: **Essential role of glutathione in acclimation to environmental and redox perturbations in the cyanobacterium Synechocystis sp. PCC 6803.** *PLANT PHYSIOLOGY* 2010, **154**:1672–1685.

48. Chardonnet S, Sakr S, Cassier-Chauvat C, Le Maréchal P, Chauvat F, Lemaire SD, Decottignies P: **First Proteomic Study of S-Glutathionylation in Cyanobacteria.** *J Proteome Res* 2014:140919143615000.

49. Kaczmarzyk D, Fulda M: **Fatty Acid Activation in Cyanobacteria Mediated by Acyl-Acyl Carrier Protein Synthetase Enables Fatty Acid Recycling**. *PLANT PHYSIOLOGY* 2010, **152**:1598–1610.

50. Klotz A, Reinhold E, Doello S, Forchhammer K: **Nitrogen Starvation Acclimation in Synechococcus elongatus: Redox-Control and the Role of Nitrate Reduction as an Electron Sink.** *Life (Basel)* 2015, **5**:888–904.

51. Flores E, Herrero A: **Nitrogen assimilation and nitrogen control in cyanobacteria.** *Biochem Soc Trans* 2005, **33**:164–167.

52. Kotze HL, Armitage EG, Sharkey KJ, Allwood JW, Dunn WB, Williams KJ, Goodacre R: **A novel untargeted metabolomics correlation- based network analysis incorporating human metabolic reconstructions**. *BMC Systems Biology* 2013, **7**:1–1.

53. Wikoff WR, Grapov D, Fahrmann JF, DeFelice B, Rom WN, Pass HI, Kim K, Nguyen U, Taylor SL, Gandara DR, Kelly K, Fiehn O, Miyamoto S: **Metabolomic markers of altered nucleotide metabolism in early stage adenocarcinoma.** *Cancer Prev Res (Phila)* 2015, **8**:410–418.

54. Takatani N, Use K, Kato A, Ikeda K, Kojima K, Aichi M, Maeda S-I, Omata T: **Essential Role of Acyl-ACP Synthetase in Acclimation of the Cyanobacterium Synechococcus elongatus Strain PCC 7942 to High-Light Conditions.** *Plant and Cell Physiology* 2015:pcv086–8.

55. Shen J, DiTommaso A, Shen M, Lu W, Li Z: **Molecular Basis for Differential Metabolic Responses to Monosulfuron in Three Nitrogen-Fixing Cyanobacteria**. *http://dxdoiorg/101614/WS-08-0241* 2009, **57**:133–

141.

56. FRIEDBERG D, SEIJFFERS J: **Sulfonylurea-Resistant Mutants and Natural Tolerance of Cyanobacteria**. *Arch Microbiol* 1988, **150**:278–281.

57. Page LE, Liberton M, Pakrasi HB: **Phycobilisome antenna truncation reduces photoautotrophic productivity in Synechocystis sp. PCC 6803, a cyanobacterium**. *Applied and Environmental Microbiology* 2012.

58. Grossman AR, Schaefer MR, Chiang GG, Collier JL: **The phycobilisome, a light-harvesting complex responsive to environmental conditions.** *Microbiol Rev* 1993, **57**:725–749.

59. Perelman A, Uzan A, Hacohen D, Schwarz R: **Oxidative Stress in Synechococcus sp. Strain PCC 7942: Various Mechanisms for H2O2 Detoxification with Different Physiological Roles**. *J Bacteriol* 2003, **185**:3654–3660.

60. Rastogi RP, Singh SP, Häder D-P, Sinha RP: **Detection of reactive oxygen species (ROS) by the oxidant-sensing probe 2“,7-”dichlorodihydrofluorescein diacetate in the cyanobacterium Anabaena variabilis PCC 7937.** *Biochem Biophys Res Commun* 2010, **397**:603–607.

61. Lea-Smith DJ, Ross N, Zori M, Bendall DS, Dennis JS, Scott SA, Smith AG, Howe CJ: **Thylakoid Terminal Oxidases Are Essential for the Cyanobacterium Synechocystis sp. PCC 6803 to Survive Rapidly Changing Light Intensities**. *PLANT PHYSIOLOGY* 2013, **162**:484–495.

62. Espinosa J, Boyd JS, Cantos R, Salinas P, Golden SS, Contreras A: **Cross-talk and regulatory interactions between the essential response regulator RpaB and cyanobacterial circadian clock output.** *Proc Natl Acad Sci USA* 2015, **112**:2198–2203.

63. Li M, Yang Q, Zhang L, Li H, Cui Y, Wu Q: **Identification of novel targets of cyanobacterial glutaredoxin.** *Arch Biochem Biophys* 2007, **458**:220–228.

64. Utkilen HC: **Magnesium-limited growth of the cyanobacterium Anacystis nidulans**. *J Gen Microbiol* 1982, **128**:1849–1862.

65. Knoop H, Gründel M, Zilliges Y, Lehmann R, Hoffmann S, Lockau W, Steuer R: **Flux Balance Analysis of Cyanobacterial Metabolism: The Metabolic Network of Synechocystis sp. PCC 6803**. *PLoS Comput Biol* 2013, **9**:e1003081.

66. Ohashi Y, Shi W, Takatani N, Aichi M, Maeda SI, Watanabe S,

Yoshikawa H, Omata T: **Regulation of nitrate assimilation in cyanobacteria**. *Journal of Experimental Botany* 2011, **62**:1411–1424.

67. Muro-Pastor MI, Reyes JC, Florencio FJ: **Ammonium assimilation in cyanobacteria.** *Photosynth Res* 2005, **83**:135–150.

68. Hosokawa N, Hatakeyama TS, Kojima T, Kikuchi Y, Ito H, Iwasaki H: **Circadian transcriptional regulation by the posttranslational oscillator without de novo clock gene expression in Synechococcus**. *Proc Natl Acad Sci USA* 2011, **108**:15396–15401.

69. Schürmann P: **Redox signaling in the chloroplast: the ferredoxin/thioredoxin system.** *Antioxid Redox Signal* 2003, **5**:69–78.

70. Díaz-Troya S, López-Maury L, Sánchez-Riego AM, Roldán M, Florencio FJ: **Redox regulation of glycogen biosynthesis in the cyanobacterium Synechocystis sp. PCC 6803: analysis of the AGP and glycogen synthases.** *Mol Plant* 2014, **7**:87–100.

71. Girotti AW: **Lipid hydroperoxide generation, turnover, and effector action in biological systems.** *J Lipid Res* 1998, **39**:1529–1542.

72. Kuo J, Khosla C: **The initiation ketosynthase (FabH) is the sole rate-limiting enzyme of the fatty acid synthase of Synechococcus sp. PCC 7002.** *Metabolic Engineering* 2014, **22**:53–59.

73. Ruffing AM: **RNA-Seq analysis and targeted mutagenesis for improved free fatty acid production in an engineered cyanobacterium**. *Biotechnology for Biofuels* 2013, **6**:1–1.

74. Ruffing AM, Jones HDT: **Physiological effects of free fatty acid production in genetically engineered Synechococcus elongatus PCC 7942.** *Biotechnol Bioeng* 2012, **109**:2190–2199.

75. Hoyle NP, O'Neill JS: **Oxidation–Reduction Cycles of Peroxiredoxin Proteins and Nontranscriptional Aspects of Timekeeping**. *Biochemistry* 2015, **54**:184–193.

76. Dietz K-J: **Peroxiredoxins in Plants and Cyanobacteria**. *Antioxid Redox Signal* 2011, **15**:1129–1159.

77. Xu Y, Mori T, Johnson CH: **Cyanobacterial circadian clockwork: roles of KaiA, KaiB and the kaiBC promoter in regulating KaiC.** *EMBO J* 2003, **22**:2117–2126.

78. Fiehn O, Garvey WT, Newman JW, Lok KH, Hoppel CL, Adams SH:

Plasma Metabolomic Profiles Reflective of Glucose Homeostasis in Non-Diabetic and Type 2 Diabetic Obese African-American Women. *PLoS ONE* 2010, **5**:e15234.

79. Fiehn O, Wohlgemuth G, Scholz M, Kind T, Lee DY, Lu Y, Moon S, Nikolau B: **Quality control for plant metabolomics: reporting MSI-compliant studies**. *The Plant Journal* 2008, **53**:691–704.

80. Xia J, Sinelnikov IV, Han B, Wishart DS: **MetaboAnalyst 3.0-making metabolomics more meaningful.** *Nucleic Acids Res* 2015.

81. R Core Team: *R: a Language and Environment for Statistical Computing*. Vienna, Austria; 2014:1–3604.

82. Benjamini Y, Hochberg Y: **Controlling the false discovery rate: a practical and powerful approach to multiple testing**. *Journal of the Royal Statistical Society Series B …* 1995.

83. Deatherage DE, Barrick JE: **Identification of mutations in laboratory-evolved microbes from next-generation sequencing data using breseq.** *Methods Mol Biol* 2014, **1151**:165–188.

Chapter 4

Discussion and Conclusions

4.1 Discussion and Conclusions

Synechococcus elongatus PCC7942, is both the premier model for a prokaryotic circadian clock as well as a successful engineering platform for a number of valuable industrial chemicals and fuels [1]. Additionally, *Synechococcus* species are ubiquitous in the environment and make a significant contribution to the global carbon cycle [2]. Thus, their metabolic regulation by light and circadian rhythms has broad implications for understanding their behavior in natural environments as well as in the context of metabolic engineering. This work investigates the importance of circadian outputs in *S. elongatus* for the control of core metabolic processes under the conditions of natural diurnal growth. Using the excellent genetic tools of *S. elongatus* [3, 4], and the extensive knowledge of its circadian mechanism [5, 6] we have set out to address four primary questions: (i) Does the circadian clock have a direct impact on metabolite levels in cyanobacteria over a diurnal cycle?; (ii) How does the timing of the circadian clock affect metabolic output under a diurnal cycle?; (iii) How does the circadian response regulator, RpaA, directly affect metabolism, and does this agree with its transcriptional output?; (iv) Why must RpaA be active at night, and what is the mechanism behind diurnal lethality observed in *rpaA*-null mutants?

Our work has shown that the *S. elongatus* circadian clock can exert very strong control over the levels of metabolites in central carbon metabolism during the day and night periods. This was observed to occur through the repression and relief of repression by the core oscillator on its output response regulator RpaA. Additionally, the timing of the core circadian oscillator, KaiC, must align with the environmental availability of light to provide optimal metabolic regulation. This is evident from the fact that when we performed experiments that locked KaiC in a morning state and placed cells in the dark, the normal night-time glycogen degradation process was attenuated and viability was significantly impacted. We also observed that although *kaiC*-null mutants do not show any visible phenotype under diurnal conditions, their metabolism at a dark-to-light transition is significantly impacted. The *kaiC*-null mutant cannot properly repress RpaA in the morning leading to the activation of night metabolic pathways, and the concentration of carbon in primary metabolic processes. Specifically show that the mechanistic importance of alignment of the clock timing with the environmental cycle is directly related to its control over the oxidative pentose phosphate pathway (OPPP) via the circadian output response regulator RpaA.

Previous work indicates that RpaA activates pathways for stored carbon degradation and reductant generation at night, and inactivation of *rpaA* results in cell death when cells enter the dark. We found that under normal conditions *rpaA* mutants generate increased levels of reactive oxygen

species (ROS) during the day period that remain present in their cells after they enter a dark period. Our data indicates that without the ability to activate the OPPP and generate reductant at night, cell death in *rpaA*-null mutants occurs due to an inability to detoxify ROS generated during the day. An ROS mediated cell death mechanism is consistent with our observation that cell death in *rpaA*-null mutants is proportional to the light intensity that cells receive during the day period of a light-dark cycle, with lower intensity daytime light allowing for survival through a dark period. Additionally, cell death can be suppressed by mutations that alleviate the production of ROS during the day period. Finally, our metabolomics data from WT and *rpaA*-null mutants at night indicates that WT cells maintain a strict level of metabolite stability, and reductant production, mediated by the RpaA activated OPPP, is a critical component to maintain this stability. The observed importance of reductant balance at night, coupled with the low level of mRNA transcription at night in *S.* elongatus [7], suggests that a significant portion of metabolic regulation during this period is driven by protein redox modification. This is consistent with the data showing that light-dark transitions can drive the redox modification of large number of metabolic proteins in cyanobacteria [8]. The interaction of circadian rhythms and protein redox regulation is emerging as a primary area of understanding for metabolic behavior under diurnal conditions.

This study addresses a critical knowledge gap in the understanding of how cyanobacteria integrate circadian and environmental signals over a diurnal cycle. Additionally, it has indicated the specific metabolic pathways that are most strongly regulated by circadian outputs, and provides significant evidence on the mechanisms behind the long-standing mystery of diurnal lethality in *rpaA*-null mutants. The connections we have built between the clock and metabolism will be invaluable for the future construction of cyanobacterial metabolic models that take into account both light and dark periods of growth, as well as the important circadian influence under these growth conditions. This type of systems level analysis will be critical for the development of cyanobacteria as a next generation engineering platform, and the ecological understanding of one of the most important primary producers on this planet.

4.2 References

1. Oliver J, Atsumi S: **Metabolic design for cyanobacterial chemical synthesis**. *Photosynth Res* 2014.

2. Bryant DA: **The beauty in small things revealed.** *Proc Natl Acad Sci USA* 2003, **100**:9647–9649.

3. Taton A, Lis E, Adin DM, Dong G, Cookson S, Kay SA, Golden SS, Golden JW: **Gene Transfer in Leptolyngbya sp. Strain BL0902, a Cyanobacterium Suitable for Production of Biomass and Bioproducts**. *PLoS ONE* 2012, **7**:e30901–15.

4. Chen Y, Holtman CK, Taton A, Golden SS: **Functional Analysis of the Synechococcus elongatus PCC 7942 Genome**. In *Advances in Photosynthesis and Respiration*. *Volume 33*. Dordrecht: Springer

Netherlands; 2011:119–137. [*Advances in Photosynthesis and Respiration*]

5. Mackey SR, Ditty JL, Clerico EM, Golden SS: **Detection of rhythmic bioluminescence from luciferase reporters in cyanobacteria.** *Methods Mol Biol* 2007, **362**:115–129.

6. Mackey SR, Golden SS, Ditty JL: **The Itty-Bitty Time Machine**. In *Advances in Genetics*. *Volume 74*. Elsevier; 2011:13–53. [*Advances in Genetics*]

7. Ito H, Mutsuda M, Murayama Y, Tomita J, Hosokawa N, Terauchi K, Sugita C, Sugita M, Kondo T, Iwasaki H: **Cyanobacterial daily life with Kai-based circadian and diurnal genome-wide transcriptional control in Synechococcus elongatus**. *Proc Natl Acad Sci USA* 2009, **106**:14168–14173.

8. Guo J, Nguyen AY, Dai Z, Su D, Gaffrey MJ, Moore RJ, Jacobs JM, Monroe ME, Smith RD, Koppenaal DW, Pakrasi HB, Qian W-J: **Proteome-wide Light/Dark Modulation of Thiol Oxidation in Cyanobacteria Revealed by Quantitative Site-specific Redox Proteomics**. *Molecular & Cellular Proteomics* 2014, **13**:3270–3285.